Cape Peninsula
University of Technology

DESIGN AND DEVELOPMENT OF AN INFRARED HEATER FOR WASTE PLASTIC GASIFICATION

by

ZUHAIR ELTIGANI MATAR HARUON

Thesis submitted in fulfillment of the requirements for the degree

Master of Technology: Electrical Engineering

in the Faculty of Electrical Engineering

at the Cape Peninsula University of Technology

Supervisor: Dr. M. Adonis

Bellville campus

August 2013

CPUT copyright information

The dissertation/thesis may not be published either in part (in scholarly, scientific or technical journals), or as a whole (as a monograph), unless permission has been obtained from the University

DECLARATION

I, Zuhair Eltigani Matar Haruon, declare that the contents of this thesis represent my own unaided work, and that this thesis has not previously been submitted for academic examination towards any qualification. Furthermore, it represents my own opinions and not necessarily those of the Cape Peninsula University of Technology.

Signed: .....

Date: .....

ABSTRACT

This research outlines the design, manufacturing and analysis of a far infrared ceramic heater for waste plastic gasification. The study includes the theoretical overview which concentrated on the mathematical modelling of the far infrared ceramic heater, as well as mathematical modelling of infrared gasifier. Secondly, the study presents an overview of the manufacturing process of the ceramic infrared heaters. Testing of the manufactured heaters has been performed to validate the efficacy of the heaters.

The model includes non-grey radiative heat transfer between the different parts of the heaters, conduction in ceramic material, convective cooling of the surface, surface balances, and blackbody radiation theories. Using infrared module voltage as input, model predictions of temperature and wavelengths using Fourier equations were found to agree well with experimental data. The ceramic infrared heaters developed in this research are fully functional and all intended test results were obtained.

The spectral analyses of different plastics (Polyethylene terephthalate, Polypropylene, Low-density polyethylene and High-density polyethylene) have been performed. ‘Heat rate’ and ‘cool rate’ of the infrared ceramic heaters have also been characterised. Gasification of plastic waste as carbonaceous material, basic reactions during gasification of plastics, and gasification products have also been discussed, including gasifier properties. The results obtained from the experiments show that using infrared heaters in gasification is practically sound because of the ability of infrared radiation to gasify waste plastics and production of syngas. This project recommended the infrared radiation because of its high efficiency in gasification of waste plastic and the production of syngas. This article reviews the infrared radiation heating and discusses the theoretical aspects of infrared radiation and the validity of infrared radiation heating in gasification of waste plastics. This research also provides a review of literature in the applications and benefits of infrared heaters.

ACKNOWLEDGEMENTS

This work has reached its successful completion mainly because of the help and encouragement of so many people. I would like to take this opportunity to extend my sincere gratitude to some very prominent figures that, through their input, made an exceptional impact.

- I would like to thank my supervisor, Dr. Marco Adonis, for his guidance and assistance throughout the time of my research to its completion.

- To the Electrical Department of Cape Peninsula University of Technology, thank you for availing me the facilities in which to conduct my research.

- Then thank you to my family, especially my dad and my mother whose financial support, understanding and words of encouragement during this research helped me focus my efforts and bring it to completion.

- To my fellow research colleagues and friends, thank you for your motivation and inspiration; it has proven invaluable.

TABLE OF CONTENTS

CHAPTER THREE: HEAT TRANSFER THEORY

CHAPTER FOUR: MODELLING OF CERAMIC INFRARED HEATER AND INFRARED GASIFIER

CHAPTER FIVE: CONSTRUCTION AND DESIGN OF INFRARED HEATER AND INFRARED GASIFIER

CHAPTER SIX: EXPERIMENTAL RESULTS

CHAPTER SEVEN: CONCLUSION AND RECOMMENDATION

LIST OF FIGURES

LIST OF TABLES

APPENDIX

NOMENCLATURE

q	Heat flux W/m^2
k_c	Thermal conductivity W/mK
T	Temperature K
h_c	Convection heat transfer coefficient W/m^2K
v	Frequency Hz
c	Speed of light $2.998.10^8 m/s$
h	Planck's constant $6.626.10^{-34} J/s$
λ	Wavelength m
e	Photon energy J
ε	Emissivity
ρ	Resistivity Ω.cm
a	Absorbtivity
t	Transmissivity
r	Reflectivity
G_λ	Spectral irradiation W/m^2
G	Total irradiation W/m^2
I_λ	Spectral intensity W/m^2
σ	Stephan Boltzmann constant $5.67\times10^{-8} W/m^2K$
C_1	First blank's law constant $3.74\times10^{-16} W/m^2$
Q	Radiative heat flux W
A	Area m^2
J	Radiosity W/m^2
F	View factor

ABBREVIATIONS

PE	Polyethylene
PP	Polypropylene
PS	Polystyrene
PET	Polyethylene terephthalate
HDPE	High density polyethylene
LDPE	Low density polyethylene
HC	Hydrocarbon
CO	Carbon monoxide
CO_2	Carbon dioxide
CH_4	Methane
H_2	Hydrogen
C	Carbon
MSW	Municipal Solid Waste
UNEP	United Nations Environmental Program
IGCC	Integrated combined cycle

CHAPTER ONE
INTRODUCTION

With today's modern quick-and-easy lifestyles, the consumption of plastics continues to increase every year; consequently, the amount of plastic waste has also increased (UNEP, 2009). The traditional manner of plastic waste disposal has been either to bury or burn the waste in landfills or incinerators, respectively. Landfills and incinerations, however, are associated with serious environmental problems; therefore various technologies have been investigated which can efficiently treat plastic waste and generate useful fuels or petrochemical feedstock in pursuit of duel environmental and economic benefits. One of these technologies involves the use of infrared energy which is considered very efficient and cost-effective. Using infrared radiant heating is preferred in heating applications in general because infrared radiation emits no harmful fumes. Infrared heat does not require air movement and therefore has no harmful emissions (Krishnamurthy *et al.,* 2008).

1.1Overview of Plastic waste consumption

The levels of consumed plastics currently, and their limited disposal procedures, grant several environmental problems. Therefore, recycling of plastics creates new opportunities to reduce the reliance on oil consumption and reduce carbon dioxide emission. In 2007, the production of plastics worldwide was estimated to be 260 million metric tons per annum, including all types of polymers such as thermosets, thermoplastics and adhesives (Jefferson *et al.,* 2009). As indicated by Andrady (2003), two thirds of the plastic production worldwide was thermosets.

National Association for PET Container Resources reported that PET is a combination of ethylene glycol and purified terephthalic acid. It is widely used for packaging soft drinks and beverages. Figure 1.1 introduces the plastic waste generation and recovery from 2006 till 2011.

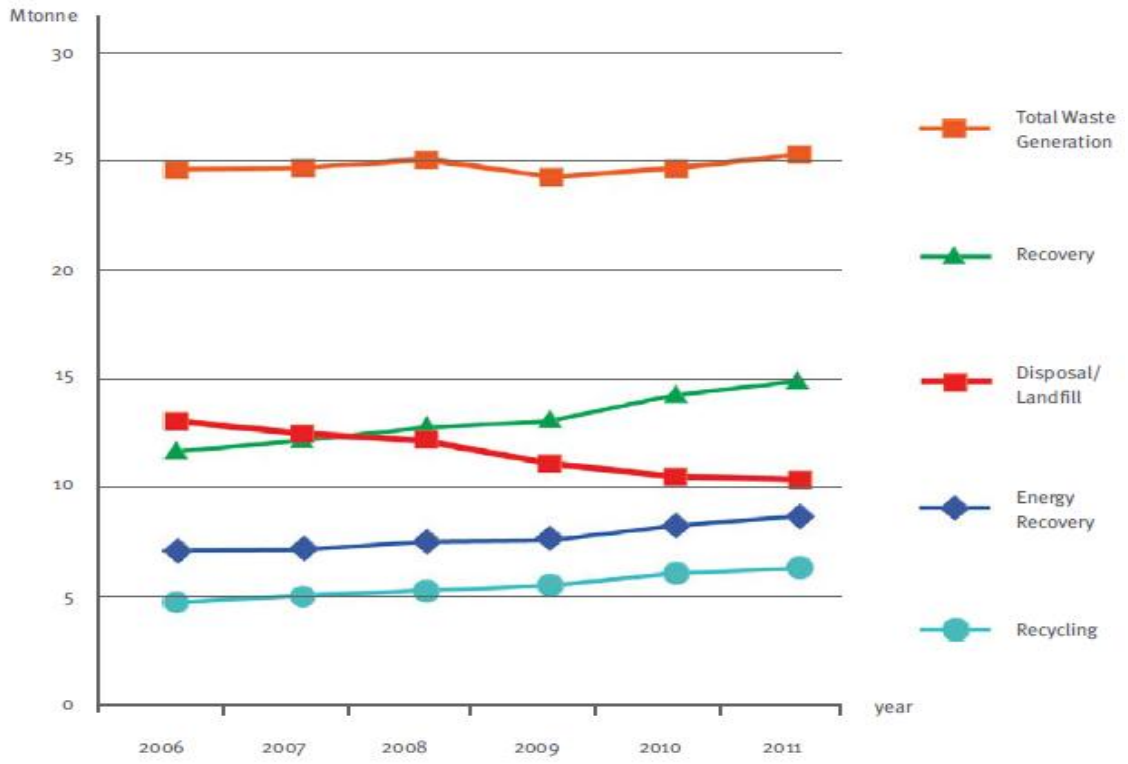

Figure 1.1: Plastic waste generation (Plastics Europe, 2012)

1.2 Problem statement

The problem addressed by this research stems from concern about the accumulation of plastic waste and the resultant negative impact to the environment. This research intends to present a physical design as well as mathematical model for an infrared gasifier with the ultimate goal of designing and manufacturing infrared gasifiers capable of transforming waste plastics into valuable fuel. The current waste disposal techniques – landfills and incinerations – each pose considerable negative impact on underground water and atmosphere.

1.3 Purpose of the research

The aim of this research is to design and manufacture ceramic far infrared heaters to be used in the gasification of waste plastics.

The main objectives of this research are as follows:

- To design, manufacture and analyse a far infrared ceramic heater for waste plastic gasification;
- To design and manufacture an infrared gasifier;
- To use plastics from waste as feedstock in order to study the influence of infrared radiation on transforming thermoset plastics into syngas; and

- To accurately and efficiently model and simulate ceramic infrared heaters that could then be used in furnaces for gasification of waste plastics

- Production of syngas using the manufactured infrared gasifier.

1.4 The research goal

The overall goal of this research is to demonstrate technical feasibility of the infrared thermal energy to gasify waste plastics and to develop a laboratory scale gasifier design for application of infrared radiation in gasification procedures.

1.5 Process modeling

The purpose is to develop and use a computational model to predict the infrared gasifier performance and operating conditions. The computational model is used to optimise and analyse data derived from experiments. LabVIEW software has been applied to test and analyse the manufactured heaters.

1.6 The design methodology

- Mathematical modeling of infrared ceramic heater as well as the infrared gasifier;
- Wavelength measurement of waste plastics using infrared spectroscopy facility, furrier transform infrared spectroscopy (FTIR). This project supports the reduction of the costs of electrical energy supply by developing a lower cost method for generating power;
- Temperature measurement using temperature sensor; and
- Data acquisition to determine characteristics of temperature sensors and temperature control.

1.7 Advantages of infrared

According to Zhongli (2010), the advantages of infrared heating are as follows:

- Lower energy consumption;

- It is clean and therefore environmentally friendly;

- Long operating life with less maintenance;

- Quick response;

- Minimize floor spacing.

1.7.1 Targeting plastic waste

Waste plastics are one of the most promising resources for fuel production because of useful gasses they contain. According to Laurence (2008), plastics do not absorb much

moisture and the water content of plastics is far lower than the water content of biomass such as crops and kitchen wastes. The conversion method of waste plastics into fuel depends on the type of plastics to be targeted and the properties of other waste that might be used in the process. Additionally, the effective conversion of plastic into energy resource requires appropriate technologies to be selected according to local economic, environmental, social and technical characteristics (Aguado & Serrano, 1999). Each type of waste plastic conversion method has it is own suitable feedstock. The composition of different plastics used as feedstock increases the probability that such composition may contain undesirable substances (e.g. additives such as flames containing bromine and antimony compounds or plastic containing nitrogen, halogens, sulphur or other hazardous substances) which pose risk to humans and to the environment (Anthony, 2003). Jenni (2005) indicated that PET plastic has high energy content, making it a strong candidate for gasification. The following Table 1.1 introduces some facts about the heat capacity for several plastics.

Table 1.1: Heat capacity of some plastics and other materials (Jenni, 2005)

Material	**Heat Capacity (MJ/kg)**
PVC	18
PE	27
PET	46
PS	41
Heavy fuel oil	41
Coal	26
Natural gas	36 (MJ/m^3) (0℃)
Milled peat	10

A study by Jones (2010) has mentioned major quality concerns when converting waste plastic into fuel resources as follows:

- Types of plastics and their consumption;
- Pre-treatment requirements;
- The combustion temperature for the conversion the energy consumption required;
- The fuel quality output, the flue gases composition (e.g. formation of hazardous flue gases such as NO_x and HCL);
- The fly ash and bottom ash composition;
- The potential of chemical corrosion of the equipment;
- Smooth feeding to convert equipment, as before their conversion to a fuel, waste

plastics undergo several pre-treatment methods to ensure smooth and efficient treatment during the conversion process;

- Different plastic waste structures (films, rigid, sheets) which insist on different pre-treatment equipment.

For effective conversion into fuel products in solid fuel production, thermoplastics act as binders which form pellets, or briquettes, by melting and adhering to other non-melting substances such as paper, wood and thermosetting plastics. Although wooden materials are formed into pellets using a pelletizer, mixing plastics with wood or paper complicates the pellet preparation process. Suitable heating is required to produce pellets from thermoplastics and other combustible waste. In liquid fuel production, thermoplastics containing liquid hydrocarbon can be used as feedstock. The type of plastic being used determines the processing rate as well as the product yield. Contaminating by undesirable substances and the presence of moisture increase energy consumption and promote the formation of by-product in the fuel production process (Anthony, 2003).

1.8 Application of infrared heating

What makes infrared radiation attractive to industry is that it is clean, has a high power output yield, and probably most importantly, is the efficiency that this kind of heating imports on the many industrial applications where it is employed (Zhongli *et al*., 2010).

1.9 Benefits of infrared radiation

Benefits of infrared radiation offering real solutions for many industries are acknowledged by a variety of industries gaining these benefits from it (Knights, 1997a). Benefits of infrared are addressed as follows:

1.9.1 Time and space saving

The floor space that is occupied by infrared radiation equipment is less than that for convection ovens. And the faster the heating process means shorter oven time. The equipment can also be added to existing convective ovens and production lines with little or no difficulty. IR ovens are easily constructed, as indicated by Howard (1996), and can also be easily reconfigured as the product requirements change.

1.9.2 Increased productivity

The speed of an infrared radiation system, which is related to the properties of infrared radiation, is a contributing factor to increased productivity. Also associated with the improved quality of the finished product is the resultant increase in productivity. The process and the system do not experience many stoppages or down time as a result of resetting the machines, factors which further contribute to the cost effectiveness of an IR system

(Howard, 1996).

1.9.3 Energy efficiency

Energy efficiency is defined as the useful energy output to the total energy input. Most of the energy in the systems that are properly designed is transferred by radiation to the material. The energy, therefore, acts directly on the material, resulting in faster processes and lowering of energy costs. Consequently, the infrared radiation heating process is of higher efficiency because energy losses are minimal. Processing time can be reduced by as much as 50%-80% when compared to convection ovens (Howard, 1996). The efficiency of the infrared heater depends on matching the emitted wavelength and the absorption spectrum of the material to be heated. The peak absorption spectrum of plastics such as polyethylene is 3.3 and 6 μm which makes it clearly more efficient to use far infrared heaters. This makes the careful selection of the correct infrared heater type important for energy efficiency in the heating process (Zhongli *et al.,* 2010).

1.9.4 Quality products

Industries in metal coating, wood, paper, glass, plastic and textiles require more lustrous, longer lasting and wear-resistant finishes. Since infrared radiation heats the material directly, there is no need to blow hot air through the oven to achieve heat transfer, translating into a superior finish and fewer rejects due to surface blemishes from entering dust (Howard, 1996).

1.9.5 Environmental impacts

Infrared technology is an environmentally friendly technique according to Zhongli *et al.* (2010). The environmental impact of an infrared radiation system is minimal and less intrusive when compared to traditional methods used previously (Broadbent, 1998).

1.9.6 Cost effectiveness

The infrared radiation products currently on the market solve the problems associated with efficiency and cost effectiveness of industrial processes. The cost effectiveness of an infrared radiation system implies that the resulting savings can be utilised in other areas in order to streamline a company's throughput. The concerns surrounding the financial viability of implementing an infrared radiation system are offset by the multiple advantages derived from such a process (Howard, 1996).

CHAPTER TWO
LITERATURE REVIEW

The traditional methods of plastic waste disposal have been either to bury or burn the waste in landfills or incinerators, respectively. Landfills and incinerations, however, are associated with serious environmental problems. Therefore various technologies have been investigated which can treat plastic waste and generate useful fuels or petrochemical feedstock in pursuit of both environmental and economic benefits. This chapter shall introduce a literature review covering the pyrolysis and gasification of plastics, as well as a review of literature concerning the infrared heating application on drying and heating.

Plastic recycling can be divided into three methods: mechanical recycling, chemical recycling and energy recovery. Feedstock recycling, which converts plastic materials into useful basic chemicals, has been recognised as an advanced technology process (Martin *et al.,* 1999). Gasification is one example of feedstock recycling technologies. In recent years, the gasification of plastics has been intensively conducted and some useful results have been drawn from various studies (Cornelia *et al.,* 2007, and Peter *et al.,* 2010).

A recent study conducted by Farah (2011) shows that around 11 billion plastic bags were used in the UAE in 2010, of which 53.7% were non-biodegradable. This means that nearly 120,000 tons of non-biodegradable plastic waste was generated in 2010 alone. This creates a problem as not every plastic bag in circulation can be recycled and unfortunately they eventually end up as litter or in landfills. Furthermore, plastics are notoriously difficult to recycle and the process of collecting them for recycling or sending to a landfill is expensive. With the ever-increasing environmental concern restrictions, it is becoming difficult to properly dispose of plastic without damaging the environment, as concluded by Baeyen (2010); therefore, the solution to this problem must be the conversion of waste plastic into useful fuel. This can be done in various ways such as pyrolysis, incineration and gasification (Arena *et al*., 2009). Each one of these methods, though, has it is own unique advantages and disadvantages. Pyrolysis and gasification are chosen over the other technologies because these two processes result in a higher yield of synthesis gas (syngas). Syngas produced from this process can then be cooled down, cleaned and combusted in gas turbine to produce electricity (Mastral *et al.,* 2003).

People have been using gasification since 1800, and since that time gasification technology has developed throughout the 19th century to provide low heating value gas for heating purposes. With the introduction of natural gas in the 20th century, and the decline of the town gas industry, gasification has become a specialised niche technology with limited

application. However, with time, the gasification processes improved and with the technological programmes, the capacities of the system have expanded steadily. Gasification in simple terms means conversion of carbonaceous fuels into gas. It is a process of chemical reactions between carbon in the feed and steam. The gasification process is one of the thermal conversions, as indicated in Figure 2.1.

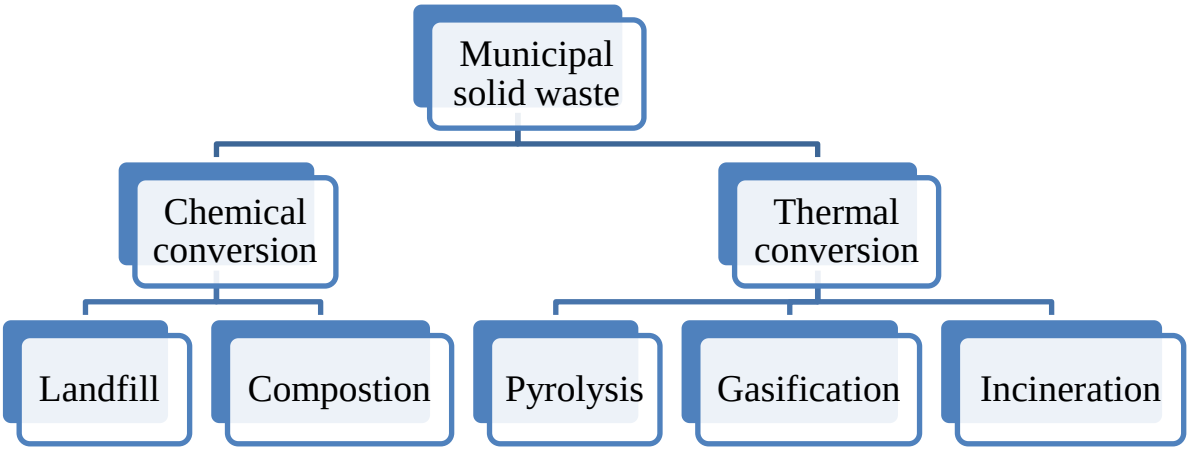

Figure 2.1: MSW management options

2.1 Gasification

The gasification process converts carbonaceous materials such as plastic, coal and petroleum into carbon monoxide and hydrogen by reacting the raw materials at high temperature with controlled amounts of oxygen or steam (Klein, 2002). The resulting gas is called ‘syngas’; it is also the method of extracting energy from different types of organic materials. In an industrial scale, gasification is currently used primarily to produce electricity from fossil fuels such as coal, where syngas are burned in gas turbine. As shown in Figure 2.2, feedstock recycling of plastics shall produce syngas. Since gasification is a process of reacting feedstock with controlled amounts of oxygen or water, Figures 2.2 and 2.3 show clearly the flow of the process.

2.1.1 The gasifier

The gasifier is the main part of any gasification system; it is the vessel where the reaction between the input feedstock and control amount of oxygen occurs at elevated high temperatures. The available gasifiers are divided according to design into ‘up draft’ and

‘down draft’ gasifiers. The gasification begins when feedstocks are fed to the gasifier with a controlled amount of oxygen; the oxygen is fed to the gasifier at the same time as the feedstock at temperatures around 450˚C. This reaction produces syngas resulting from the breakdown of the feedstock molecules.

2.1.2 Syngas

Syngas is a mix of carbon monoxide and hydrogen. It is an ideal replacement for fossil fuels in conventional combined heat, power units and power generation systems. Syngas consists of hydrogen and carbon monoxide and, according to Jenni (2005), the ratio of the hydrogen and carbon monoxide depends on the hydrogen and carbon content of the feedstock and the type of the gasifier used.

The ratio of hydrogen and carbon determine the product to be manufactured: electricity, chemicals, fuels, or hydrogen. For example, refineries use syngas consisting primarily of hydrogen, and chemical plants use syngas with roughly equal proportions of hydrogen and carbon monoxide. Syngas is 50% the density of natural gas and can be used as fuel in the same way as natural gas. Products made from syngas are shown in Figure 2.4.

Syngas can also be used in the following ways:

- To displace natural gas or residual oil in existing electricity generating equipment;

Or

- To generate renewable thermal power.

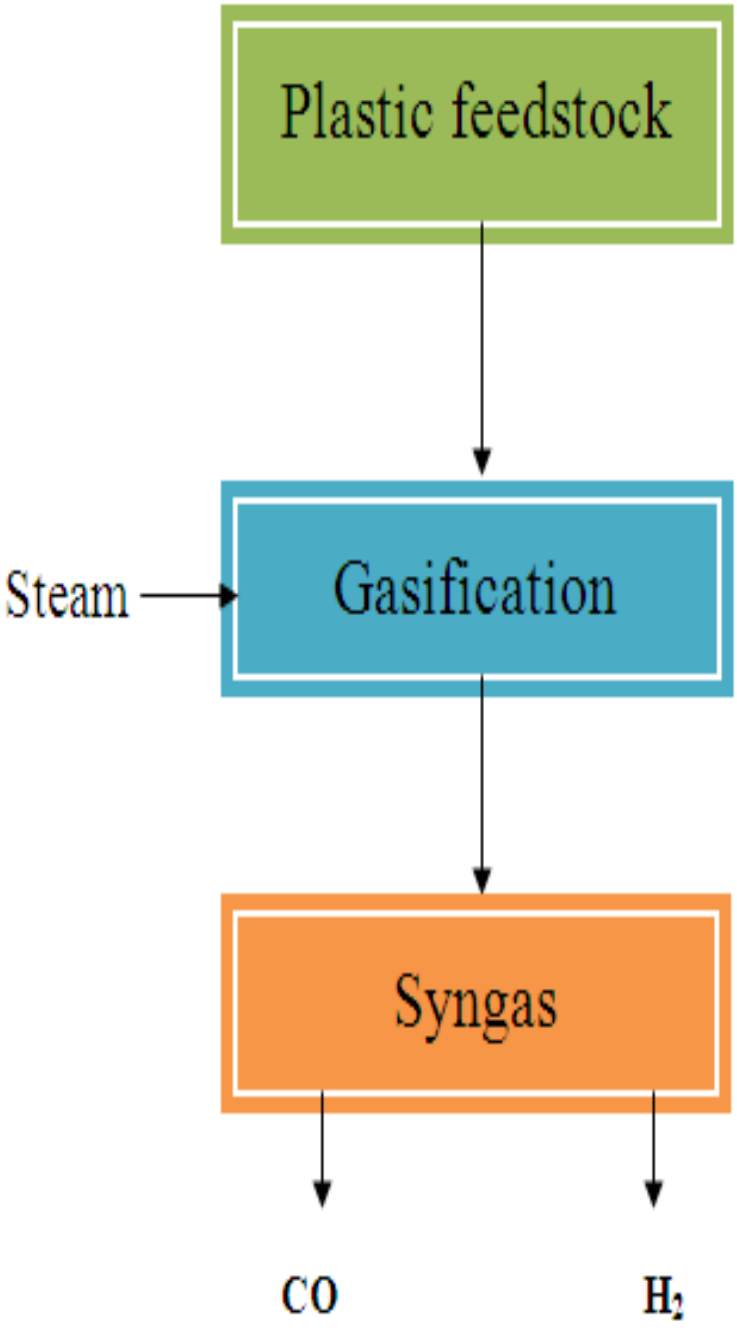

Figure 2.2: Plastics gasification

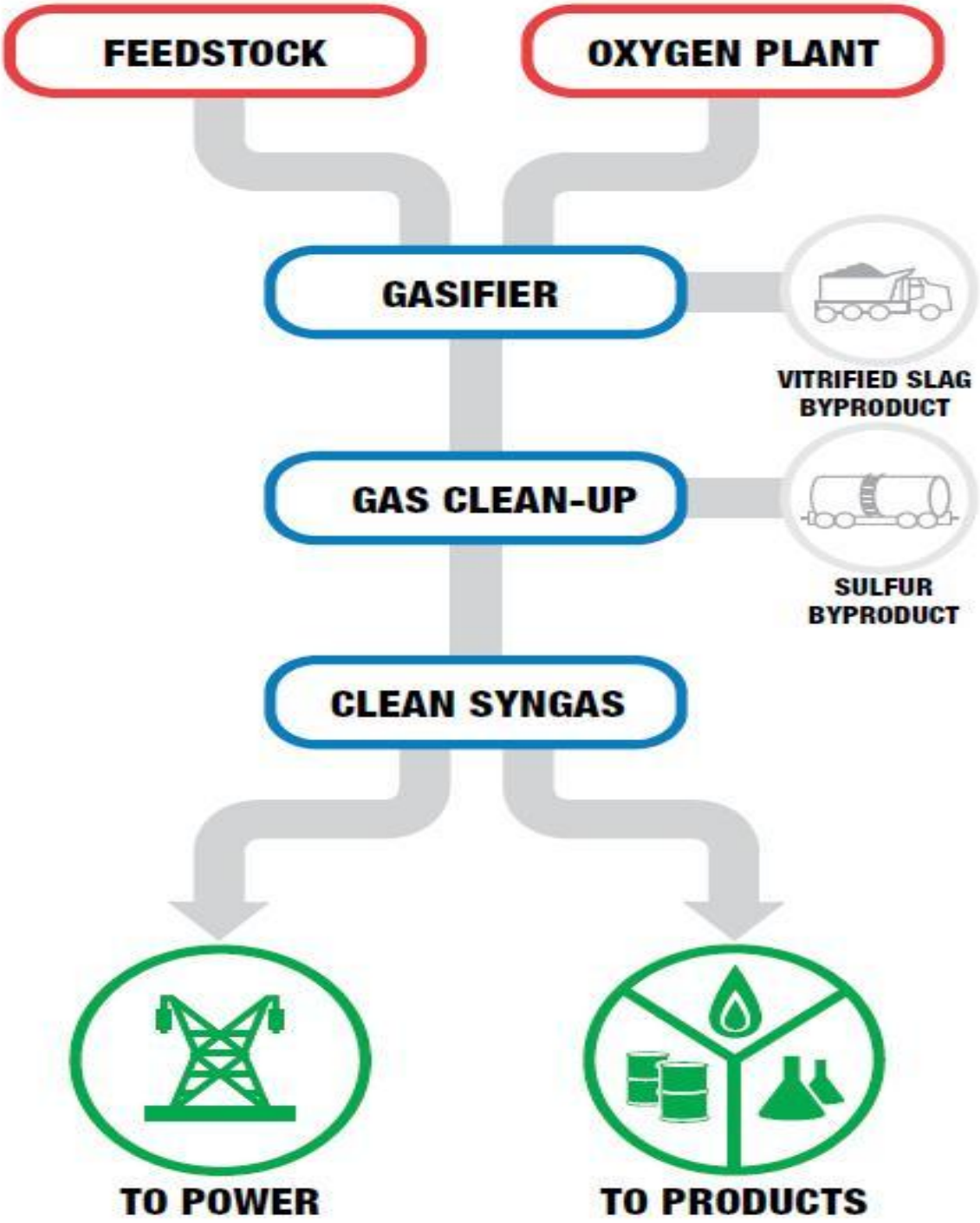

Figure 2.3: Gasification process (Gasification council, 2010)

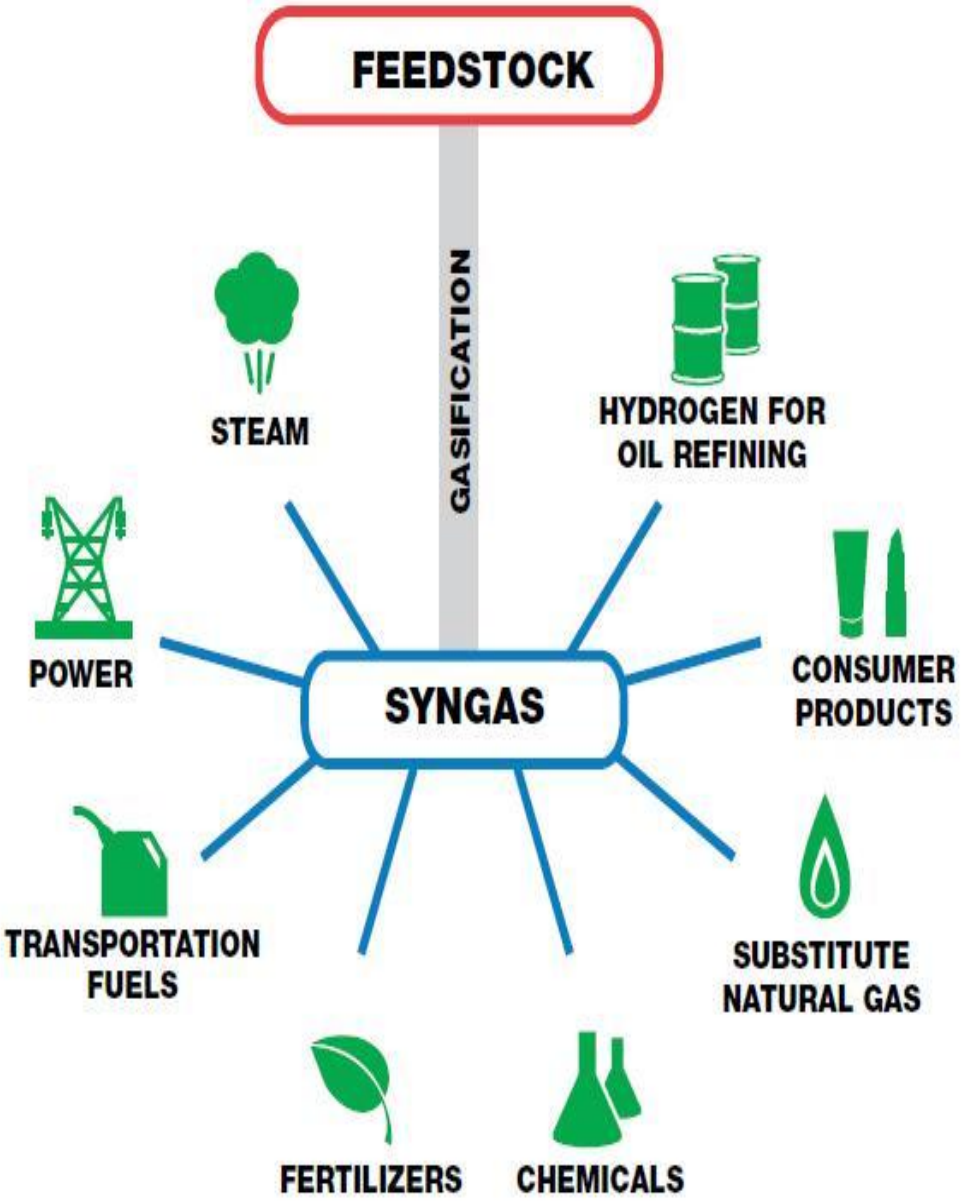

Figure 2.4: Gasification products (Gasification council, 2010)

The basic reactions during the gasification of carbonaceous materials are shown below:

- Raw Material Decomposition

$$C_x + H_y \rightarrow xC + \frac{y}{2}H_2 \quad (2.1)$$

- Reaction With Oxygen

$$C + \frac{1}{2}O_2 \rightarrow CO \quad (2.2)$$

$$C + \frac{1}{2}O_2 \rightarrow CO_2 \quad (2.3)$$

$$H_2 + \frac{1}{2}O_2 \rightarrow H_2O \quad (2.4)$$

$$C_xH_y + \left[x + \frac{y}{4}\right]O_2 \rightarrow xCO_2 + \frac{y}{2}H_2O \quad (2.5)$$

$$C_xH_y + \left[\frac{x}{2} + \frac{y}{4}\right]O_2 \rightarrow xCO + \frac{y}{2}H_2O \quad (2.6)$$

- Reaction with water

$$C + H_2O \rightarrow CO + H_2 \quad (2.7)$$

$$CO + H_2O \rightarrow CO_2 + H_2 \quad (2.8)$$

$$C_xH_y + xH_2O \rightarrow xCO + \left[\frac{y}{2} + x\right]H_2 \quad (2.9)$$

- Reactions with CO_2

$$C + CO_2 \rightarrow 2CO \quad (2.10)$$

$$C_xH_y + xCO_2 \rightarrow 2xCO + \frac{y}{2}H_2 \quad (2.11)$$

- Methanation Reaction

$$CO + 3H_2 \rightarrow CH_4 + H_2O \quad (2.12)$$

$$CO_2 + 4H_2 \rightarrow CH_4 + 2H_2O \quad (2.13)$$

2.1.3 Gasification review

A two-stage thermal gasification of plastics has been developed by Toshiro and Yoshika (2000). Polyethylene (PE), polypropylene (PP) and polystyrene (PS) have been gasified using this two-stage thermal degradation. Plastics have been transformed to liquid and then to gas in the gasification stage. The total gases yielded from the gasification stage were 80, 70 and 6.6%wt for PE, PP and PS respectively. The main components were methane and gaseous olefins such as ethylene and propylene; carbonaceous residue or coke was less than 1%wt. Pyrolysis process of plastics produced high calorie gas with low coke ratio and aromatic oils such as benzene, toluene and xylene (BTX).

Toshiro and Yoshika (2000) studied the use of external heating to improve the quality of gaseous products and efficiency of gasification. The concept of the two-stage pyrolysis gasification was to convert plastics to liquid products at low temperature and then to gasify the liquid hydrocarbons. It was found that using two-stage pyrolysis gasification remarkably reduced the amount of coke. The results of the liquefaction stage concluded that the yields of the gaseous products were very low because the temperature of the reaction was relatively low.

The dependence of the gas yielded such as methane and ethylene increased with the temperature, but the gaseous products heavier than C_3 components decreased with the temperature; the maximum gas yielded was at 750˚C. At higher temperatures, gas components having a carbon number larger than 3 turned BTX by intermolecular condensation. The total gases yielded in this study were higher than that in a one-stage gasification process. It was recommended that sub products such as oil and coke can be used as heating sources for the pyrolysis process.

High calorie gas with low coke formation has been produced: the gas yielded for PE was 80% wt and 74% wt PP based on weight of each polymer. At 800˚C the produced gasses were methane and gaseous olefins for PE and PP; sub products were aromatic oils such as

BTX. Takatoshi *et al.* 2001 studied an entrained flow gasification process which converted waste plastics to energy at a high energy recovery rate. The plastics fed into gasifier were < 8mm in size and the other inputs to the gasifier were air and oxygen.

The organic substances in the gasifier went first through pyrolysis process, partially combusted and then converted to synthetic gas (CO, H2). At a high temperature over 1600 K, the lower heating value of the produced gas was over 4.2 MJ and the cold gas efficiency was approximately 60%.Other inert substances in the waste such as ashes and metals were melted into slag and condensed on bag filters: the bag filters and water scrubber removed impurities such as dusts, heavy metals and hydrogen halides from the product gases. Solid hydrocarbons which include char and soot were removed at a hot cyclone and on the bag filter.

Recycling of waste electronics and electrical have been implemented by Takashi and Yamawaki (2003) and plastics have been gasified at temperatures up to 1200˚C. Then shock cooling was done to cool down the reaction temperature to about 200˚C and the decomposition was done at a resident time of 2.5 seconds and a decomposition rate of 99.99%.

The study of gasification of waste electronics concluded that gasification of plastics containing brominated flame retardants can be achieved to prevent the generation of brominated dioxins and to prevent the regeneration of brominated dioxin, similar to the experience with chlorinated dioxins under the proper operating conditions.

Gasification of 100%wt polypropylene waste was carried out by Jesu *et al*.(2008). The objective of this particular study was to compare the effectiveness of tar elimination by dolomite and olivine in the gasifier bed. The study concluded that the dolomite was more active for tar elimination than olivine for the same amount in the gasifier: the reduction of tar contents with dolomite was 92% whereas with olivine it was 40%. Olivine was preferred as the gasifier bed material because it doesn't have as many high amounts of particulates as dolomite. Canadian Plastics Industry Association and the Environmental and Industry Council (2004)have reported that wastes can be transformed into products that could be used as a source of chemicals or clean burning fuels. The report showed that the chemical process of gasification is markedly different from that of incineration. According to the report, gasification is designed to maximise the conversion of feedstock to carbon monoxide (CO) and hydrogen (H_2) while incineration converts the feedstock into carbon dioxide (CO_2) and water (H_2O).

The report indicated that the typical operating temperatures of the gasifiers were around

1200˚C to 2000˚C. Thermal decomposition of the feedstock occurred in this temperature range because the chemical bonds are broken thermally at high temperatures. In addition, a gasifier operates within an atmosphere deficient in oxygen. This is called a 'reducing atmosphere'. Such an atmosphere prevents the formation of the oxides of sulphur and nitrogen that contribute to the formation of smog and acid gases. The report addressed two reasons that prevent dioxins and furan from being present in the syngas:

- First, high temperature in the gasification process destroys any dioxins or furan components or precursors in the feed.
- Secondly, Secondly, the reducing environment precludes the formation of free chlorine from HCL, thereby limiting chlorination of any species in the syngas.

Tsuji and Hayatamam (2007) investigated the gasification of waste plastics PE and PS using steam reforming. The carbon conversion increased with the increase in temperature during the gasification process. The high temperature applied showed great influence on the steam reforming process, which in turn increased hydrogen and decreased the methane formation. The yielded carbon monoxide was also found to increase with the increasing temperature. When steam-to-carbon ratio has been varied at fixed temperature 1023K, it was found that carbon conversion increased by increasing steam-to-carbon ratio. Increasing the steam-to-carbon ratio also increased the gas composition of hydrogen and carbon dioxide according to water / gas shift reaction. Wu and Williams (2010) studied pyrolysis and gasification of post-consumer municipal plastic wastes, concluding that gasification temperature had an important influence on the product yielded and gas composition. The hydrogen composition in the gas increased with increasing temperature, as did the overall gas yielded. The composition of carbon monoxide also increased with increasing the gasification temperature. The steam-to-fuel ratio was also studied and it was reported that increasing the steam-to-fuel ratio increased the hydrogen production and decreased the carbon monoxide production. He *et al.* (2009) analysed the syngas production from the catalytic gasification of waste polyethylene; the study consisted of steam gasification of waste polyethylene using Al_2O_3 as catalyst in fixed bed reactor.

Gas compositions were studied at different temperatures: higher temperatures increased the CO and H2along with significant decreases in the methane production. The lower heating value of syngas decreased when temperature was increased. Mastral *et al*. (2003) carried out experiments to analyse the gas yield composition from pyrolysis and gasification processes performed at temperatures higher than 700˚C. Air was used as a gasifying medium. The CO yield increased with temperature and water shift reactions. The yield of H_2increased at higher temperatures and methane was too strongly influenced by high

temperatures.

2.2 Pyrolysis

Pyrolysis is a thermochemical decomposition of organic materials at elevated temperature in the absence of oxygen. Pyrolysis typically occurs under pressure and at operating temperatures above 340˚C (Sajid *et al.,* 2010). In general, pyrolysis of organic substances produces gas and liquid products while leaving solid residue richer in carbon contents. Pyrolysis of waste plastic is one of the routes to waste minimisation that has been attracting attention in recent years. The products of pyrolysis have considerably reduced viscosity which can be used either as fuel directly or as feedstock for refineries. Pyrolysis transfers large amounts of heat to materials in the absence of oxygen to break them down into simple compounds. Pyrolysis has been investigated previously for plastic recycling just to produce fuel but without any effort to separate assorted plastics for chemical value. In the subsequent section, previous research projects and reports that have been introduced in the areas of pyrolysis and gasification of plastics will be discussed.

2.2.1 Plastic pyrolysis review

Hojo Unity Company has developed a recycling system and apparatus that can liquefy plastics, turning it into fuel oils (Hironari *et al.,* 2005). The process started by feeding plastics of different types to the pyrolysis oven. In the oven, plastics were melted and evaporated at 350˚C to 400˚C, as at that temperature the heavy hydrocarbon molecules were decomposed to lighter molecules. The gas was condensed and then cooled down using air and water. This process provided recovered fuel from a wide range of waste, not only plastics.

During the process, the plastics were melted and evaporated, then condensed, thereby extracting the energy contained in the carbonaceous material. When catalyzers were used to convince the reaction, the decomposition of the raw materials was much easier and quicker. It has been noticed also that the output products differ according to the raw plastic used. The total products yielded were 30 to 40% wt of the raw plastics. According to the reaction nature 100% from polyethylene PE and PP, PS gave 70 to 90% liquid fuel, 3 to 6%, and non-condensable gas, 7 to 14% solid residue. When waste plastics were mixed with wood, paper and metal, the percentage of valuable recovery decreased and solid residue increased, and when water was contained in the waste, the report recommended that it is better to vaporise it in an early stage. For the safety of the plant, pressure management was considered a very important factor, especially in gasifier design. The pressure was kept under 100 Pa all the time in order to prevent air from leaking into the gasifier. The study indicated that the gasifier was built out of steel because steel can resist corrosion. The

metal catalysers used were Nickel, Copper and ceramic in the shape of punched plate or wire mesh type. The pyrolysis process gave different products depending on the raw materials that fed to the gasifier. The temperature of the heating oven was measured using thermometers placed in the oven space. It was concluded that the time required for the pyrolysis must be taken into consideration from the moment the raw materials were put in the gasifier till the emission of gas stopped.

Recycling of plastic waste produced by industries and cities has been a major concern in both developed and developing countries. Previously, waste plastics were recycled in several ways: mechanically transformed into construction materials or low quality resin, or converted into palletised fuel. But these methods of recycling are not environmentally friendly as these pellets generate too much heat and unfavourable emissions accompanied with high hydrocarbons. The new plastic recycling system constructed by Hojo Unity Company has the ability to recover 80 to 90% fuel from waste plastics by pyrolysis and a liquefaction process. The recovered oil is a valuable alternative fuel and can be used in boilers and diesel engines.

Kiran *et al.* (2000) have investigated thermal degradation of plastic waste using the pyrolysis methodology, and thermo gravimetric analysis has been applied as well to determine decomposition mechanisms and kinetics. The experiment was implemented at low temperature and was carried out in a fixed bed reactor. The products obtained from the process depended on the temperature range, residence time and feeding arrangement. Polyethylene (PE) was used with 13mm diameter and polystyrene (PS) with a 5mm size. Samples of 5 grams were heated to a temperature of 600˚C at a heating rate of 5C minutes and then held by the system for15 minutes and left to cool down for two hours. The pyrolysis of (PE) then gave green wax and gas, and the pyrolysis of (PS) gave brown coloured oil collected in the condenser. At a ratio of 20:80, 50:50, and 80:20 of PE:PS, the oil production decreased linearly with the increase in the PE content of the feed but total gas production increased. The mixing ratio of PE and PS had little effect on the residual char. In the final yield results, PS gave higher liquid yields than PE. Waste PE yields were 37% styrene monomer and toluene. Naphthalene and exylene PE pyrolysis process also yielded propenylbenzen and butenylbenzen. At the end of the experiment, it was concluded that the gas production in the case of PE was higher than that in PS.

In a fast pyrolysis of plastic waste conducted by Scott *et al.* (1990), three of the most common polymers - polyvinyl chloride, polystyrene, and polyethylene - were selected for the tests. Pyrolysis of polyvinyl chloride (PVC) was conducted at 520˚C. HCL was the main gaseous products and its yield was about 99% of the total output. Other liquids and gases

were difficult to identify. Then the experiment stopped because of the corrosion of the reactor, while the pyrolysis of polystyrene was performed at three different temperatures: 532˚C, 651˚C, and 708˚C. The main product in all cases was styrene. The other products were toluene and ethylbenzene. The pyrolysis of polyethylene yielded at temperature >700˚C gas containing ethylene, propylene, butyene and some other light hydrocarbons. A pyrolysis gasification process was performed on refused plastic fuel (RPF) to maximise the fuel gas H_2. Various catalysts and steam were added to the reactor. The maximum fuel gas yielded was 92.6% from RPF and it was attained when Mg and Fe_2O_3 had been used as catalyst. In addition, the temperature always had a significant influence during the reaction regardless of the presence of catalysts.

Stefan (2006) proposed a two-step process to produce hydrogen from plastics. The first step was pyrolysis of the plastics and the second, catalytic steam reforming of the paralysed gases and vapours. The report proposed an integrated process in which the volatile product of plastic pyrolysis will be used as feedstock for catalytic steam reforming, and a microscale reactor system was interfaced with molecular beam mass spectrometer.

A fluidised bed with 120 grams of sand was used, operated at 600˚C to 700˚C; hot steam flowing at 180 to 240 gram per hour (g/h) was used as fluidising gas. The tests were conducted on several types of plastics: polyethylene, polypropylene, polystyrene and polyethylene terephalate (PET). The yielded gas composition remained unchanged but hydrogen exceeded 70% of the total volume of the yielded gas and 92% of the carbon that was contained in the polypropylene converted to carbon oxide. The temperature change had no visible influence on the produced gas during the experiment; therefore, pyrolysis of polypropylene at 600˚C produced hydrocarbons that can be reformed.

The hydrogen produced in this experiment was 34g per 100g polypropylene, and the maximum amount of hydrogen produced was 42.9g per 100g propylene. At 650˚C as temperature of pyrolysis zone and 800˚C as temperature of reforming zone, the hydrogen production from polyethylene was 80% of the stoichiometric, and0.5 gram per hour (g/h) hydrogen was produced during the pyrolysis; reforming of 60 gram per hour (g/h) of polypropylene and 14.3 gram per hour (g/h) was also produced during pyrolysis.

Gasification of post-consumer municipal solid plastic waste for hydrogen production has been reported by Chunfei *et al.*(2009). In this research, the pyrolysis gasification process was investigated using a two-stage catalytic steam reaction to produce hydrogen gas. The process depended on three parameters: 1) catalyst to plastic ratio, 2) gasification temperature, and 3) water injection rate. Electron scanned microscopy (ESM) and temperature programmed oxidation (TPO) were used for the analysis. When gasification

temperature and water injection rate increased, the hydrogen production also increased. The study indicated that the coke formation decreased due to the use of catalysts, but the formation of coke was maximised at 700˚Cand a water injection rate of 4.74 grams per hour. High density polyethylene and polyethylene terephthalate were used in this experiment. At a certain amount of catalysts, production of hydrogen gas was significantly increased, but at the same time, when catalysts to plastic ratio increased, there were no considerable changes in the gas yielded; however, the amount of coke decreased. The amount of the product yielded increased when the gasification temperature increased, but there was no significant change in hydrogen production at the beginning. When water injection rate increased, the total gas yielded increased as well. The total gas yielded increased with no influence of hydrogen production; at the same time, when CO_2 concentration increased, the hydrogen production has also increased. Table 2.1 summarises the gasification and pyrolysis review.

Table 2.1: Literature review of gasification and pyrolysis processes

Material	Reaction type	Temperature	Yields	Author
PE, PP, PS	Two stage reaction	750˚C	Methan, ethylene, propylene	Tohiro and yoshika, 2000
Waste Plastic	Entrained flow	1600˚C	2.4MJ lower heating value gases	Takatoshi et al. 2001
Waste electronics	-	1200˚C	-	Takashi yamawaki, 2003
PP	Bed reaction	-	-	Jesu *et al*. 2008
Raw plastic waste	Bed reaction	1200 - 2000˚C	CO, H_2	CPIAEIC, 2004
PE, PS	Steam reforming	1023k	CO, CO_2, H_2,CH_4	Tsuji and Hayatama, 2007
Municipal plastic waste	Steam reforming gasification	-	CO, H_2	Wu and Williams, 2010
PE	Steam reforming gasification	700˚C	CO, H_2, CH_4	Mastral *et al*. 2003
Pyrolysis review				
PE, PP, PS	-	350-400˚C	liquid fuel	Hironari *et al*. 2005
PE, PS	Fixed bed reaction	600˚C	Styrene monomer, toluene, naphthalene and exylene	Kiran *et al*. 2000
PVC, PS, PE	-	520˚C	Styrene, toluene , ethylbenzene	Scott*et al*. 1990
PE, PP, PS,PET	Steam reforming	600˚C to 700˚C	CO, CO_2, H_2	Stefan *et al*. 2006
HDPE, PET	Catalytic steam pyrolysis gasification	700˚C	H_2	Chufei *et al*. 2009

Wenyi (2010) studied the effects of gasification temperature, pressure, and steam-to-fuel ratio on a biomass gasification process. The model was an isothermal model with no pressure loss. It was reported that an increase in steam-to-fuel ratio increased hydrogen yield while an increase in temperature or pressure led to decrease of hydrogen production. Tables 2.2, 2.3 and 2.4 include the concluded results.

Table 2.2: Temperature property (Zhong, 2010)

Material	Particle size	Experimental conditions	Temperature range (˚C)	yields			
				H_2	CH_4	CO	CO_2
Plastic waste	5 mm	Steam gasification, N_2 used as carrier gas	600 – 900	H_2, CH_4, CO, CO_2			
PE	5 mm	Steam catalytic gasification	700 - 900	H_2, CH_4, CO, CO_2			
PP	2 mm	Steam catalytic gasification, N_2 used as carrier gas	600 - 900	H_2, CH_4, CO, CO_2			
PS	2 mm	Steam catalytic gasification, N_2 used as carrier gas	800 - 850	H_2, CH_4			
PP	2 mm	Steam catalytic gasification, N_2 used as carrier gas	800 - 850	H_2, CH_4			
HDPE	2 mm	Steam catalytic gasification, N_2 used as carrier gas	800 - 850	H_2, CH_4			
HDPE	0.225 mm	Air and N_2 were used.	640 - 850	H_2, CH_4, CO, CO_2			

Table 2.3: Equivalent ratio (Zhong, 2010)

Material	Particle size	Experimental condition	Equivalence ratio range	yields			
				H_2	CH_4	CO	CO_2
`PS	2 mm	Steam catalytic gasification, N_2 used as carrier gas	0.1 – 0.4	H_2, CH_4, CO, CO_2			
PP	2 mm	Steam catalytic gasification, N_2 used as carrier gas	0.1 – 0.4	H_2, CH_4, CO, CO_2			
HDPE	2 mm	Steam catalytic gasification, N_2 used as carrier gas	0.1 – 0.4	H2, CH4, CO, CO2			
PP	2 mm	Air gasification	0.2 – 0.45	H_2, CH_4, CO, CO_2			

Table 2.4: Steam to fuel ratio (Zhong, 2010)

Material	Particle size	Experimental condition	Steam to fuel ratio range	Yields			
				H_2	CH_4	CO	CO_2
`PP	2 mm	Steam catalytic gasification, N_2 used as carrier gas	1.9 – 14.2	H_2, CH_4, CO, CO_2			
PS	2 mm	Steam catalytic gasification, N_2 used as carrier gas	1.9 – 14.2	H_2, CH_4, CO, CO_2			
PP	2 mm	Steam catalytic gasification, N_2 used as carrier gas	1.9 – 14.2	H2, CH4, CO, CO2			
HDPE	2 mm	Steam catalytic gasification, N_2 used as carrier gas	1.9 – 14.2	H_2, CH_4, CO, CO_2			
Waste plastic	5 mm	Steam catalytic gasification, N_2 used as carrier gas	1.9 – 14.2	H_2, CH_4, CO, CO_2			

2.3 Disposal of plastics

2.3.1 Incineration

To incinerate a consignment of MSW is to convert it to an ash having about a tenth of its original volume. The ash is abundant with a strong propensity to adhesion and to plant surfaces which soon corrode as a result. Gilpin *et al*. (2003) have also defined incineration as one of the waste management strategies where municipal solid waste is burned, including plastics, and thereafter hazardous substances may be released into the atmosphere. The most important function of the incineration is destruction of microorganisms. Incineration of MSW normally results in carbon dioxide release. Such wastes as paper and cardboard, if taken to landfills, start to release methane after decomposing over time. It is also well known that methane is a much more powerful greenhouse gas than carbon dioxide. Figure 2.5 shows the emission of powerful greenhouse gases into the atmosphere.

Figure 2.5: Incineration reactors (LAW, 2002)

2.3.2 Landfill

Landfill is a piece of land set for the purpose of disposal of solid waste, either municipal trash, such as waste coming from homes, or hazardous such as toxic chemicals. As a consequence of disposing plastics in landfills, considerable amounts of end-of-life plastics have accumulated in landfills resulting in both waste management issues and environmental damage (Barnes *et al.,* 2009; Gregory, 2009; Oehlmann *et al.*, 2009).

Hazardous waste refers to any material that may cause risk to health, safety, or property, especially those materials that are toxic, corrosive, reactive or ignitable (Fred, 1994). The amount of MSW generated plays an important role in health effects on human life, especially if all amounts generated went to landfill sites and incinerators. Jones, (2010) represented reviews on MSW amounts generated in some countries, as shown in table 2.4.

Detrimental health effects from exposure to hazardous waste can include cancer, birth defects and genetic mutations. Exposure to harmful chemicals can come several sources:

Air: Toxic chemicals from the soil can be vaporised in areas such as basements, causing high concentrations of hazardous chemicals gases in homes (Fred, 1994).

Soil: If a former landfill or waste site is developed as commercial or residential property without going through proper abatement or remediation measures, soil can remain contaminated long after waste dumping has ceased. Brown *et al.* (1988) have indicated that harmful chemicals may be absorbed through the skin after contact with contaminated soil,

vegetables and other edible plants grown in such soil that absorbs chemicals. Waste management companies use incinerators or landfills to settle the waste. Landfills are mostly used to settle the waste into the ground by compressing the materials that cannot be recycled or burned or degraded. Such materials have proven to be hazardous to our health as well as to our environment. Landfill sites need to be well designed and well-planned sites; therefore, the implementation of continuous monitoring is essential. Decompressed solid waste, such as plastics buried under ground, do not get decompressed; after a site has been closed, this will create significantly more hazardous problems for the environment, land, water, air and human beings.

Water: if harmful chemicals are present in the soil surrounding a water supply, these chemicals can seep into the water supply and cause harmful effects, even in miniscule amounts. The U.S Environmental protection agency (2011) estimated that between 0.1% and 0.4% of usable surface aquifers are contaminated by industrial impoundments and landfills. Dumps and landfills are a threat to water supplies when water percolates through waste, picking up a variety of substances such as metals, minerals, organic chemicals, bacterial viruses, explosives, flammables and other toxic materials, as the water then becomes contaminated (Brown *et al.*,1988). Therefore, according to Alfred *et al.* (2012), the negative impact of landfills on both human health and the environment can be concluded as follows:

- Contamination of ground and surface water
- Emission of methane and VOCs (Volatile organic Compounds)
- Dumping and littering beside landfill will increase;
- Noise due to truck traffic
- Impaired view
- Decreased property values

Table 2.4: MSW places and amounts (Jones, 2010)

Place	**Amount of MSW**
London, Ontario	267000 tones in 2006
Kumasi, Ghana	365000 tones in 2006
China	180 million tones expected for 2010
UK	34.8 million tones in 2007/2008
USA	190 million tones in 2009
Australia	43.8 million tones in 2006/2007
South West England	522 kg per resident in 2001

2.4 Plastic as feedstock

Plastics in general, particularly the polyolefins, have high calorific value and its chemical contents are carbon and hydrogen (Stefan *et al.,* 2006). Thus plastic waste can be a very good candidate for the gasification process. But the plastic waste needs to be resized from common large sizes to about 5cm or less in diameter, so that the feeding process can run smoothly. The gasification of high density polyethylene normally produces carbon monoxide and hydrogen. These materials can be used to produce some other chemicals such as ethylene from which the polyethylene is produced. South Africa relies on coal to generate electricity by burning of the coal. Gasifying waste plastics using good conversion efficiency could provide more benefits in terms of reductions of greenhouse gas emissions that are much better than mechanical recycling of plastic. Plastics comprise a relatively small portion of municipal solid waste stream, generally 8 to 11% by weight. Even with this percentage, plastic waste can be collected to operate small 5-megawatt gasifiers for producing electricity for local grid. The U.S. Department of Energy (2010) studied a process to generate five megawatts of electricity at an efficiency of 37%. The average of the process requires a feedstock delivering 48.65 megajoules of energy per hour. As an example, high density polyethylene (HDPE) has a calorific value of 43.5 MJ kilograms. Therefore, the operation of a 5-megawatt facility would require 1118 kilograms of HDPE per hour, 26.8 tons per day or 9800 tons per year. Detailed analysis of the plastics stream in Canada shows that 58% of the plastics are considered to be recoverable while the remaining 42% are said to be unrecoverable because the materials have been too badly contaminated by or mixed with other garbage. The average per capita generation of municipal solid waste as recently measured in five communities across Canada is 350 kilograms. On this basis, a region having a population of just over 1 million could provide plastic feed to a 5-megawatt gasifier for generating electricity. A 5-megawatt generator is sufficient to supply the annual electrical needs of approximately 4600 Canadian homes.

2.5 Recycling plastics

Recycling is a process that allows waste to be reintroduced into the consumption cycle, though generally the recycled products are of lower quality than the original ones. The recycling process can only be applied when the amount of energy consumed in therecycling process is lower than the energy required for the production of new materials. There are two different approaches for recycling plastics: mechanical and feedstock recycling. In mechanical recycling, plastics are recycled back to polymers, whereas in feedstock recycling, plastic wastes are transformed into chemicals or fuel (Jefferson *et al.*, 2004). Plastic materials can also be formed into different shapes depending on the process of

thermoforming, such as extrusion, molding, coasting or spinning. Modern plastics have some desirable characteristics such as excellent thermal properties and resistance to acids. Monomers can be put in series to form polymers, and monomers will have certain characteristics depending on the configuration and the polymerisation degree. According to Figure 2.6, polymers are divided into three types:

- Linear polymer
- Branched polymer
- Cross linked polymer

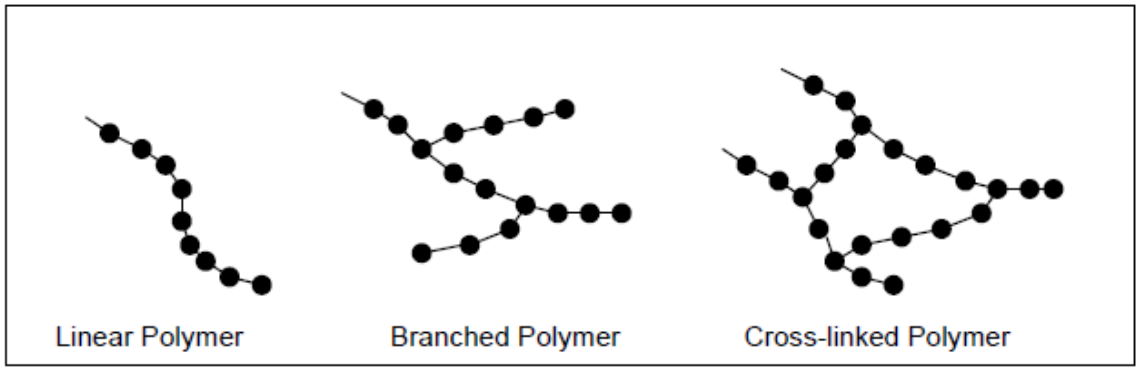

Figure 2.6: Polymers structure (Aguado, 1999)

2.5.1 Mechanical recycling

Mechanical or material recycling of plastics involves a number of treatments and operations; for example, mechanical recycling may involve separation of plastics by resin, washing to remove dirt and contaminants, grinding and crushing to reduce the plastic particle size, extrusion by heat and processing into new plastic goods. Thermosets cannot be remolded by the effect of heat; therefore, this type of recycling is mainly restricted to thermoplastics. Mechanical recycling is limited by the compatibility between the different types of polymers when mixed (Jefferson *et al.,* 2004). Presence of low amounts of PVC in recycled PET strongly reduces the commercial value of the latter due to the possible release of hydrogen chloride during the PET processing. This problem is enhanced by the fact that PVC and PET are difficult to separate from other plastic waste. Another difficulty with mechanical recycling is the presence in plastic wastes of products made of the same resin, but with different colors, which usually impart an undesirable gray color to the recycled plastic. Factors such as temperature, ultraviolet radiation, oxygen and ozone can affect polymers and make them suffer certain degradation. The progressive in length and partial oxidation of the polymer chains results from the degradation; therefore, recycled polymers necessarily

have less value than the virgin ones. To achieve a higher quality of recycling, plastics must be separated by resin prior to the remolding step.

2.5.2 Feedstock recycling

The limitation of mechanical recycling encourages researchers to investigate new viable and potential recycling methods such feedstock. According to Fisher (2003), feedstock recycling applies when the polymer is decomposed to its basic chemical molecules. An advantage of feedstock recycling is the recovering of the petrochemical constituents of the polymer. It is also called 'chemical recycling' as this recycling process is based on thermal degradation of polymers. Chemical agents and catalysts are also used to yield different products ranging from the starting monomer to mixers of compounds (mainly hydrocarbons) with possible applications as a source of chemicals or fuels. The products yielded from the decomposition of plastics are similar to those of their counterparts prepared by conventional methods. Feedstock recycling process has been classified to the following:

- Thermal decomposition of polymers by an inert atmosphere.
- Catalytic cracking and reforming in which the polymer chains are broken down by the effect of catalyst, promoting cleavage reactions.
- Hydrogenation where the polymer is degraded by the combined action of heat, hydrogen and, in many cases, catalysts. There are three main factors determining the profitability of these alternatives: 1) the degree of separation required in the raw wastes; 2) the value of the product obtained; and 3) the capital investment in the processing facilities.

In all of the previous feedstock methods, plastic wastes need some pre-treatment and separation operations, which inflate into additional costs.

2.6 Recyclable plastics

The most common recyclable plastics are Polyethylene, polypropylene, polystyrene, polyvinyl chloride and polyethylene terephthalate.

2.6.1 Energy recovery

Plastics are materials of high calorific value; therefore, plastic waste greatly contributes to the energy produced in incineration plants. It can also be used as fuels in a number of applications such as power plants and industrial furnaces. However, the relationship between PVC content in the waste stream and dioxin concentration has not been clearly demonstrated. It seems that the formation of dioxins depends mainly on the incineration conditions rather than on the waste composition; therefore, only the non-recyclable and non-energy valuable wastes can be disposed of in landfills. In general, however, most of

the plastic waste is still disposed of in landfills. In fact, rapid growth in feedstock recycling has been observed in recent years in developed countries (Cornelia *et al.,* 2007). There are several reasons for the lack of recycling of plastic waste, especially compared to other solid materials such as paper, cardboard and glass. A number of problems rise from the large variety of chemical compositions and properties of the different types of plastics which escalate the difficulty of establishing a general recycling procedure.

In addition, plastic wastes are mainly contained in MSW mixed with other solids; consequently, costly and complex separation treatments must be applied to obtain a plastic waste stream having a more or less homogeneous composition. The low density of most plastics makes it necessary to deal with large volumes of waste in order to produce a given mass of recycled materials.

2.6.2 Economic and environmental impact of plastic wastes

From an economic point of view, plastic can be an important source of valuable chemicals such as hydrocarbon. It also has calorific value similar to that of fuel and higher than that of coal deeming plastic a valuable fuel. A study by Ojolo (2012) showed that plastic wastes represent a significant environmental impact due to the following facts:

- Because of their resistance to degradation, plastic materials exist for an extremely long time when disposed of in landfills.
- Some plastics have been successfully synthesized.
- Slow degradation of plastics is responsible for progressive reduction of landfill capacity.
- The risks of accidental fires with highly polluting emissions increased in landfill containing large amount of plastics.
- Plastic waste accounts for about 25% of all solid waste accumulated in landfills.
- Plastic waste contains additives such as fillers, stabilizers, plasticizers, reinforcing, agents, and colorants.

Both organic and inorganic compounds are added to plastics to improve and modify their properties, containing, in many cases, heavy metals. Thus, according to the United States Environmental Protection Agency (2010), plastics contribute 28% of all cadmium present in MSW and about 2% of all lead. As a consequence of their low density, plastics cause a greater visual impact on disposal than many other materials. Similarly the light weight of plastic waste greatly increases collection and transportation cost. For example, to recover one ton of used plastic, it is necessary to collect about 20,000 plastic bottles. Because plastic wastes are found in MSW mixed with other solid wastes, complex and costly separation steps are required to produce used plastic stream of relatively high purity.

Despite all these problems, substitution of plastics by other materials is not environmentally sound. Energy requirements for polyethylene grocery sacks are 20 to 40% lower than paper, while generating about 75% less solid waste, 65% less atmospheric emissions and 90% less waterborne waste. Replacement of about 200 to 300 kg of conventional materials in modern cars by plastics leads to reduction in the fuel consumption by 750 litres over a lifespan of 150 000 km if the whole automotive sector of western Europe is considered. This reduction would cause a decrease in the oil consumption of 12 million tons and in CO_2 emissions of 30 million tons each year (Akitsugu, 2004).

2.7 Power generation using gasification

Widely used technology that produces power from gasification, known as integrated gasification combined cycle (IGCC), is a technology that combines gas turbine with steam turbine to generate electricity (Androutsopoulos, 2001). IGCC first combusts the syngas in the gas turbine to produce electric power; at the same time, since the reaction is exothermic, the resultant heat from the reaction is then converted to steam, collected and fed to the steam turbine in order to generate more electricity.

2.7.1 Economics of gasification

Compared to the conventional combustion systems gasification technology in terms of operating cost, gasification is a far lower cost because gasification can use veryinexpensive feedstock input (plastic waste) and convert them to high value yields. Plastic gasification systems can be sustainable. Ultimate sustainability of plastics gasification is, then, achieved by number of factors:

- Maintaining certain level of plastic waste as input;
- Reducing the energy input to the gasification systems; and
- Reducing the external impacts on ecosystems

Gasification technologies according to Androutsopoulos (2001) have opened newhorizons on extracting valuable energy from the waste while simultaneously reducing disposal impact. Gasification economic benefits can therefore be concluded as follows:

- The gasification products (syngas) are marketable.
- Gasification units require less emission control equipment because they generate fewer emissions, further reducing plant operating costs.
- Investment in gasification injects capital into the economy (building large scale

plants using domestic labor and suppliers) creating domestic jobs.

2.8 Infrared heating of plastics

The amount of radiant energy emitted from a heat source is proportional to the surface temperature and the emissivity of the material as described by the Stefan Boltzmann's law. Commonly available infrared sources include heat lamps, quartz lamps, quartz tubes, metal sheath elements, ceramic elements, and ceramic, glass or metal panels. Each of these sources has unique physical characteristics, operating temperature ranges and peak energy wavelengths. Most infrared heaters consist of lamps emitting one specific peak wavelength corresponding to fixed surface temperature. The type of IR emitter and control of the accurate wavelength should be considered for optimal processing. Bishof (1990) presented one example of a product: a new infrared curing system especially in-vented for manufacturing technology of surface mounted device (SMDs). Accurate wave-length control achieved by adjusting the source temperature validated that the lower side components could be kept below 80˚C while the board surface was cured up to 120˚C. It was noted that tight control of IR wavelengths allowed infrared radiation to emit the spectrum where a material had relatively high absorptive. Simulation of quartz tube used in the thermoforming process has been investigated by Brogan *et al.* (1996), with the conclusion from the experiment that infrared heaters can accurately be used in thermoforming of plastics. Sweeney *et al.* (1995) investigated a reduction of infrared heating cycle time in processing of thermoplastic by increasing the speed of the infrared heating cycle. Some process parameters had been varied to obtain optimum process conditions, such as heater power, heater to composite distance and composite thickness. Thermocouples were fitted to a number of heaters so that heater temperature versus heater power curves was obtained. The output from the heater thermocouples was sent to a 32 channel data acquisition board which is connected to a computer, where standard programme converts to millivolt output. It was been recommended that heater to composite distance can be varied according to the oven design.

Radiant heating of plastic panels has been investigated by Sweeney *et al.* (1995). In this study, a simple radiation model was used to determine the one-dimensional temperature distribution through the absorber. Results were presented comparing the model against experiment. No significant work, though, has been published on optimisation of the IR heating of plastic panels. Scobbo (1990) determined optimum heating and forming times for thermoforming of a panel of graphite fibre reinforced composite. Results presented showed the transient temperature profiles through the thickness for one specimen thickness of 2mm placed in a thermoforming oven, set at its maximum temperature of 538˚C.

A mathematical model which determines the heat transfer to thermoplastic piece was carried out by Cunnigham*et al*. (1996). Within the project there were three heating techniques: radiant heating, contact heating, and convection heating. In the case of radiation, an enclosure analysis was used to calculate the radiation heat exchange between all surfaces within the enclosure. Their analysis assumes that varying the set-up of a bank of heaters had an effect on product being heated. The model successfully predicted heat up curves for IR vacuum, contact and convection heating. Lebaudy and Grenet (2010), in a study of heating simulation of multilayer preform have used quartz radiators as infrared radiation sources in plastic processing. It was noticed that change in temperature leads to change in the distribution of the radiation intensity with wavelength. The Lambert Bouguer law was used to describe the spectral absorption characteristics of the plastic. The study found that it was advantageous to describe the absorption behavior in terms of penetration depth. In an experiment conducted by Monteix *et al.* (2001), a control volume model was used to compute the radiative heat transfer during the infrared heating stage. In this method the temperature balance including radiative transfer (thermal power absorbed by the polymeric sheet from the infrared heaters) was integrated over each control volume and time. Lloyd *et al.* (2003) have discussed the characterisation of the radiant emitters used in the food processing; a comparison of the radiant emissions from short, medium and long wavelength as thermal radiant emitter systems has been done. The measurements included heat flux intensity, emitter surface temperature and spectral wavelength distribution. Heat flux measurements were found to be highly dependent on the incident angle and the distance from the emitter facing. The maximum heat flux measured was 5.4w/$m^{2.}$ Emitter surface temperature measurements showed that short wavelength radiant systems had the highest surface temperature.

Sakai *et al.* (1994) and Hebbar *et al.* (2004) have applied the infrared radiation on drying applications, proving its validity for the application in addition to the low cost application. It has some advantages such as low investment cost, easy assembly, high rating of heating and drying, uniform temperature of the product during drying, high process control and clean working conditions (Sandu, 1986). infrared also offers many advantages over conventional drying such as a decreased drying time, high energy efficiency, high finished products, uniform temperature in the products while drying, a reduced necessity for air flow across the product (Sharma *et al.,* 2005). Combining far infrared and convective drying of barley, Afzal *et al.* (1999) discovered that the drying process implemented via infrared and hot air had a greater synergic effect as compared to drying via infrared and hot air alone. Various models for describing infrared drying of rough rice have been developed by Hanzawa (1994), Abe *et al.* (1990) and Cihan *et al*. (2007).

Petterson and Stenstrom (1998) developed a model for an electric infrared paper dryer that included a non-grey radiative heat transfer between the different parts of the infrared heater as well as conduction in reflector material and convective cooling of surfaces. A combined infrared and hot air dryer was developed for drying vegetables by Hebbar *et al.* (2004). Lampinen *et al.* (1991) conducted some studies concerning infrared paper drying with regards to radiative exchange but cautioned that their results were only quantitative due to the assumptions made on temperature that are ambiguous. Petterson (1998), on assumption of temperature, developed a model for which the results and the energy surface balance could not be tallied. Sakuyama *et al.* (1995) used a selective infrared heating of both aluminum oxide heater and a halogen heater as infrared sources to develop a new reflow soldering technique. The aluminum oxide heater radiates intensive infrared rays between 5μm and 8 μm that are readily absorbed by a glass-epoxy substrate, whereas the halogen heater radiates intensive infrared rays between 1μm and 2μm that are readilyabsorbed by the resin used in quad flat packages.

A study by Bolshakov *et al.* (1976) suggested that a maximum transmission of infrared radiation should cover the spectral wavelength of 1.2 μm obtained by analysis of thetransmittance spectrograms of lean pork for deep heating of pork. A two-stage frying process consisted of the first stage, to aim surface heat transfer by radiant flux with a maximum of 3.5μm to 3.8μm, and the second stage, to achieve greater penetration of heat transferby radiant flux with a maximum of 1.04 μm. Higher moisture content and sensory qualityof the products were obtained using combined far infrared and near infrared heaters, compared to the conventional method. A similar study explored by Dangerskog (1979) used two alternative types of infrared radiators for frying equipment: 1) quartz tube heaters whose filament temperature was 2340˚C at 220V rating, corresponding to a maximum of 1.24 μm as near infrared region, and 2) tubular metallic electric heaters at a temperature of 680℃ at 220V, corresponding to a maximum of 3.0 μm as far infrared region.It was observed from the study that both penetration capacity and reflection increased as the wavelength of the radiation decreased, indicating that although the short wave radiation had a higher penetrating capacity than the long wave radiation, the heating effects were almost the same due to body reflection.

CHAPTER THREE

HEAT TRANSFER THEORY

Chapter Three shall introduce the infrared theory and the thermal radiation laws governing the heat transfer mechanisms, as well as the radiation exchange between surfaces in an enclosure.

3.1 Electromagnetic spectrum

Different types of radiation exist within an electromagnetic spectrum. Among them are sunlight, heat, X-rays, radio-waves and Gamma rays. Infrared rays are classed under and described according to their position on the electromagnetic spectrum and their radiations are organised by wavelength or frequency. All electromagnetic waves obey the following general equation:

$$\lambda v = c \qquad (3.1)$$

Where c is the velocity of light, the frequency and is the wavelength. All electromagnetic waves propagate at the velocity of light but are different in frequency and wave length from one another. Figure 3.1 shows the electromagnetic spectrum:

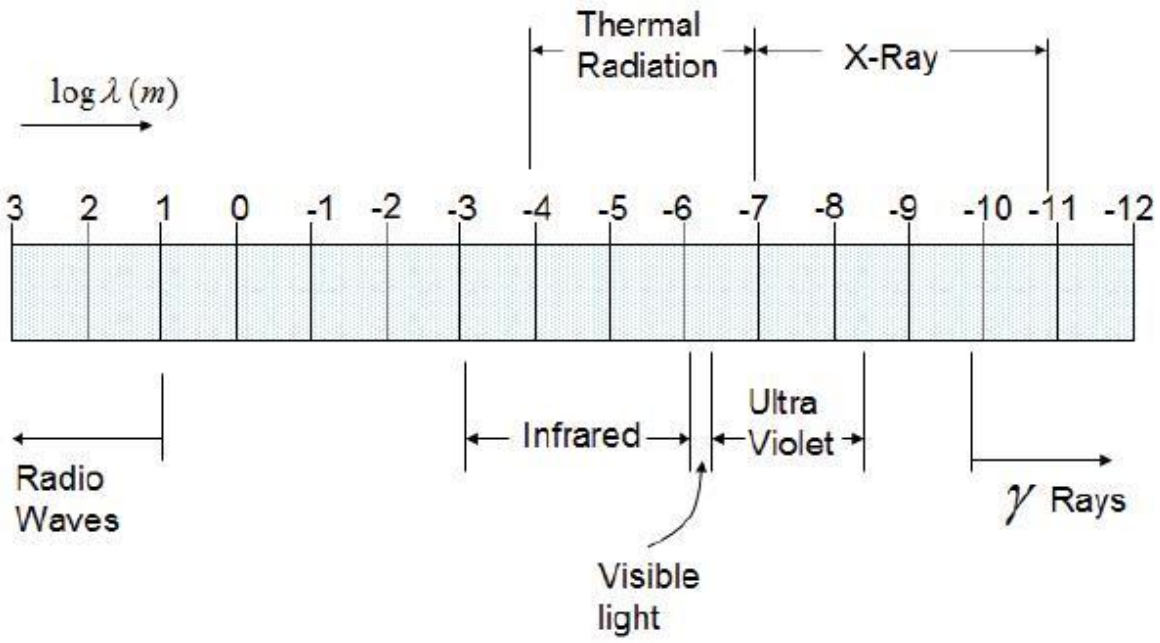

Figure 3.1: Electromagnetic spectrum (Chris, 2009)

2.3 Modes of heat transfer

To determine the temperature distribution in a medium, it is necessary to solve the appropriate form of the heat equation. However, the solution depends on the physical conditions existing at the boundaries of the medium, on whether or not the situation is time dependent, and on conditions existing in the medium at some initial time. With regard to the boundary conditions, there are three kinds commonly encountered in heat transfer. The first kind is the constant surface temperature. This condition is closely approximated, for example, when the surface experiences convection with an extremely high convection coefficient. Such conditions occur with boiling or condensation, and in both instances the surface remains at the temperature of the phase changes process.

The second kind is the constant surface heat flux. The heat flux is related to the temperature gradient at the surface by Fourier's law. This condition could be realised by bonding a thin film or patch electric heater to the surface or by irradiating the surface with heat lamp. A special case of this condition corresponds to perfectly insulated, or adiabatic, surface for which the gradient is zero. If there is symmetry in the temperature distribution, a surface corresponding to the maximum or minimum temperature could also represent an adiabatic surface.

The third kind is convection surface condition. This condition corresponds to the existence of convection heating or cooling at the surface. Heat transfer is the process by which energy moves from a hot source to a cold sink. Heat is transferred via three modes: conduction, convection and radiation (as explained in Table 3.1). Conduction occurs when heat diffuses through a solid or a fluid that is not in motion within molecules and when a temperature gradient exists (Chris, 2009). Convection occurs within molecules of fluid in motion. Radiation occurs when the energy is transmitted without the need of a medium by electromagnetic phenomenon. Heat transfer by thermal radiation takes place in the range of wavelength 1μm to 100μm.

As thermal radiation does not require the use of medium to transfer energy, its use has become the dominant mode of heat transfer in low pressure (Adrian, 2003). The aim of this study is to focus on the far infrared radiation spectrum of the electromagnetic wave.

Table 3.1: Modes of heat transfer

Conduction (via direct contact)	Convection (via fluid)	Radiation (via electromagnetic radiation)
Conduction is the direct flow of heat through a material resulting from physical contact.	Heat transfer between a surface and adjacent fluid (gas, air or liquid) and by the flow of the fluid from one place to another induced by temperature.	No transfer medium is required It is the transfer of thermal energy through matter of space by electromagnetic waves.

3.2.1 Conduction

Conduction is the transfer of heat from material to another at a molecular level. The material may be solid or fluid. Conduction heat transfer occurs when the temperature gradient exists in a medium (Chris, 2009). Fourier's law of heat conduction is expressed in term of heat flux Q, the temperature gradientdT/dx, the area A and the thermal conductivity k:

$$Q = -kA\frac{dT}{dx} \tag{3.2}$$

The temperature gradient$dT/dx$is always negative and the sign shows that the heat flows from high temperature to low temperature and therefore, down the temperature gradient. In addition, the other property that characterizes the heat transfer by conduction is the thermal diffusivity. It describes the capability of a material to transfer thermal energy in relation to it is capability to keep that energy where as the thermal conductivity varies with temperature (Chris Long, 2009). The equation that defines the thermal diffusivity is

$$\alpha = \frac{k}{\rho c} \tag{3.3}$$

Where ρ is the density of material and c is the specific heat capacity.

3.2.2 Convection

Convection heat transfer is the process that is accomplished by motion of fluid. Newton's law of cooling rate expresses the convection mode between a surface and a fluid.

$$Q = h_c A(T_1 - T_2) \tag{3.4}$$

According to the nature of the flow, two ways of conduction can be expressed such as natural convection and forced convection.

3.2.3 Radiation

Radiation heat transfer uses invisible electromagnetic waves from an energy source e.g. heat from the sun. Infrared heaters are radiant heaters that emit radiant energy which

passes through space in the form of electromagnetic waves. Infrared energy does not depend on air for transmission and is converted to heat upon absorption by the work piece. As a result, infrared heaters which produces infrared energy provides for efficient heat transfer without contact between the heat source and the work piece.

All objects above absolute zero temperature radiate infrared energy with warmer objects radiating more energy than cooler objects. Infrared energy radiating from a hot object such as heating element, strikes the surface of a cooler object (work piece), is absorbed and converted to heat energy. Paint drying by radiant heaters is a typical application of infrared heating. The most important principle in infrared heating is that infrared energy radiates from the source in straight lines and does not become heat energy until absorbed by the work product.

Conduction and convection are effective over short distances, whereas radiation can be effective over long distances. For example, the transfer of heat from the surface of the sun to the earth through the vacuum of space occurs exclusively by radiation. Another distinguishing feature between conduction and convection on the one hand and thermal radiation on the other is the difference in their temperature dependencies. For the vast majority of conduction applications heat transfer rates are as well described by Fourier's law

$$q_x = -k\frac{dt}{dx} \tag{3.5}$$

Where$q_x$conducted heat flux in the x direction, T is temperature and k is the thermal conductivity of the medium. Similarly, convective heat flux may usually be calculated from correlation such as:

$$q = h_c(t - t_\infty) \tag{3.6}$$

Where h is known as the convective heat transfer coefficient, and t_∞ is a reference temperature. While k and h may depend on temperature, this dependence is usually not very strong. Thus, for most applications conductive and convective heat transfer rates are linearly proportional to temperature differences. As can be seen, radiative heat transfers is generally proportional to differences in temperature to the fourth or higher power, i.e.

$$q \propto T^4 - T_\infty^4 \tag{3.7}$$

Therefore radiative heat transfer becomes more important with rising temperature levels and may be totally dominant over conduction and convection at very high temperatures.

3.4 Thermal Radiation

Thermal radiation is the rate that energy is transferred from a surface to another by means of electromagnetic waves and unlike conduction and convection heat transfer, thermal radiation does not require the use of a medium between elements. Radiation is also proportional to the difference of temperature to the fourth power.

Infrared radiation is the part of the electromagnetic spectrum that is predominantly responsible for the heating effect of the sun. Infrared radiation as mentioned before can be classified into three ranges such as

- Near-infrared (NIR)
- Mid-infrared (MIR)
- Far-infrared (FIR).

Infrared waves constitute part of the electromagnetic spectrum alongside other waves. The many types of electromagnetic radiation are produced through diverse methods. Gamma rays are produced by nuclear reactions, the bombardment of metals with high energy electrons results in X-rays, microwaves are produced by special types of electron tubes for example klystrons and magnetrons and radio waves by the agitation of certain types crystals or through the flow of alternating current in electric conductors. Of interest in heat transfer is thermal radiation, which is emitted as a results of the vibrational and rotational motions of molecules, atoms and electrons of a substance. Temperature is a measure of the strength of these events at the microscopic level.

Heat transfer application wavelengths between 10^{7}m and 10^{13}m (ultraviolet, visible and infrared) are most important in electrical engineering and will be mainly considered here. The term thermal radiation which will be commonly used to describe the science of heat transfer caused by electromagnetic waves is transferred by electromagnetic waves or photons which may travel over long distance without interacting with a medium thus making it important in vacuum and space applications.

Thermal radiative energy may be viewed as consisting of electromagnetic waves as predicted by electromagnetic wave theory or as consisting of mass less energy photon particles called photons as predicted by quantum mechanics (Modest, 2003). Both concepts are used interchangeably because none completely describe all the radiative phenomena that have been observed.

All electromagnetic waves propagate at the speed of light through any medium. The speed of light depends on the medium through which it travels and it described by the formula:

$$v = \frac{c}{\lambda}$$

Electromagnetic waves travel considerably slower through dielectric, which have refractive indices between 1.4 and 4, and they hardly penetrate at all into electrical conductors (metals). Each wave may be identified either by it is frequency v, wavelength λ, wavenumber **η** and angular frequency ω through the formula:

$$v = \frac{\omega}{2\pi} = \frac{c}{\lambda} = c\boldsymbol{\eta} \tag{3.8}$$

Each wave or photon carries with it an amount or energy ε, determined from quantum mechanics as:

$$\varepsilon = hv \tag{3.9}$$

When heat is transferred to a surface by electromagnetic radiation, incident radiation may be absorbed, transmitted or reflected as shown below:

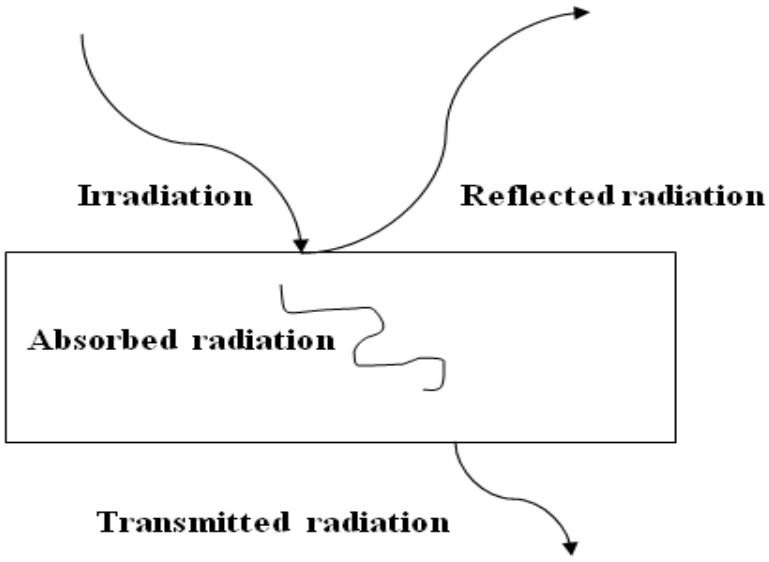

Figure 3.2: Extinction of radiation

3.5 Basic Laws of Heat Transfer

3.5.1 Planck's Law

Planck's law describes the spectral radiance of electromagnetic radiation at all wavelengths emitted in the normal direction from a blackbody at a temperature (T) as a function of frequency (v). The formula is given as:

$$E = h\nu / (e^{h\nu/kt} - 1) \quad (3.10)$$

In order to understand the spectral distribution of infrared radiation from a source, it is imperative to understand Plank's law, as Plank's law gives the spectral radiation from blackbody source. That is a source that emits 100% infrared radiation at a single given temperature. It is important to understand at this point that, in practice, infrared sources are made up of thousands of point sources that are all at different temperatures. Each point of source will have a different spectral distribution and the combination of point of sources will make up the entire spectral distribution. This means only approximation of the spectral distribution using an average surface temperature and emissivity value can be done.

Plank's law curves show that the spectral radiance of the source increases proportionally with the source temperature. The radiant infrared output from the source increases as the temperature of the source increases. The overall infrared emission from a given source is equal to the area under the associated Planck's law curve. By integrating Planck's law at a given temperature with respect to the wavelength, the amount of infrared emission within a range of wavelengths can be calculated. As the temperature of the source increases, the peak wavelength of the source becomes shorter, as seen in Figure 3.3. When the temperature of the source becomes too high, a noticeable amount of energy is emitted from the source as light. Plank's law can be applied to estimate the total amount of radiative heat flux when the specific temperature of the heating element is known. An energy balance to assess the amount of energy emitted from the IR source, proportionally directed through a conveying chamber known as waveguide to the surface of the materials at the receiving end, is known as ‘view factor’. Hence the actual amount of heat flux absorbed by material can be estimated by calculating the total emissive power and view factors from the source to the target.

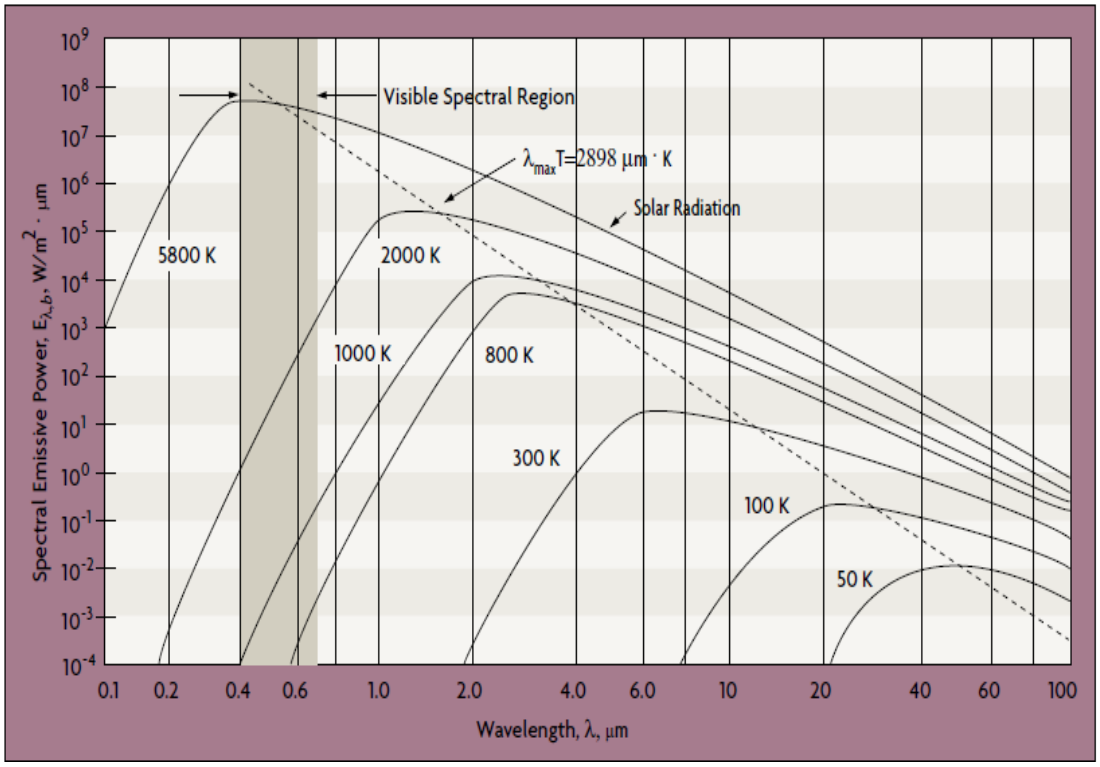

Figure 3.3: Plank's prediction of blackbody (Omega, 1998)

3.4.2 Wien's displacement law

Wien's law states that the wavelength distribution of radiated heat energy from a black-body at any temperature has essentially the same shapes as the distribution at any other temperature, except that each wavelength is displaced, or moved over.

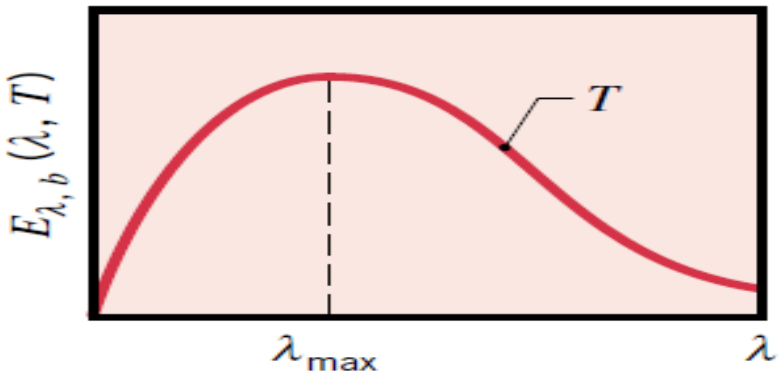

Figure 3.4: Wien's law (Michael, 2003)

Wien's displacement law is the wavelength at which the emissive power$E_{\lambda,b}$ is maximum.

$$\lambda_{max}T = 2897\ \mu m.K \tag{3.11}$$

3.5.3 Stefan Boltzmann Law

Stefan Boltzmann law of radiation states that as the temperature of a heat source is increased, the radiant output increases to the fourth power of its temperature (Shumacher, 1996).

$$E = kT^4 \tag{3.12}$$

3.5 Emissivity

The emissivity of a surface is defined as the ratio of the radiation emitted by a real surface to the ratio of the radiation emitted by a perfectly radiating ideal surface (blackbody). Similar to other food radiative properties, emissivity depends on the wavelength of radiation incident on the food, which in turn depends on the emission characteristics of the source of radiation (emitter). The emissivity at a specified wavelength is called the 'spectral emissivity'. For plant materials such as leaves, for example, the emissivity is typically above 0.97 regarding the radiation source. Wien's displacement law indicates that the peak of the emission decreases with increasing temperature.

$$\lambda_{max}T = 2897.8\ \mu m.k$$

3.6 Emissive power

The radiative heat flux emitted from a surface is called the 'emissive power', E. Electro-magnetic radiation is emitted randomly in all directions continuously by every medium depending on the temperature and property of the material. Total and spectral emissive powers are distinguished, so that:

$$E(T) = \int_0^\infty E_\lambda(T,\lambda)d\lambda \tag{3.13}$$

3.7 Irradiation

Radiation emanates from emission and reflection which occurs at other surface or from surroundings and radiation sources. The term irradiation is a radiative flux that represents the incident radiation which surrounds radiation from all directions.

Spectral radiation is defined as the rate at which radiation of wavelength is incident on a surface, per unit area of the surface and per unit wavelength interval. If the total irradiation represents the rate at which radiation is incident per unit area from all directions and at all wavelengths, which gives:

$$G = \int_0^\infty G_\lambda(\lambda) d\lambda \tag{3.14}$$

3.8 Radiosity

The term 'radiosity' accounts for the radiant energy leaving a surface. The spectral radiosity is defined as the rate at which radiation of wavelength leaves a unit area of the surface, per unit wavelength interval:

$$J_\lambda = E_\lambda + G_{\lambda,ref} \tag{3.15}$$

3.9 Blackbody radiation

A blackbody may be viewed as an object that absorbs completely radiant energy. It is an ideal body that allows all the incident radiation to pass unto it and absorbs all the incident radiation. In other words, it is a perfect absorber as it does not reflect nor transmit energy (Siegel, 1992).

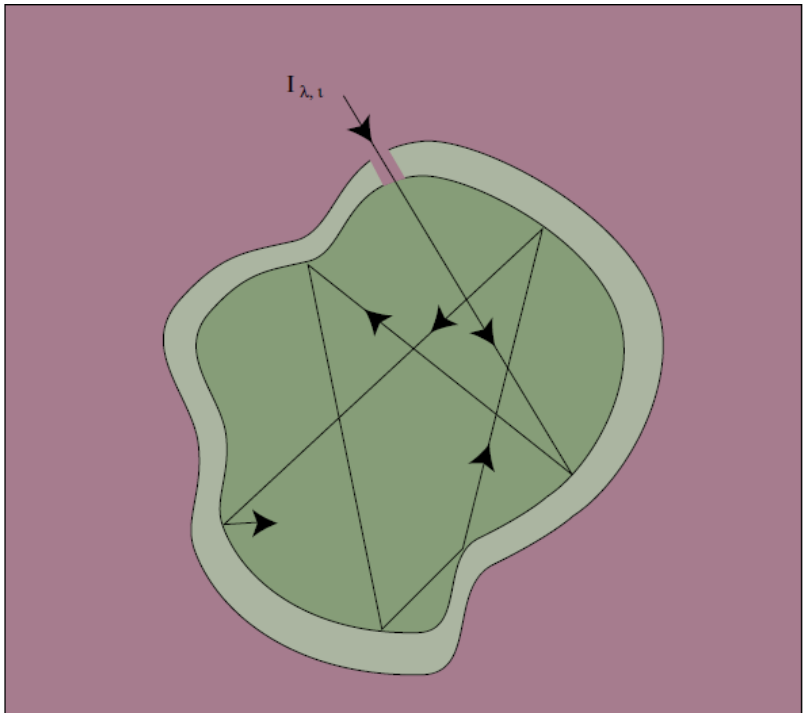

Figure 3.5: An isothermal blackbody cavity (Omega, 1998)

The energy balance within a blackbody can be calculated using incident radiation which may be absorbed, reflected or transmitted. The radiation energy balance expressed in a body is given as follows:

$$\alpha + \tau + r = 1 \tag{3.16}$$

For opaque medium $\tau = 0$, therefore$\alpha + r = 1$.

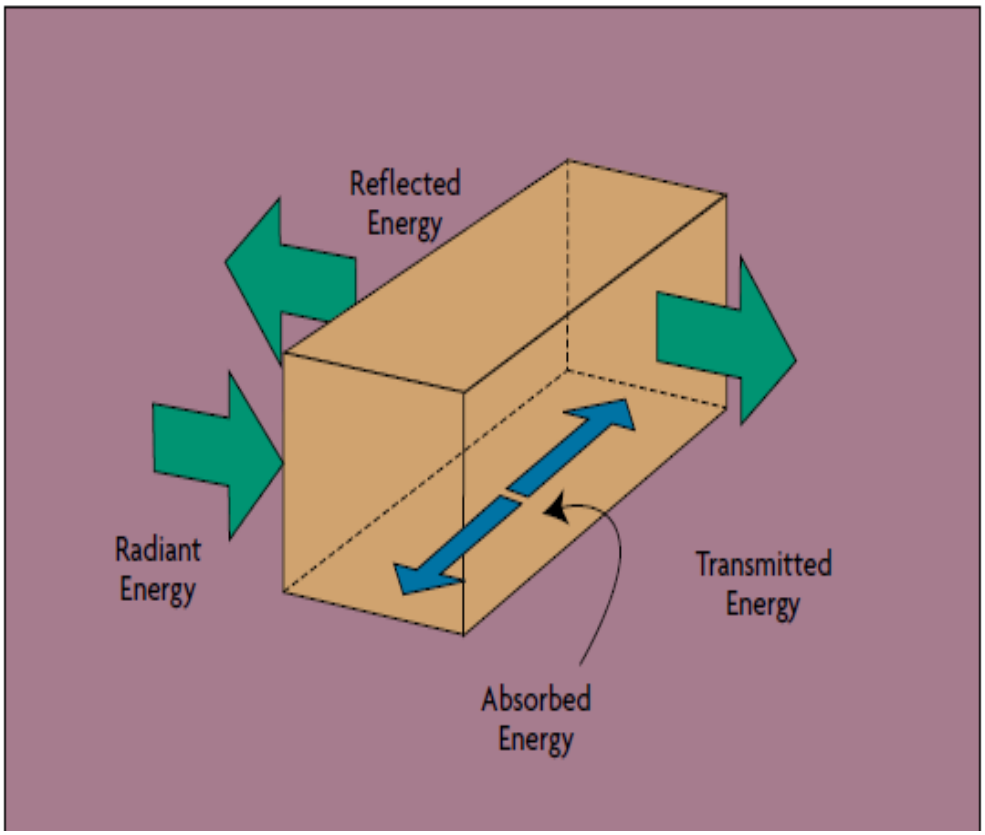

Figure 3.6: Radiation energy balance (Omega, 1998)

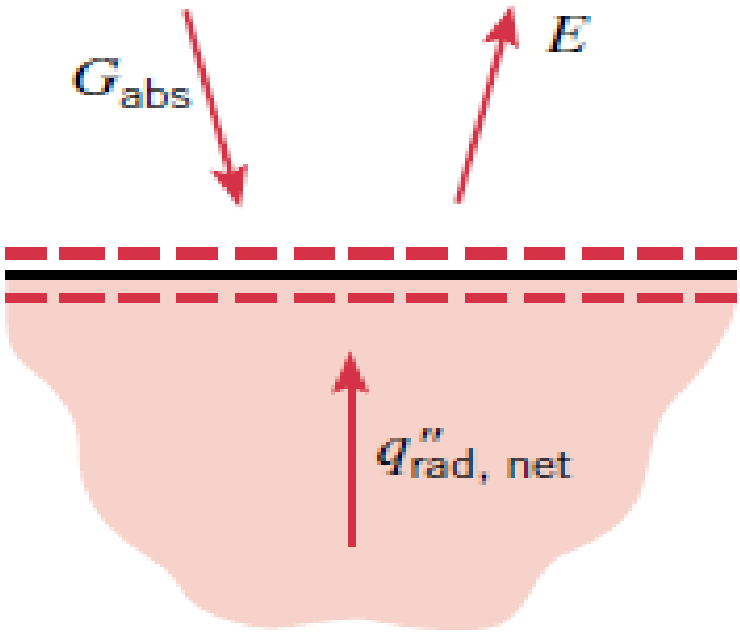

Figure 3.7: Surface energy balance (Michael, 2003)

Then the net radiative flux leaving the surface can be expressed as follows

$$q_{rad,net} = E - G_{abs} \qquad (3.17)$$

3.10 Radiative exchange between surfaces in an enclosure

Radiation leaves a surface due to both direct emission and reflection (radiosity), and experiences absorption and reflection upon reaching a second surface. This depends on the surface geometry and orientation as well as on their radiative properties and temperatures. The geometrical features can be established using the view factor which can also be used to treat black surface exchange.

3.10.1 View factor

The view factor accounts for the geometrical features for the radiation exchange between two surfaces. The view factor F ij is defined as the fraction of the radiation leaving surface i that is intercepted by surface j. For the arbitrarily oriented surfaces Ai and Aj:

$$F_{ij} = \frac{q_{i \to j}}{A_i j_i} \qquad (3.18)$$

Where $q_{i\to j}$is the radiative flux leavingA_i that is intercepted byA_j;$j_i$is the radiosity of surface A_i, which represent the radiative flux leaving A_i in all directions. It is assumed that the surfaces are isothermal, diffuse and have uniform radiosity.

The reciprocity relation for the arbitrarily oriented surface which is a relationship involved in the view factor is recognized as useful in determining one view factor from knowledge of the other and can be written as follows:

$$A_i F_{ij} = A_j F_{ji} \tag{3.19}$$

Whereas for enclosed surfaces, the summation rule can be applied to each of the N surface in the enclosure

$$\sum_{j=1}^{N} F_{ij} = 1 \tag{3.20}$$

This rule follows from the requirement that all radiation leaving surface i must be intercepted by the enclosure surfaces. The term Fij in the summation represents the fraction of the radiation that leaves surface i and is directly intercepted by i. The definition given in Equation 3.20 expressed as the sum of the view factors from surface i of an enclosure to all surfaces in the enclosure, including itself, must equal unity. If a view factor to be determined for certain geometry is not available in the standard tables and charts, the superposition rule is useful. The view factors of known geometries are added or subtracted so as to closely approximate the required geometry. The following Figures 3.8 and 3.9 represent view factors for two plates in different orientations:

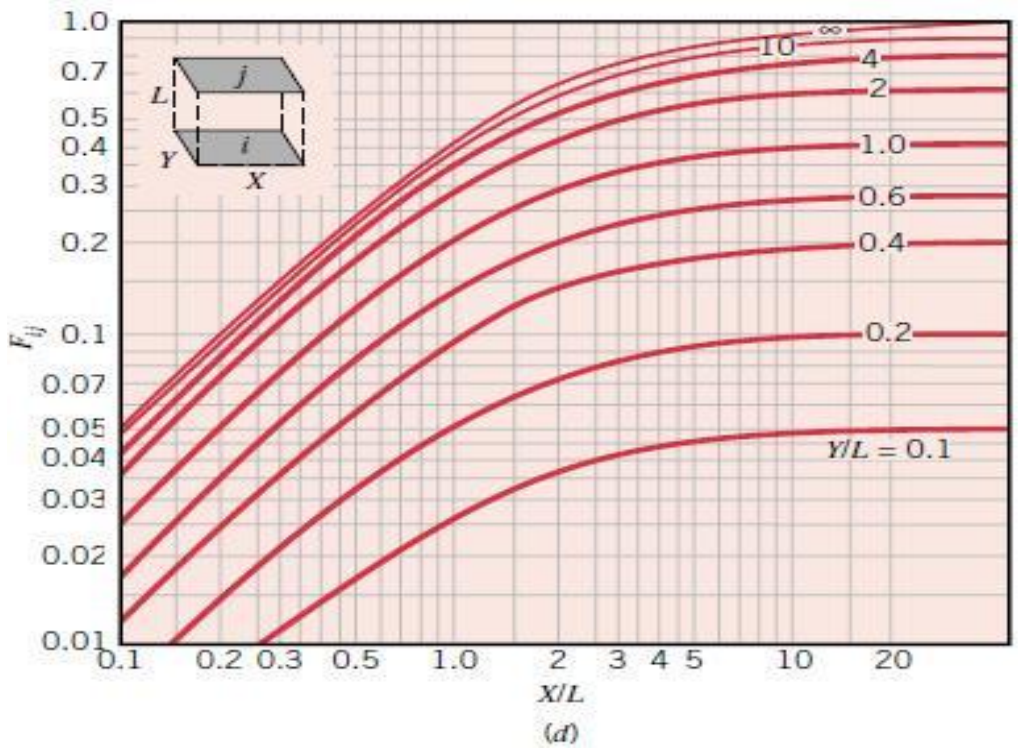

Figure 3.8: View factor of parallel plates (Michael, 2003)

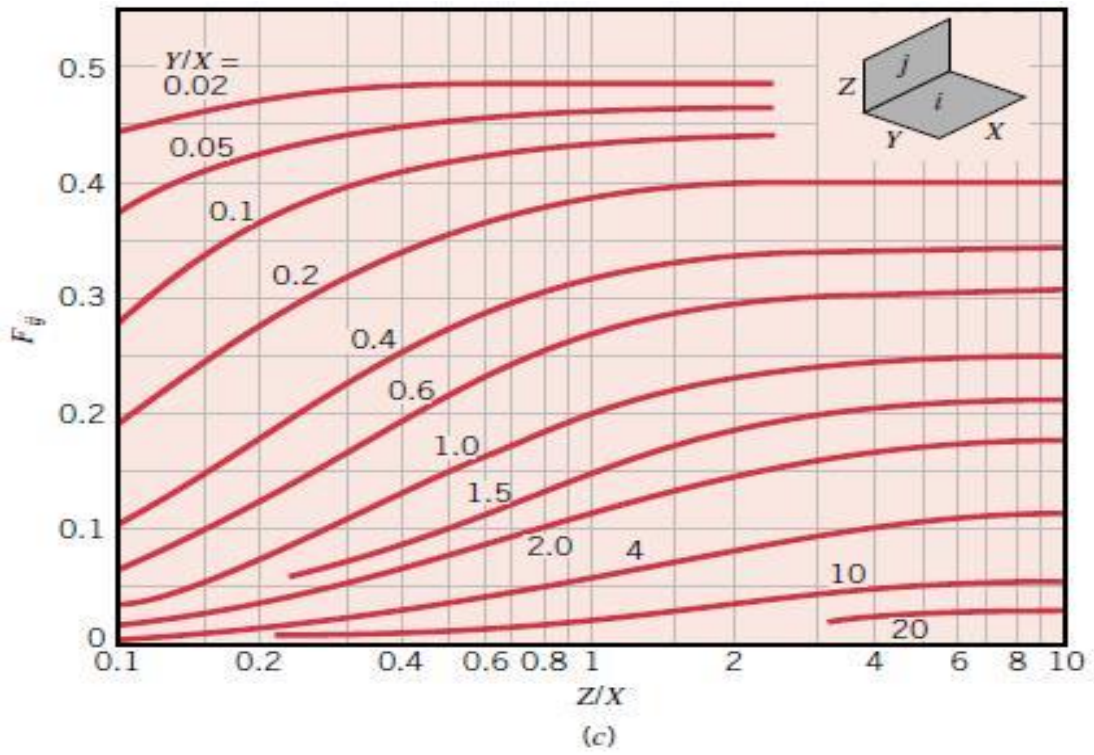

Figure 3.9: View factor of perpendicular plates (Michael, 2003)

3.10.2 Radiative exchange between black surfaces

Emission and reflection are both ways through which radiation may leave a surface. The investigation of radiation exchange between surfaces, in general, is complicated because of reflection: a radiation beam leaving a surface may be reflected many times, with partial absorption occurring at each surface, before it is finally absorbed. The analysis is greatly simplified if the surfaces involved can be approximated as blackbodies because of the absence of reflection. Consider radiation exchange between two back surfaces of arbitrary shape,$q_{i\to j}$ is the rate at which radiation leaves the surface i and is intercepted by surface j, it follows that

$$q_{i\to j} = (A_i J_i) F_{ij} \qquad (3.21)$$

3.10.3 Radiative exchange between diffuse grey surfaces enclosure

Radiation exchange formulas are available for blackbodies. Because these results can differ considerably from the practical realisation, usefulness is generally limited to analytical analysis. A blackbody is an idealisation that can be closely approximated by some surfaces, but never accurately achieved. Calculations involving real non-blackbody surfaces do present increased mathematical complications; therefore, these calculations invariably assume certain conditions. The calculations involved in analysing radiation exchange can be simplified by making certain assumptions. These conditions include the following:

- The surface surface of the enclosure is isothermal, which is by a uniform radiosity and irradiation.
- Surface behavior is opaque, diffuse and grey.
- The medium within the enclosure is non-participating.

The aim of many calculations is to determine the net radiative heat flux q_i, knowing the temperature T_i associated with each surface of an enclosure. The radiosity J is defined as the total diffuse energy leaving a surface through emission and reflection. Whereas the radiosity of a blackbody is given by $J = E_h = \sigma T^4$. such that it is radiosity equals it is emissive power since it does not reflect any radiation.

CHAPTER FOUR

MODELLING OF CERAMIC INFRARED HEATER AND INFRARED GASIFIER

This chapter shall introduce the mathematical model of the ceramic infrared heater as well as the mathematical model of the gasifier enclosure. The thermal system is described here using mathematical representation. Several heaters are commercialized to meet client specific needs. Application of heaters may vary from drying, heating in food industry or for household applications, to boiling, and furnace application for commercial building (Roth, 2007). Infrared heaters, also called infrared radiant heaters as referring to the sun, operate not-surprisingly in a manner similar to the sun.

This chapter shall introduce the mathematical model of the ceramic infrared heater as well as the mathematical model of the gasifier enclosure. The thermal system is described here using mathematical representation. Several heaters are commercialised to meet client specific needs. Application of heaters may vary from drying, heating in food industry or for household applications, to boiling, and furnace application for commercial building (Roth, 2007). Infrared heaters, also called infrared radiant heaters as referring to the sun, operate not-surprisingly in a manner similar to the sun.

4.1 Infrared heaters classifications

Emitters are broadly classified into three categories according to wavelength of radiation - namely shortwave, medium wave and long wave emitters - though the boundary between them is not very precise.

4.1.1 Short wavelength heaters

Short wave emitters emit infrared rays of wavelength ranging from 0.7 to 1.4μm, which is closest to visible spectrum, giving a bright white appearance, with the corresponding radiator temperature being around 1300K and 2600K. These types of emitters are often considered the most powerful because they can achieve the highest power densities, up to more than 300 KW^2, and are very responsive as they can attain the maximum temperature within a few seconds. They are used extensively for industrial processes such as preheating, metal casting, powder coating and adhesive bonding.

4.1.2 Medium wavelength heaters

Medium wavelength heaters emit a radiation spectrum of wavelength ranging from 1.4 to 3.0 μm at radiator temperature of 850K-1200K and power density of up to 90 kWm^2. They appear as a bright orange glow and have a response time of about a minute. Medium wave emitters are used extensively for the drying and curing of food products.

4.1.3 Long wavelength infrared heater

Long wavelength radiators have a radiation temperature of 500 - 800K, which corresponds to a spectrum of wavelength more than 3.0μm. They attain a power density up to 40 kWm^2.The emitter appears dull orange and in many cases is not even perceivable to the human eye. This type of emitter takes more than five minutes to reach its peak emissive power (Anon, 2009). Long wave infrared emitters create a stream of hot air that is useful for processes requiring a combination of convection and radiation heating. Basically two types of infrared emitters are conventionally used in industry: electric infrared emitters and gas fired infrared emitters. Electric infrared emitters can emit any wavelength beginning from short to long wave, depending on the voltage supplied to the emitters. In contrast, gas fired infrared emitters are restricted to medium or long wavelength range heaters.

4.1.4 Types of infrared radiation emitters

The basic form of an IR emitter is a heating element sealed inside enclosure or embedded inside a ceramic body. The heating element is a high resistance wire (Nichrome wire, tungsten) that resists the passage of the current, resulting in radiant energy. The reflector-type incandescent lamp is one of the IR emitters that operate in the wavelength region, while quartz tubes and resistance elements operate as medium to long wave infrared emitters.

4.1.5 Ceramic infrared radiation emitter

Ceramic IR heaters are made of heating elements (iron, chrome and aluminum) which is embedded in a ceramic body (as shown in Figure 4.1) in addition to a fibre blanket at the back of the heater behind the heating element to work as a reflector. The heating element is embedded inside the ceramic body thereby providing protection for the heating element against thermal cracking and oxidation damage. When voltage is applied, the surface of the ceramic becomes hot and acts as an emitter of radiant heat energy. Ceramic infrared heaters operate in medium to long wave spectrum providing infrared radiation with peak values between 3.3μm and 5.7μm and temperatures up to 500˚C and power density ranging from10 to 60 kWm^2 and energy efficiency about 96%. Table4.1 presents the filament specifications at various diameters and lengths.

In order to study the heater, a schematic of the heater has been developed, as shown in Figure 4.1. The radiation heat transfer is described similarly to that suggested by Petterson and Strenstrom, (2000) as believed that radiation is assumed to be diffuse and the model for radiation exchange will have to be non-grey for simplification purpose. For the geometry of the FIR heater, a symbol is allocated on each surface with regards to the radiosity, Ji and irradiation, Gi.

Table 4.1: Calculated resistance and length of wire

Diameter (mm)	**Length (m)**	**Area (mm^2)**	**Resistivity (ρ)**	**Resistance @ (20˚C)**	**Power (kW)**
0.35	12	0.096	1.09	136.25	0.36
0.5	14	0.196	1.09	77.86	0.62
0.5	18	0.196	1.09	100.10	0.48
0.5	22	0.196	1.09	122.35	0.40
0.5	35	0.196	1.09	194.64	0.25
0.5	42	0.196	1.09	233.57	0.21
0.5	50	0.196	1.09	278.06	0.17
0.3	3	0.707	1.09	46.25	1.05
0.3	4	0.707	1.09	61.67	0.78
0.3	5	0.707	1.09	77.09	0.63
0.3	6	0.707	1.09	92.50	0.52

Table 4.2: Types of infrared emitters (Alan, 1998)

	G-30 bulbs	**T_3 Quartz lamp**	**Quartz Tubes**	**Metal Radiant Tube**	**Panel Heaters**	**Ceramic Element**
Heated element	Tungsten filament	Tungsten filament	Nickrom wire	Nickrom wire or Fe-Cr, AL wire	Fe-Cr-AL wire	Fe-Cr-AL
Intensity	Short wave high intensity	Short wave high intensity	Medium wave medium intensity	Medium wave medium intensity	Medium or long wave medium to low intensity	Medium or long wave medium to low intensity
Temperature	400-2900°F	400-2900°F	1800-1400°F	1400-100°F	1300-400°F	1300-400°F
Brightness	Bright white	Bright white	Cherry red	Dull red	No visible light	No visible light
Usual range of peak energy wavelength	1.15-1.16 μm	1.15-1.16μm	2.3-2.8μm	2.8-3.6μm	3.2-6μm	3.2-6μm
Percent radiant	72-86%	72-86%	40-60%	45-53%	20-50%	20-50%

Percent convective	28-14%	28-14%	60-40%	55-47%	80-50%	80-50%
Response to heat up/ cool down	1 second	1 second	30 seconds	2 minutes	5 minutes	5 minutes
Watt density W/sq.in	10 – 15	50 – 1200	10 – 80	10 – 35	10 – 30	10 - 40

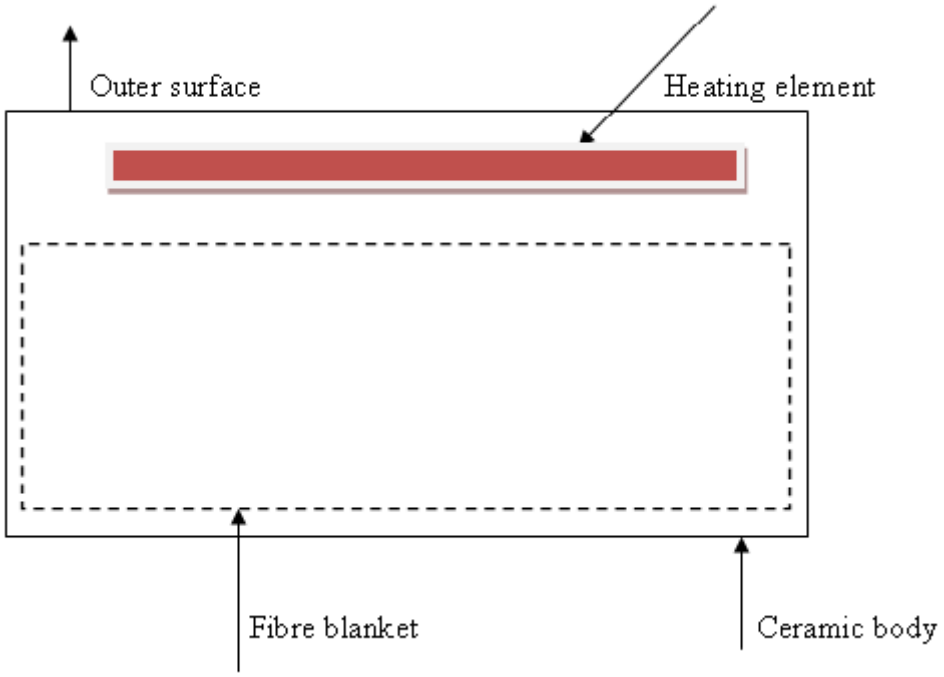

Figure 4.1: Schematic of infrared heater

4.1.6 Conduction Heat Transfer within a Plastic Sample

Prediction of conduction heat transfer within the plastics can be calculated under steady state condition as follows

$$Q = K\frac{T_1 - T_2}{X}At \tag{4.1}$$

Where Q is the quantity of heat transfer, therefore the rate of heat flow can also be calculated from

$$\frac{dQ}{dt} = K\frac{T_1 - T_2}{X}Aor\frac{dQ}{dt} = -KA\frac{dt}{dx} \tag{4.2}$$

Equation (4.1) relates the rate of heat flow $\frac{dQ}{dt}$to the temperature gradient in the plastic $\frac{dT}{dx}inx$ direction (one dimensional heat conduction). $\frac{dQ}{dt}$(Heat flux) is measured in Jm^2s. Fourier's equations are the base of calculating conduction heat transfer

$$\rho c\frac{dT}{dt} = \nabla k\nabla T \tag{4.3}$$

Where$\nabla = {}^{d}/_{dx} + {}^{d}/_{dy} + {}^{d}/_{dz}$ (ρ) (c) are density and specific heat respectively.

4.1.7 Boundary Conditions

Temperature distribution can be represented as one-dimensional as T(x, t) and T(x, y, t), T(x, y, z, t), and as two and three-dimensional respectively. The plastic sample is assumed to be initially at uniform temperature T, thus T = T at t = 0 or T = T (X, Y, Z, 0) Separation of the variable method has been used for solving partial differential equation; in this case, this method has been used to solve the one-dimensional unsteady state temperature distribution in plastic samples.

$$\frac{dT(x,t)}{dt} = \alpha\frac{d^2T(x,t)}{d^2x} \tag{4.4}$$

Or it can also be represented as the product of a spatial function X(x) and time function T (t) as follows:

$$T(x,t) = X(x).T(t) \tag{4.5}$$

Substituting (4.4) into (4.5)

$$\frac{1}{\alpha}\frac{dT}{dt} = \frac{1}{x}\frac{d^2X}{dx^2} \tag{4.6}$$

Thus$T(t) = Ae^{-b^2t}$

$$X(x) = B\cos\ (bx) + \mathrm{C}\sin(bx) \tag{4.7}$$

From (4.4), the solution is

$$T(x,t) = [D\cos(bx) + \mathrm{E}\sin(bx)]e^{-b^2t} \tag{4.8}$$

4.3 Mathematical modelling of an enclosure

Designing an efficient energy system requires accurate predictions of heat transfer rates in these systems. Three modes of heat transfer exist: two modes (conduction and convection) represent the heat transfer rates proportional to the differences in temperature, whereas in the third mode (radiation), the heat transfer rates are proportional to the differences of the fourth powers of the temperature. Prediction of thermal radiation in enclosures becomes very important for the determination of radiative heat transfer in designing high temperature energy conversion devices (boilers, heating furnaces and incinerators). For calculating the radiative heat transfer rates in a particular energy conversion system, the following equation is formulated, combining conduction, convection and radiation in one equation, therefore:

$$\rho C_v\left(\frac{dT}{dt} + v\nabla T\right) = -\nabla.(-K\nabla T + qR) - \rho\nabla.v + \mu\varphi + Q \tag{4.9}$$

Equation 4.9 represents the general equation to calculate the heat transfer rates for energy conversion system, considering convection, conduction and radiation. Howell (1983) has concluded that the following features should be in any numerical method that calculates heat transfer within enclosure:

- Capability to handle multi-dimensional and complex enclosure geometry;
- Good accuracy under all conditions: non-scattering or anisotropic; scattering, grey or non grey, Iso-thermal or non Iso-thermal participating media;
- Ease of application;
- Ease of generalization: flexibility in choosing the different order of approximations;
- Availability of the accurate intensity field and the integrated quantity;
- Computational compatibility with conductive and convective heat transfer codes;
- Low computation cost.

4.3.1 Discrete Transfer Method

The discrete transfer method provides a solution to the radiative heat transfer equation by calculating the intensity of radiation along a particular direction. Same as the control volume method, this method also divides the physical domain into sub-domains. In the control volume sub-domains, the temperature and the absorption coefficient are constant. In each small control volume there is a central point, a point representing a centre of semi-hemisphere divided into a number of solid angles. Solid angles then represent a path along which the radiative equation is given (Carvalho, 1998). It was proposed by Shah (1979) that the discrete transfer method assumes that radiation emitted from surface element in specific ranges of solid angles can be approximated by a single ray. It solves the radiative heat transfer tracing a particular ray when travelling from surface to another. The intensity along a particular path is given by the following:

$$\frac{di}{ds} = -ki + \frac{k\sigma T^4}{\pi} \tag{4.10}$$

Where i is the intensity, s is the path along which ray is travelling, k is the absorption coefficient and σ is the Stefan Boltzmann constant. The above equation can be integrated to give the following:

$$i_{n+1} = i_n \exp(-k\Delta s) + \frac{k\sigma T_c^4}{\pi}(1 - \exp(-k\Delta s)) \tag{4.11}$$

Where i_{n+1} and i_n are the intensity of the ray on entry and exit, Δs is the distance travelled in the control volume, T_c^4 is the temperature of the control volume at the centre. Therefore the change in the intensity along a particular path can be calculated from the above equation. Incident flux may then be calculated using the numerical quadrature.

$$\bar{q} = \sum i_w^- (\theta, \varphi) \cos\theta \sin\theta \, \Delta\theta \Delta\varphi \tag{4.12}$$

It has been proven by Lockwood and Fontes (1981) that this method can accurately handle radiative heat transfer problems in two and three-dimensional geometries, increasing the number of rays. Murthy and Choudhary (1992) have also used this method to calculate the radiative heat transfer in two and three-dimensions.

4.3.2 Finite Volume Method

The finite volume method is more likely comparable to discrete ordinate method, it also divides the total volume into small control volumes, then a calculation of the intensity over

the total solid angle 4π is achieved taking the integration over each individual control volume.

4.2.3 Discrete ordinate method

Analysis of combined conductive and radiative heat transfer in a two-dimensional rectangular enclosure using the discrete ordinate method has been investigated by Taik (1990) to calculate the conductive and radiative heat transfer in a two-dimension enclosure. The study found that the discrete ordinate method is highly integrated with other methods. In addition, the discrete ordinate method does not take much time to give accurate solutions. This method has also been defined by Farias (1998) as a method that represents the radiation intensity of the system depending on the direction of the radiation. The total solid angle around each point is normally segmented into smaller solid angles. It is also depends on differential equations to calculate the radiation intensities in a particular direction. The discrete ordinate method has been used by Sgalari *et al.* (1998) to investigate the photo catalytic processes. The results reported showed that in a case of comparison between the discrete ordinate method and the Monte Carlo method, the two methods show cohesive agreement. The discrete ordinate method has less computation time but that depends on the thickness of the object to be processed and the phase function. It was concluded that the discrete ordinate method can accurately represent the radiation transmission in a photochemical reactor and it was also concluded that this method is not a time-consuming method as compared to the Monte Carlo method. Conductive and radiative heat transfer has been modelled by Mahapatra (2004). In this study the discrete ordinate method has been used to develop a model that describes radiation conduction interaction within enclosure. It was found that the discrete ordinate method is accurate when the processed material is relatively thin. It was also noticed that the increase in the radiative transfer is influenced by the increased emissivity and decreased optical thickness.

4.2.4 Monte Carlo method

Radiative heat transfer flux in a cylindrical furnace has been calculated by Steward (1969) using the Monte Carlo method. Steward has compared the Monte Carlo method with the interchange method in terms of handling the radiative heat flux and temperature distribution within a furnace enclosure. It was been found that Monte Carlo method was more accurate and favourable in handling the variation of temperature since the geometry is changing The Monte Carlo method in radiative heat transfer has also been discussed by Howell (1998). The Monte Carlo method is reportedly the most accurate method that can handle the radiative heat transfer phenomena. Therefore, the Monte Carlo method is statistical sampling technique that can actually simulate all the physical processes. Because of its accuracy, the Monte Carlo method has been applied to a variety of heat transfer problems.

The Monte Carlo method is considered a reference when discussing radiative heat transfer problems with respect to other methods (Viskanta & Menguc, 1987). However, the disadvantages of the Monte Carlo method are that it is a time-consuming method and statistical complication of the results makes it difficult for the Monte Carlo method to be used as a reference method. A report by Carvalho (1998) stated that as this method is basically a statistical method, it can calculate the path of a photon travelling in a particular direction. It traces the path till the photons get totally absorbed by a particular medium. It describes the emitting energy in form of bundles so that the number of bundles always determines the flux of the emitted energy. Absorption and reflection coefficient play an important role in the heat balance in the system; that means a photon is emitted in a certain direction that is randomly chosen and then there is a probability that this photon will get absorbed either by the wall or by the gas that occupies the enclosure. In order to get accurate results from the Monte Carlo method, large numbers of samples of energy bundles need to be considered.

4.2.5 Moment method

Leon *et al.* (1987) have reviewed the use of the moment method in radiation from flanged parallel plates. The review found that the moment method is accurate and efficient in handling the reflection coefficient. In this method radiation intensity is represented as follows:

$$i(X,Y,Z,\theta,\varphi) = A_{\circ} + \sum_{n=1}^{N} [\xi^n A_{n,x} + \eta^n A_{n,y} + \mu^n A_{n,z} \quad (4.13)$$

As represent function of locations and **ξ**, and μ correspond to direction cosines in x, y, z directions (Viskanta and Menguc 1987).

4.2.6 Zonal method

The Zonal method is a method used in calculating the radiative heat transfer equation to describe the radiation phenomena in combustion furnaces. The Zonal method divides the radiative enclosure into small zones; then it calculates the direct heat exchange between the zones, dividing the system into smaller zones using simultaneous solutions. The Zonal method has the ability to describe the temperature profile and heat flux distribution within a surface. The disadvantage of the Zonal method is the difficulty of handling complex geometries in terms of calculating the direct heat exchange between zones. It has also been found that the finite difference method can be coupled with the Zonal method to accurately handle the flow rate and the energy equation difficulty (Carvalho, 1998).

This method is also known as Hottel's Zone method as developed by Hottel and Cohen (1958). In the Zonal method, the direct exchange areas $s_i s_i$ are determined and the total

exchange areas SjSjare also determined. The radiant balance calculated for each zone can then be calculated from the following formula:

$$Q_i = Q_{E,i} - \sum_{j}^{N} S_i S_j \,.\, E_j \tag{4.14}$$

The formula above calculates the net heat flow from an object i, subtracting the received radiation from all N surfaces enclosure and the emitted radiation$Q_{E,i}.E_j$ Is the total blackbody emitted fluxσT_j^4. Zonal method has been applied by Liu and Tiwari (1994) to solve radiative heat transfer equation in non gray, anisotropic scattering media.

4.2.7 Flux method

The solid angle is discretized into a number of discrete directions, with intensity considered to be uniform over a given interval over the solid angle (Khalil *et al.,* 1982). The number of discrete directions determines the multi-flux method results; therefore, two fluxes and four fluxes will result as a consequence of dividing the solid angle uniformly into two and four divisions respectively. This method relies on representing the radiative heat transfer problem by solving the partial differential equations. The Flux method calculates the angular intensity variation (Carvalho, 1998).

4.2.8 Ray tracing method

The Ray tracing method is a method that describes the path of a photon, widely used in heat transfer applications as it allows the tracking and simulation of reflection and absorption of thermal radiation (Cosson *et al*., 2010).

4.2.9 Net radiation method

A portion of the irradiation striking surface K will be reflected from K. Let K be a diffuse surface. In that case the reflected radiative flux from A_K will be:

$$dq_{\lambda,ref,K} = \rho_{\lambda,K} G_{\lambda,K} d\lambda \tag{4.15}$$

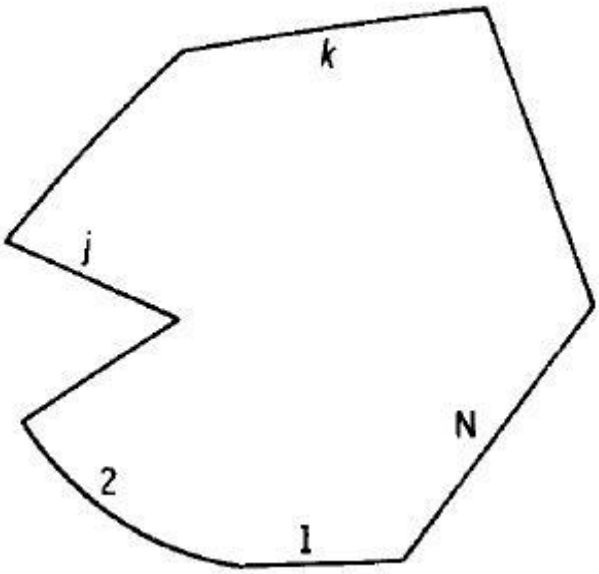

Figure 4.2: Enclosure of N discrete surfaces (Siegal, 1992)

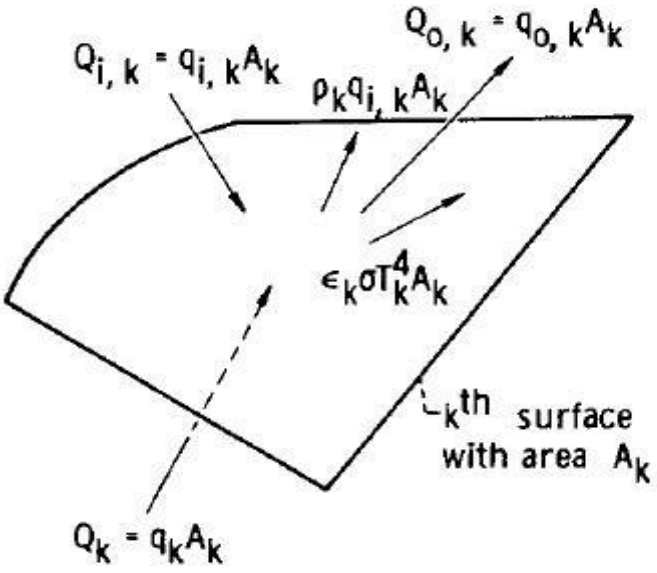

Figure 4.3: Energy incident and leaving a surface (Siegal, 1992)

The radiosity of a surface is a combination of the emitted and reflected radiation, given by the following formula:

$$J_{\lambda,K} = \text{emitted} + \text{reflected flux} = \varepsilon_{\lambda,K} E_{\lambda b,K} + \rho_{\lambda,K} G_{\lambda,K} \qquad (4.16)$$

The radiation energy balance on K can be represented as:

$$dq_{\lambda,K} = (\text{out going} - \text{incoming radiation}) = J_{\lambda,K}d\lambda - G_{\lambda,K}d\lambda \qquad (4.17)$$

Therefore irradiation on A_K is:

$$G_{\lambda,K}A_K = \sum_{j=1}^{N} J_{\lambda,j}A_j F_{J-K} \qquad (4.18)$$

Or

$$G_{\lambda,K} = \sum_{J=1}^{N} J_{\lambda,j}F_{K-j} \qquad (4.19)$$

4.2.9.1 Grey surfaces

Because wavelength dependent properties are often not available, the net radiation method is quite often applied under the further assumption that all surfaces in the enclosure are gray. Therefore, the three basic equations can be integrated over wavelength to become:

$$J_K = \varepsilon_K E_{b,K} + \rho_K G_K = \varepsilon_K \sigma T_K^4 + (1-\varepsilon_K)G_K \qquad (4.20)$$

$$q_k = J_k - G_K \qquad (4.21)$$

$$G_K = \sum_{j=1}^{N} J_j F_{K-j} \qquad (4.22)$$

G_K Can be found from Eq (4.21) and substituted into Eqs (4.19) and (4.22), giving:

$$J_K = \varepsilon_K \sigma T_K^4 + (1-\varepsilon_K)(J_K - q_K) \qquad (4.23)$$

$$J_K = \sigma T_K^4 - \frac{(1-\varepsilon_K)}{\varepsilon_K} q_K \qquad (4.23a)$$

$$J_K = q_K + \sum_{j=1}^{N} J_j F_{K-j} \tag{4.24}$$

If the radiosity is not required, then it can be eliminated from the equation set by substituting Eq. (4.23a) into Eq (4.24) to give:

$$\sigma T_K^4 - \frac{1}{\varepsilon_K} q_K = \sum_{j=1}^{N} [\sigma T_j^4 - \frac{(1-\varepsilon_j)}{\varepsilon_j} q_j] F_{K-j} \tag{4.25}$$

4.3 Mathematical modelling of infrared radiation heater

Heaters differ in design by virtue of arrangement of current leads, shapes, and presence or absence of reflectors, although all have filament as a common feature. The filament determines the energy characteristics of heaters and accounts for the wide range of designs (Petrovskii, 1998). The most important parameters of any heater are the surface load, efficiency and durability.

Here we shall consider the design of a ceramic infrared heater which has a surface temperature lower than 800℃. The heater is made of ceramic body with resistance wire (filament) embedded in it. There is a fibre blanket placed just behind the filament to avoid heat loss from the back of the heater. These fibre blankets exhibit outstanding insulating properties at elevated temperatures and can withstand temperatures to the value of 1300℃. They also have excellent thermal stability, low heat storage, are free of binder or lubricant and immune to thermal shock (thermal ceramics).

Ceramic infrared heaters are designed to emit wavelengths in the far range at certain operational powers and temperatures. As voltage is applied to the leads, there are current and resistive loses in the filaments that translate into heat build-up. The higher the temperature, the higher the filament resistivity, and hence the reduction in the amount of current and power consumed. The rise in temperature filament results in heat transfer by means of conduction to the ceramic body and then radiation to the surrounding. The passage of electric current through a filament when voltage is applied is given by the following:

$$i(t) = \frac{U}{R}(1 - e^{k_1}) + c_2 e^{k_2} k_{1,2} = -\frac{1}{2RC}\left[1 \pm \sqrt{1 - \frac{4CR^2}{L}}\right] \tag{4.26}$$

Where c_2 is constant.

$$k_1 = {}^{R}/_{L}$$

$$k_2 = {}^{-1}/_{RC} + {}^{R}/_{L}$$

The mechanism involved in the heat transfer in ceramic heaters is conduction from the filament to the ceramic body. A Fourier equation can be used to calculate the rate of heating and cooling of the heater:

$$T = T_1 + (T_0 + T_1)e^{\frac{2Na_t^2}{r_0}} \tag{4.27}$$

Where ($a = c_p\lambda$).

Where T, T_0, T_1 are the running temperature of the surface of the heater after the time$t$, the initial temperature of the heater, and the temperature of the medium respectively, a is the diffusivity, equal to the product of the heat capacity of the heater, its density and the thermal conductivity of the insulating sheath, N is the heat transfer coefficient characterizing heat exchange with the medium, r is the depth of penetration of the heat pulse.

The heating element reliability and stability are determined by the extent to which the heater remains constant over its service life. The relation in equation (4.28) describes the rate of degradation.

$$\xi = \xi_0 \exp\left[-\frac{Q}{RT}\right] \tag{4.28}$$

Where ξ_0 is a constant dependent on the composition and method of production of the material of the conducting phase, the electrical insulator, or the casing, Q is the energy of activation of the aging process, which depends on the ambient conditions and the thermo-mechanical stability of the material of the heater, T is the working temperature of the heater.

4.3.1 Energy balance

Energy balance is when the rate at which energy is transferred from the heater surface to the surface of the target is equal, given mathematically as follows:

$$\mathrm{E_{out}} - \mathrm{E_{in}} = 0 \tag{4.29}$$

Considering ceramic heaters as having a resistance wires of diameter D and length L initially at thermal equilibrium with the ambient air and its surroundings, this equilibrium condition is only distributed when an electric current I is passed through the wire. An equation that could be used to compute the variation of the wire temperature with time

during the passage of the current is developed using the first law of thermodynamics, often used for determining unknown temperatures. Relevant terms involve heat transfer by radiation from the surface of the heater, internal energy generation due to electrical current passage through the wire, and a change in internal energy storage. For determining the rate of change of temperature and applying the first law of thermodynamics to a system of length L of the wire, it follows that:

$$E_g - E_{out} = E_{st} \tag{4.30}$$

Where the energy generation due to the electric resistant heating is given by:

$$E_g = I^2 R_e L \tag{4.31}$$

Energy outflow due to net radiation leaving the surface is given by:

$$E_{out} = \varepsilon\sigma(\pi DL)(T^4 - T_{sur}^4) \tag{4.32}$$

The change of energy storage due to the temperature change is:

$$E_{st} = \frac{dU}{dt} = \rho c V \frac{dT}{dt} \tag{4.33}$$

Where ρ and c are the density and specific heat, respectively of the wire material and V is the volume of the wire $V = \left(\frac{\pi D^2}{4}\right) L$

Substituting the rate equations into the energy balance, it follows that:

$$I^2 R_e L - \varepsilon\sigma(\pi DL)(T^4 - T_{sur}^4) = \rho c \left(\frac{\pi D^2}{4}\right) L \frac{dT}{dt} \tag{4.34}$$

Hence the time rate of change of the wire temperature is:

$$\frac{dT}{dt} = \frac{I^2 R_e L - \varepsilon\sigma(\pi D)(T^4 - T_{sur}^4)}{\rho c \left(\frac{\pi D^2}{4}\right)} \tag{4.35}$$

The heat transfer is defined as one dimensional conduction in the reflector which itself is considered as an opaque body. The equation in the reflector is defined as:

$$\frac{\partial T_r}{\partial t} = \frac{K_c}{\rho C p} \frac{\partial^2 T_r}{\partial x^2} \tag{4.36}$$

Since there is an insulation blanket, the boundary condition at the back of the heater is:

$$\frac{\partial T_r}{\partial_x} = 0 \tag{4.37}$$

The boundary conditions at the front surface of the heater involve radiation and it is represented as follows:

$$-K_c \frac{\partial T_r}{\partial_x} = \varepsilon\sigma A(T^4 - T_{sur}^4) \tag{4.38}$$

4.3.2 Physical properties of ceramic infrared heaters

The change in temperature of a ceramic heater depends solely on the temperature of the heating element embedded inside the ceramic. Equations 4.26 and 4.27 describe the phenomenon involved in the process. Ceramic IR heaters operate in the region of medium to far wavelengths. Here we shall consider heating elements, fibre insulation materials and the ceramic body.

4.4.3 Heating element

Infrared source is a heating element converting voltage into heat, and the heat then radiated in the form of electromagnetic radiation. Infrared sources are available in different forms and shapes, operating under different wavelengths and temperatures. The selection of an IR source for a particular application depends on the wavelength under which the heater is operating. In the case of selecting an infrared heater for plastic gasification purposes, the heater should be able to provide wavelengths in the range of a long wavelength region in order for the plastic to absorb the source radiation. The ideal infrared sources for plastic gasification are the wide panel infrared heaters such as ceramic coated and quartz face, because their operating temperatures fall in the range 94˚C to 934˚C; therefore, they provide peak wavelengths of 2.2 micron to 7 microns. The heating element considered in this design is Nickel-chromium (80 Ni, 20 Cr) as it is widely used as a heating element in industrial furnaces as well as in electric household appliances. This element has special advantages in that it has very good mechanical and physical properties, as shown in Table 4.3.

Table 4.3: Physical and mechanical properties of Nickrothal alloy, (Nikrothal Handbook, 2001)

	Nickrothal 80	**Nickrothal 70**	**Nickrothal 60**
Maximum continuous operating temperature ℃	1200	1250	1150
Resistivity at 20˚C, $\Omega mm^{-2}mm^{-1}$	1.09	1.18	1.11
Density, g/cm^3	8.3	8.1	8.2
Coefficient of thermal expansion, K^{-1} 20-750˚C	17.10^{-6}	16.10^{-6}	16.10^{-6}

Thermal conductivity at 20˚C W m^{-1} K^{-1}	15	13	13
Specific heat capacity KJ/kg^{-1}, 20˚C	0.46	0.46	0.46
Melting point ˚C	1400	1380	1390
Mechanical properties			
Tensile strength, Nmm^{-2}	750	875	750
Yield point, Nmm^{-2}	450	450	450
Hardness, Hv	180	185	180
Elongation at rupture, %	30	30	30
Tensile strength at 900˚C, Nmm^{-2}	100	120	100
Creep strength at 800˚C, Nmm^{-2} 100℃, Nmm^{-2}	15 4	15 4	15 4
Emissivity, fully oxidized condition	0.88	0.88	0.88

Table 4.4: Emissivity of some metal sources (Industrial heating, 1998)

Metal	**Polished**	**Oxidized**
Aluminum	0.05	0.15
Brass	0.09	0.60
Cast Iron	0.21	0.71
Copper	0.02	0.60
Galvanized Steel	0.02	0.76
Gold	0.018	----
Lead	0.08	0.70
Nickel	0.06	0.90
Stainless Steel	0.17	0.85
Tin	0.18	0.60
Zinc	0.03	0.50

Resistance wire, otherwise known as heating element, is probably the most important material in the manufacturing of this kind of heater as it determines the power, temperature and wavelength of the heater. It is eminent to take into consideration the length and diameter of the wire as these are essential determining factors for acquiring the resistive and irradiational values. The type of wire in use here is the Nikrothal80, a high grade austenitic alloy which is specially suited in the electrical appliance industry due to its malleability and strength at high temperatures. It has also gained many advantages as a

result of its mechanical properties in the hot state. Nikrothal 80 is used in appliances such as flat irons, ironing machines, water heaters, plastic molding dyes, soldering irons, metal sheathed tubular elements and cartridges. The Nikrothal 80 has superior life compared to the competitive Nickel Chromium alloys because of the extremely good adhesion properties of the surface oxide. To calculate resistance of wire and output power of heater, the formulas below are used:

$$R = \rho\left(\frac{l}{A}\right)(\Omega) \tag{4.39}$$

Where R= resistance, l = length, A= area, ρ = resistivity.

Power

$$P = IV \tag{4.40}$$

Where V= Voltage (220 single phase), R= Resistance (Ω).

4.3.4 Radiation network

The mechanism of irradiation is the quantity of far infrared radiation (FIR) irradiated from the ceramic FIR heater. It is therefore the sum of the quantity of FIR energy delivered to the surroundings with the quantity of energy delivered by the resistance wire. In other words:

$$Q_{ir,FIR} = Q_{ir,FIR_h} + Q_{ir,wire} \tag{4.41}$$

The heat energy radiated by the heater is:

$$Q_{ir,FIR_h} = \sigma\varepsilon_h A_h T_h^4 \tag{4.42}$$

The convection heat transfer of air to the surface is expressed as:

$$Q_{conv} = h_{conv} A_s (T - T_\infty) \tag{4.43}$$

The current flow, as it is comparable to the heat transfer in the enclosure, can be established by comparison. By determining the resistance, we can determine the net radiation exchange between the heater, the filament wire and the surroundings.

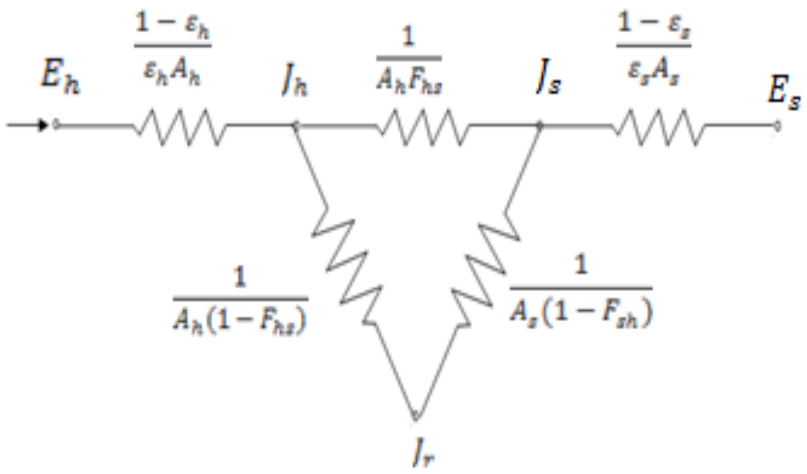

Figure 4.4: Series-parallel radiation network of three surfaces (Michael, 2003)

The equation that determines the net radiation exchange between the heater and the surface can be written as follows:

$$q_{hs} = \frac{E_h - E_s}{\left(1 - \frac{\varepsilon_h}{\varepsilon_h A_h}\right) + \left(\frac{1}{A_h F_{hs}}\right) + \left(1 - \frac{\varepsilon_s}{\varepsilon_s A_s}\right)} \tag{4.44}$$

$$q_{hs} = \frac{\sigma\left(T_h^4 - T_s^4\right)}{\left(1 - \frac{\varepsilon_h}{\varepsilon_h A_h}\right) + \left(\frac{1}{A_h F_{hs}}\right) + \left(1 - \frac{\varepsilon_s}{\varepsilon_s A_s}\right)} \tag{4.45}$$

$$q_{hs} = \frac{\sigma\left(T_h^4 - T_s^4\right)}{R_{net}} \tag{4.46}$$

Where $R_{net} = \left(1 - \frac{\varepsilon_h}{\varepsilon_h A_h}\right) + \left(\frac{1}{A_h F_{hs}}\right) + \left(1 - \frac{\varepsilon_s}{\varepsilon_s A_s}\right)$

4.3.5 Insulation fibre

A fibre blanket is one of the materials used in ceramic heaters to prevent heat from escaping through the back of the heater. This can be considered as a reflector in that it reflects the infrared waves, forcing it to focus in one direction. Two materials of slightly similar properties will be employed in this experiment to give different views on their applications. The materials used in this case are applied by thermal ceramics.

4.3.5.1 Fibre blanket

This is a blanket made from high temperature insulation wool exhibiting outstanding insulating properties at elevated temperatures. The blanket has an excellent thermal stability and has an original soft fibrous structure up to maximum continuous use temperature. It

contains neither binder nor lubricant and does not emit any fume or smell during the first firing. Furthermore, it is flexible and easy to cut shape and easy to install. It can withstand temperatures of up to 1260˚C. According to thermal ceramic manufacturers, it has the following features:

- Excellent thermal insulating performances
- Unaffected by most chemicals except hydrofluoric and phosphoric acids and strong alkalies.
- Excellent thermal stability: fibers have good resistance to devitrification
- The combination of long spun fibers and the needling operation produce tough, resilient and strong blankets, which resists tearing both before and after heating.
- Free of binder or lubricant
- Thermal stability
- Low heat storage
- Good sound absorption
- Flexible and resilient
- Immune to thermal shock
- No reaction with alumina based in application in the range of the typical use temperature
- Exonerated from any carcinogenic classification under nota Q of directive 97/69 EC.

CHAPTER FIVE

CONSTRUCTION AND DESIGN OF CERAMIC INFRARED HEATER AND INFRARED GASIFIER

Making a ceramic heater needs thorough preparation prior to even starting the process. The mold and slip must be prepared in order to get the right shape and size. Molds are usually made out of Plaster of Paris (POP), wax, wood, aluminum and any other material that can be curved into a desired shape. The mold selected for this project is POP mold because POP molds allow for the repetition of complicated patterns and creation of forms not possible to construct efficiently using any other pottery technique.

5.1 The mold board

Mold boards are made out of wood or aluminum. Polywood can also be used but needs mold soap to be applied as a release agent. Wood must be assembled to the desired shape and size and then fastened together. If the boards are cut accurately at the corners, the assembled form will keep the plaster from leaking without needing to seal joints with clay.

5.2 Making the mold

First determine the number of sections the mold will have and identify the location of the plug hole. Molds are typically in four pieces - the bottom, two sides and the top - but could differ according to desired shape. A two-piece mold has been used for this project. When determining the size of the template, accommodate for clay shrinkage in the final heater; for example, using a clay body that shrinks at 12%, a 4.5 mold should be used for a101.6mm heater.

5.3 Steps for Preparing Plaster

According to Jones (2008), there are ten steps to perfect plaster. Whether a drying bat is needed, a simple hump mold, or making a slip mold, mixing plaster is needed. Getting the plaster right requires a bit more than just dumping and mixing.

- Prepare the work area ensuring it is clean and tidy. A clean container for the plaster, a scale for weighting the plaster, a measuring cup for the water and a rinse bucket is required. Plaster should not be disposed down the drain as this can form rock-like mass that will block the drain.
- Mixing water should be at room temperature or (21˚C). Too warm water results in plaster setting too fast and vice versa. Use clean, drinkable tap water or distilled water metallic salts, such as aluminum sulfate, can accelerate the setting time, and soluble salts can cause efflorescence on the mold surface.
- Plaster is calcined, meaning chemically bound water has been driven through heating. If the plaster has been sitting around in a damp environment, it will have

lumps in it, in which case it is no longer usable. Plaster should be fresh, stored no more that 6 months and completely free of moisture.

- Measure out sufficient amount of required materials. To determine required amount, estimate the volume in cubic inches then divide by 231 to give gallons or by 58 to give quarts. Deduct 20% to allow for the volume of plaster. Refer to table 5.1.
- Slowly sift the plaster into the water. Once all the plaster is in, allow to soak (slate) for one minute without any agitation. Mix plaster with clean stick until it becomes a heavy cream consistency. This should take ideally 2 to 3 minutes, but can happen anywhere from 1 to 5 minutes. Mixing time affects absorption rates; longer mixing time produces tighter and less-absorptive molds.
- After mixing, tap the bucket on a hard surface to release trapped air. Pour the plaster carefully into the mold board. Fill up all deep areas so the slurry flows evenly across the surface of the mold. Once the mold is poured, tap the table slightly to release some more air bubbles.
- After about 30-45 minutes, the plaster would have cooled. When plaster sets, it heats up of a chemical reaction. Take the form (boards) apart. If the board sticks, give it tap from the mold and it will pop off. Drying mold properly promotes good strength development, uniform absorption and reduced efflorescence.

Table 5.1: Water to plaster mixing chart (Bill, 2008)

Water	Plaster
1 quart	2 lbs. 14 oz. (1,293 grams)
1 ½ quarts	4 lbs. 4 oz. (1,937 grams)
2 quarts	5 lbs. 11 oz. (2,585 grams)
2 ½ quarts	7 lbs. 2 oz. (3,230 grams)
3 quarts	8 lbs. 9 oz. (3,878 grams)
3 ½ quarts	10 lbs. (4,522 grams)
1 gallon	11 lbs. 6 oz. (5,171 grams)
1 ½ gallons	17 lbs. 2 oz. (7,756 grams)
2 gallons	22 lbs. 13 oz. (10,337 grams)
2 ½ gallons	28 lbs. 8 oz. (12, 923 grams)
3 gallons	34 lbs. 3 oz. (15,503 grams)

5.4 Preparing Ceramic Slip for Casting

'Slip' is clay in liquid form that is poured into plaster molds to make caste ceramic figures. According to Paul (2010), instructions on how to make slip is given as follows:

- Mix minerals of kaolin, ball clay, feldspar and silica water. Make sure there is enough slip to fill the mold. Stir well and ensure even thickness all through.

- Test slips specific gravity to determine if the water to clay ratio is correct before deflocculating. To determine specific gravity, which is a comparison of the weight of 100 ml of water (which is 100g and therefore has specific gravity of 1) with the weight of 100ml of the slip you are working with, fill 100 ml of slip in a graduated measuring container, put it on scale and see how much it weights in grams. Divide the weight by the weight of an equivalent volume of water (100g). These workouts by moving the decimal point on your measurement slip to the left by two places to get the specific gravity of the slip, example 175g = 1.75 specific gravity. Different clay bodies have different optical specific gravities that are determined by trail and error. Specific gravity is simply a tool to adjust the slip to meet requirements for particular casting projects. Ideally, specific gravity of 1.80 is recommended. If you have higher value and wish to bring it down, just add little water, few drops at time to your slip, mix and re-test.

- Once specific gravity is known, add deflocculates to the slip to make it fluid so it can be poured. A few drops of deflocculates go along way. The consistency of cream is what is needed. So over deflocculating should be avoided. Scoop some of the slip to see how it pours.

5.4.1 Processing

- Prepare mold by making sure it is clean and dry, a thin coating of dish soap or any other lubricating agent is applied to the inside of the mold for easy removal of the ceramic. Assemble pieces of mold together and strap them tightly together with bands or tapes.

- When desired consistency of pourable ceramic is achieved, slowly pour the mixture into the mold but remember to insert the resistance wire and insulation fiber. Ensure walls of clay are not thinner than approximately 3/16 inch.

- When the correct thickness of the wall is complete, pour out the excess slip, clean off the opening of the mold and leave to set for about 45 minutes.

- Remove the straps and gently take one side of the mold a part. If it still feels sticky do not remove the mold and leave to dry for another 30 minutes.

- When complete dry, remove the mold and the molded clay can either let air dry or can put in oven on 300 degree for 30 minutes.

- When complete dry, paint or glaze as desired and fire.

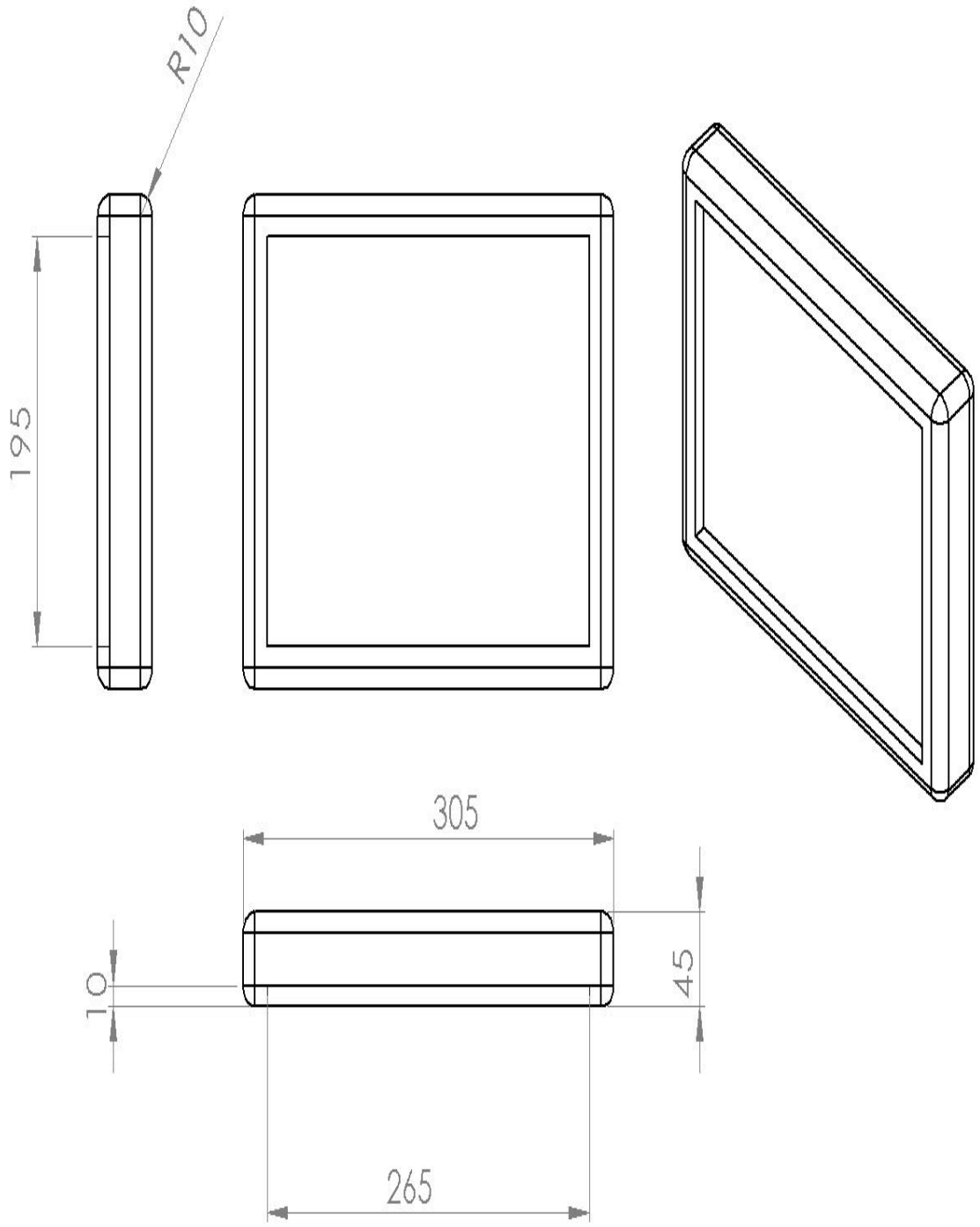

Figure 5.1: Schematic diagram of top part mold with dimensions

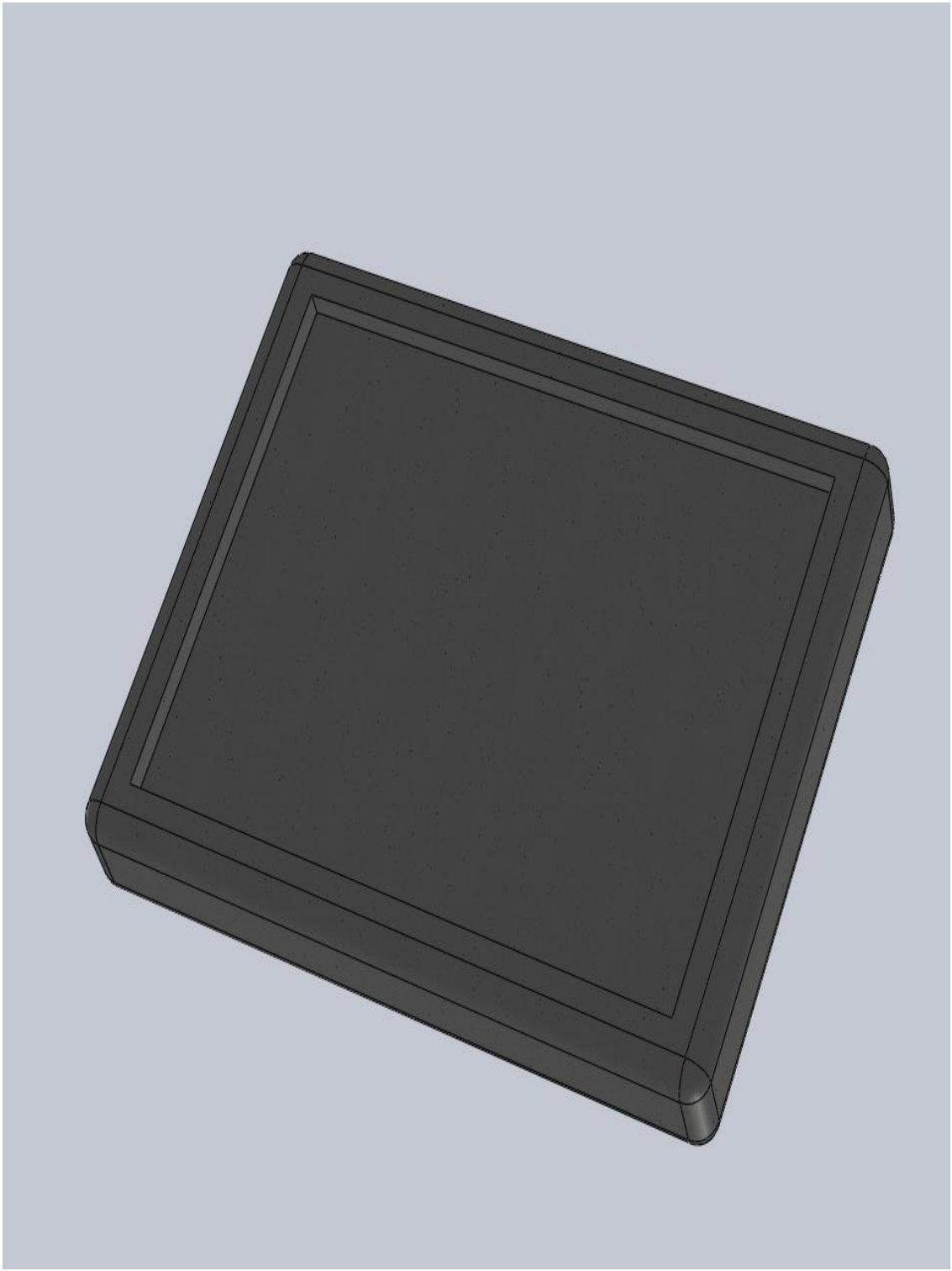

Figure 5.2: Sketch diagram of top part of mold

Figure 5.3: Actual photo of bottom part of mold (top view)

Figure 5.4: Actual photo of bottom part of mold (rear view)

Figure 5.5: Sketch diagram of bottom part of mold (rear view)

5.5Ceramic Heater Manufacturing

After the backside and front were made, the heating element (NiCr, 80 20),at a length of35 meters and diameter of 0.5cm,was then carefully placed in a zigzag form inside the inner surface of the front side. A fibre blanket (insulator) was also placed to cover the heating element, then the backside and front heater sides were carefully joined together and the two lead heating elements were taken through a hole at the back of the heater. Figures 5.6 to 5.8 represent the schematic diagrams in millimetres, assembling and manufacturing the actual ceramic heater:

Figure 5.6: Actual photo of heating element on the top part

Figure 5.7: Actual photo of the bottom part of the heater

Figure 5.8: Actual photo of the fibre blanket covering the heating element

5.6 Design of the gasifier

The design of an aluminum rectangular gasifier has been considered prior to gasification stage. Since aluminum is considered an effective reflector, the gasifier body was made of aluminum to reflect as much thermal radiation as possible for preventing thermal radiation from escaping outside the enclosure. A fibre blanket was also attached to the gasifier corners to further prohibit thermal radiation from escaping. This project focused on considering the design and manufacturing of ceramic infrared heaters as well as infrared gasifiers for the gasification of plastic. The experiment concentrated on the characterisation of the heaters, the heater configuration and the production of the syngas. The manufactured aluminum gasifier contains the following three things: 1) gasifier box, 2) lid of the reactor, and 3) the mesh of the reactor.

5.6.1The gasifier box

There is a need for a reactor gasifier for optimum high yield of gaseous products and low coke production to perform an experiment concerning waste plastic gasification. This is achieved by developing a small scale gasifier to successfully experiment on common waste plastics by applying the gasification process using an infrared heater. The reactor is designed with specifications to accommodate the designed infrared heaters up to a maximum size of 260 x 190 mm. The reactor material is aluminum, joined together by the aluminum angles. The fibre blanket is also used to aid with heat retention within the gasifier. The gasifier design specifications and description of gasifier are shown in Tables 5.2 and 5.3. The different schematic views of the gasifier design in millimeters are shown in Figures 5.9 and 5.10. The visual view of the reactor can be seen in Figures 5.11, 5.12 and 5.13. The gasifier lid is designed to cover and retain heat inside the box. The lid has a smoke filter for the yield gases that will be possible during the gasification process. The lid is shown in Figure 5.14. The mesh of the gasifier is the holder of the plastics during experiment.

5.6.2 The construction of gasifier

There are important factors to note during the construction of the gasifier. These include measurements, cutting of the plate, bending of the plate, hole-drilling and assembling. Figures 5.15 to 5.20 demonstrate the flow of these processes.

Table 5.2: Gasifier design specifications

	Size (mm)
Reactor length	280X280
Reactor height	366
Material thickness	2

Heater wires outlets holes diameters	10
Smoke hole diameter	20
Mesh hole diameter	36

Table 5.3: Description of gasifier design

Description	**Quantity**
Outlet leads	4
Angle plate	4
Heater holders	4
Reactor holders	2
Mesh	1

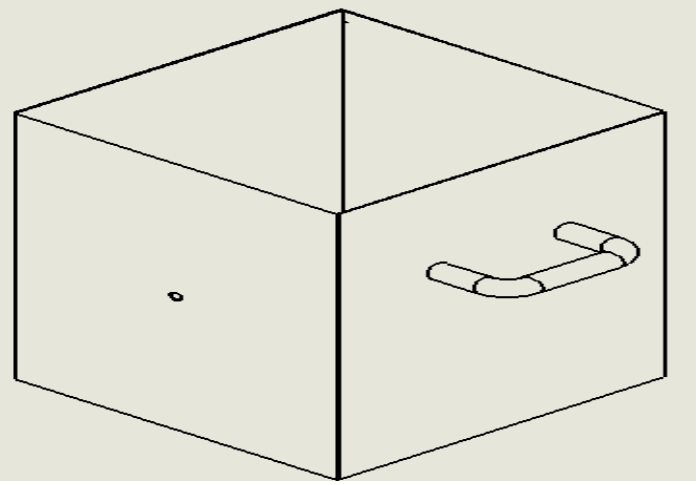

Figure 5.9: Gasifier design

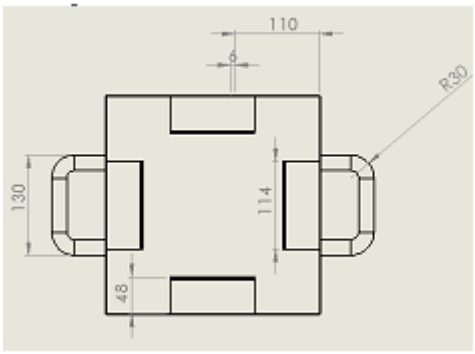

Figure 5.10: Schematic diagram of top view of gasifier

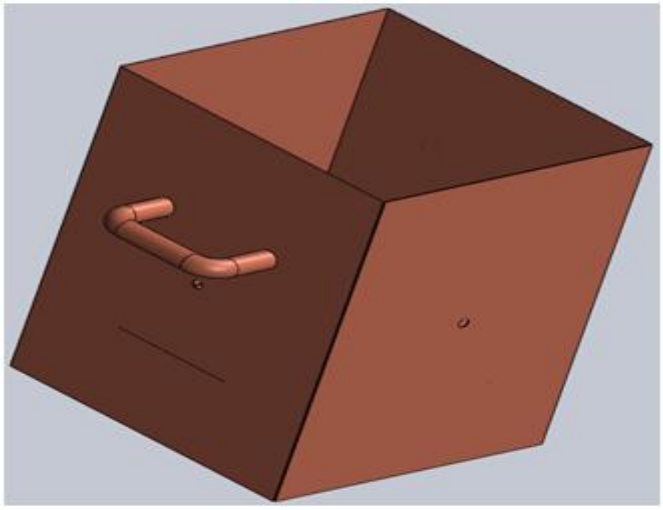

Figure 5.11: Side view of the gasifier

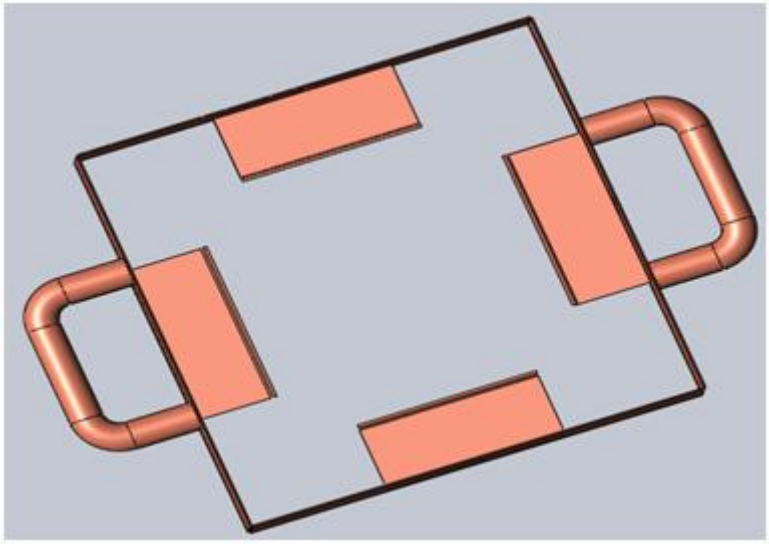

Figure 5.12: Top view of the gasifier

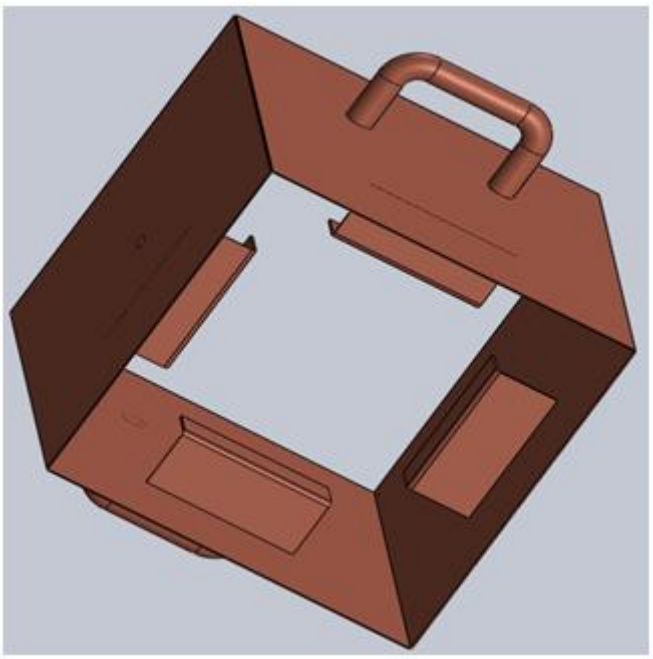

Figure 5.13: Side view of the gasifier

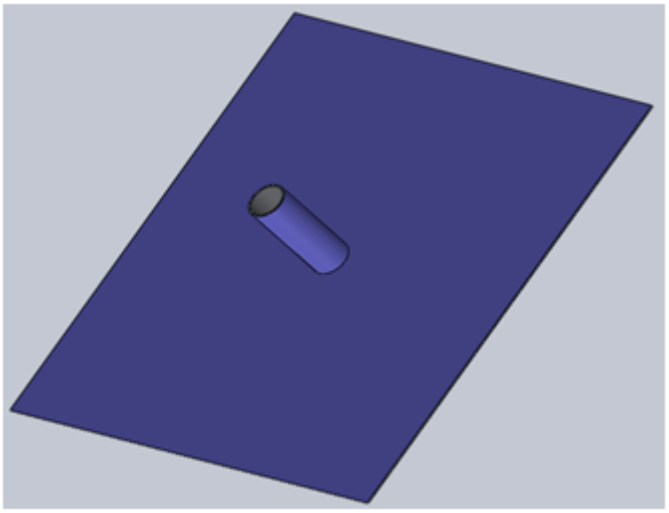

Figure 5.14: The gasifier box lid

Figure 5.15: Bended angle plates

Figure 5.16: Bended heater holders

Figure 5.17: Drilling of holes

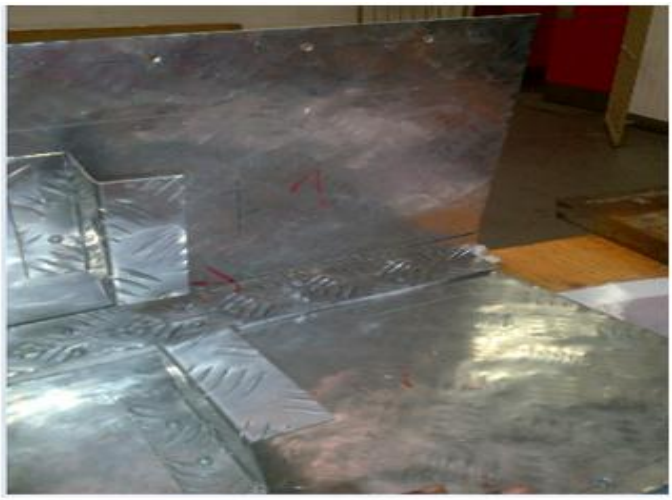

Figure 5.18: Assembling of gasifier

Figure 5.19: Final assembly of the gasifier

Figure 5.20: Top view of gasifier with heaters

CHAPTER SIX
EXPERIMENTAL RESULTS

This chapter shall introduce wavelength measurements of the plastic samples as well as the testing of the manufacturing infrared heaters using LabVIEW and signal express software. It will also explain the gasification experiment.

6.1 Wavelength measurement

Different samples of plastic waste have been tested in terms of absorbtivity and transmitivity in order to determine the exact wavelengths at which high density polyethylene, low density polyethylene, polypropylene, and polyethylene teraphthalate perfectly absorb infrared radiation. The results showed that the absorption of the infrared radiation by any sample of plastics strongly depends on the thickness of the sample: the thinner the sample the better and stronger the absorption, while the opposite also held true - the thicker the sample the poorer the absorption.

6.2 Perkin Elmer Spectrum 100 FTIR Specifications

The PERKINELMER spectrum 100 series spectrometers is the facility used in this experiment to determine the wavelength peak values of the plastic samples, it has the following specifications:

- It has a large, purgeable sample compartment.
- The instrument can operate in ratio, single beam or interferogram mode.
- For the spectrum 100 FT-IR an optical system that gives data collection over a total range of 7800 to 370 cm^{-1} with best resolution of 0.5 cm^{-1} .
- The instrument is connected to a PC, either point to point or over a network, which utilizes spectrum software. This software enables to control that instrument and manipulate the spectra that to be collected.
- Ambient temperature of 5˚C - 40˚C.
- A maximum ambient relative humidity of 80% for temperature up to 30˚C.

6.2.1 Electrical Requirements

- The spectrum 100 FT-IR operates on electricity supplies of 50-60Hz and in the 100-230V range without any adjustment.
- A nominal power consumption of the instrument is 120W
- The line supply must be within 10% of the nominal voltage.

Infrared energy travels in the form of electromagnetic waves, does not require any medium to travel and it can be directed and focused in particular direction which means that it is easy to control, It is only heats a body when absorbed.

6.3 Infrared spectroscopy

Infrared spectroscopy is a technique for identifying the chemical compounds of samples (Smith, 2011). It depends on the fact that different materials absorb infrared radiation at different wavelengths. Fourier Transform Infrared Spectroscopy (FTIR) is a device used to identify the wavelengths at which PET, PP, HDPE, LDPE absorb, reflect and transmit infrared radiation, thereby leading to the choice of the right infrared heater.

6.3.1 Principles of infrared analysis

There are several modes to obtain IR spectra of a sample.

6.3.2 Transmission infrared

In this technique, an infrared beam is passed through a sample (PET), the outgoing portion of the infrared energy is detected, and then the incoming and outgoing infrared beams are measured with respect to wavelength to generate spectrum.

6.3.3 Diffuse and specular reflectance

This technique depends on two types of reflections that occur when an infrared beam falls on a sample surface: specular and diffuse reflections. Specular reflection occurs when infrared energy is directed toward a surface of a solid sample; the specular infrared energy that is reflected in this case corresponds to the portion that is not absorbed by the sample. Diffuse reflection, on the other hand, occurs when an IR beam falls on the surface of the sample; it penetrates into the surface of the sample and then remerges after reflecting off an internal portion of the sample.

6.4 Characterisation of plastics

The purpose behind using Furrier Transform Infrared Spectroscopy is to identify different groups by their different vibration modes. The samples are placed inside the FTIR, making sure that the beam penetrates the sample. The facility was closed, and then sample testing was conducted. Table 6.1 represents the thickness of the plastic samples used in these

tests:

Table 6.1: Thickness of plastic samples

Plastic sample	**Thickness**
HDPE	1mm
LDPE	0.1mm
PET	0.5mm
PP	1mm

Before closing the FT-IR facility, considerable amount of atmospheric carbon dioxide goes in. In order to avoid the influence of carbon dioxide inside the machine, the facility was left for 10-15 minutes.

Procedure of plastic samples spectral properties measurement (transmitivity, absorbtivity) using a Perkin-Elmer FTIR spectrometer. The measured transmitivity is plotted versus wavelength. It appears from these experimental data that the samples are transparent at short wavelengths and part of the medium wavelengths. In addition, the plastic samples are opaque to wavelengths in the far infrared range.

In the FTIR device options the following have been adjusted:

- The sample scan time has been adjusted to 16 scans.
- The background scan time has also been adjusted to 10 scans.
- In the resolution box the adjustment interred was $4cm^{-1}$
- The range of the spectrum is chosen to be from 4000 to $450cm^{-1}$

The data is collected and a signal is plotted in 2 dimensional axes XY, the Y axes represented the transmittance and the X axes represented the range of the spectrum or the wave number in cm^{-1}.

Transmittance measurement of LDPE, HDPE, PET and PP using a FTIR was conducted and is shown in figures 6.1 – 6.4.Sample wavelength measurements were implemented to determine the IR absorption wavelength.

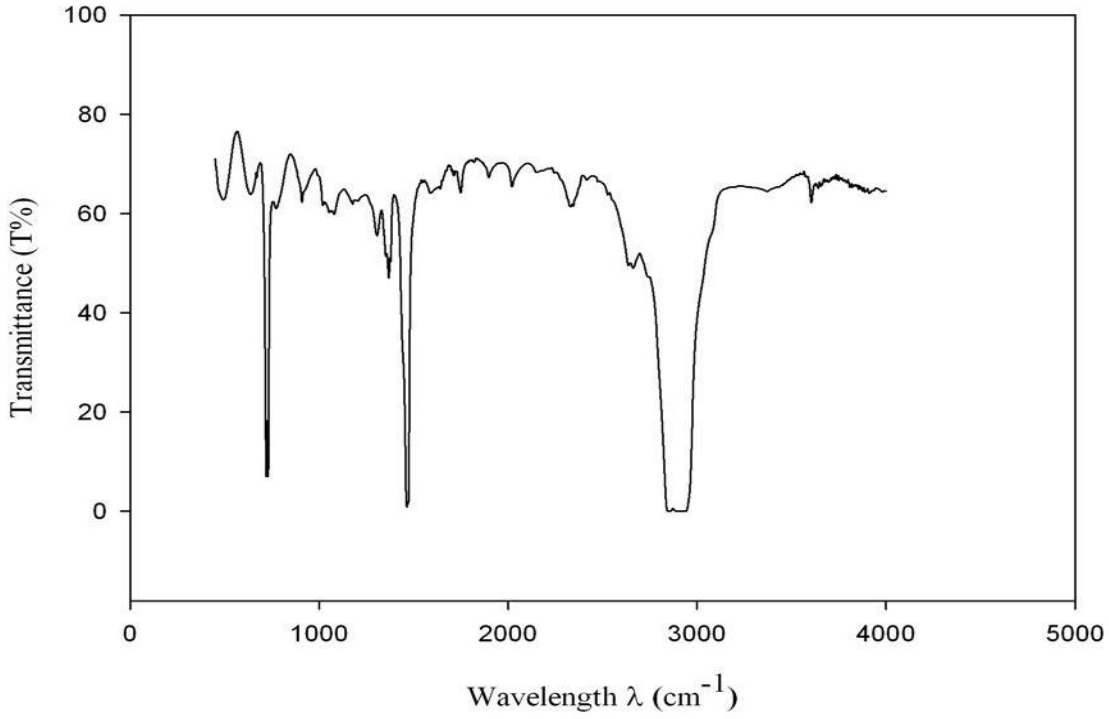

Figure 6.1: Transmittance of Low density polyethylene

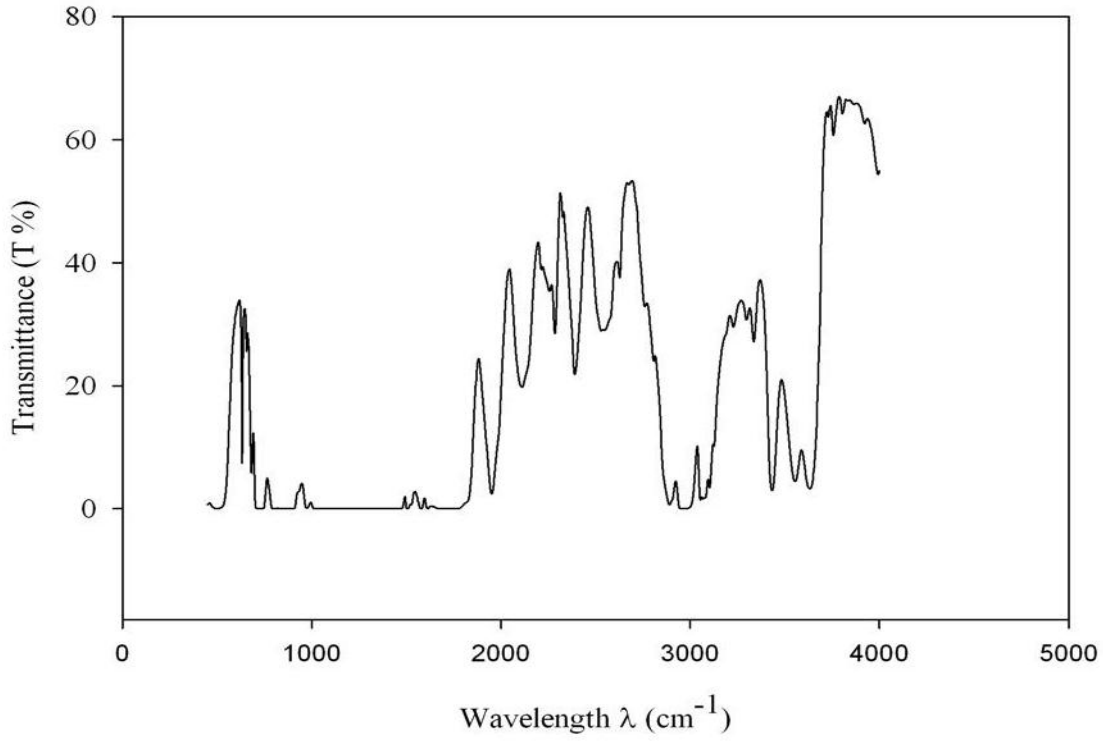

Figure 6.2: Transmittance of Polyethylene teraphthalate

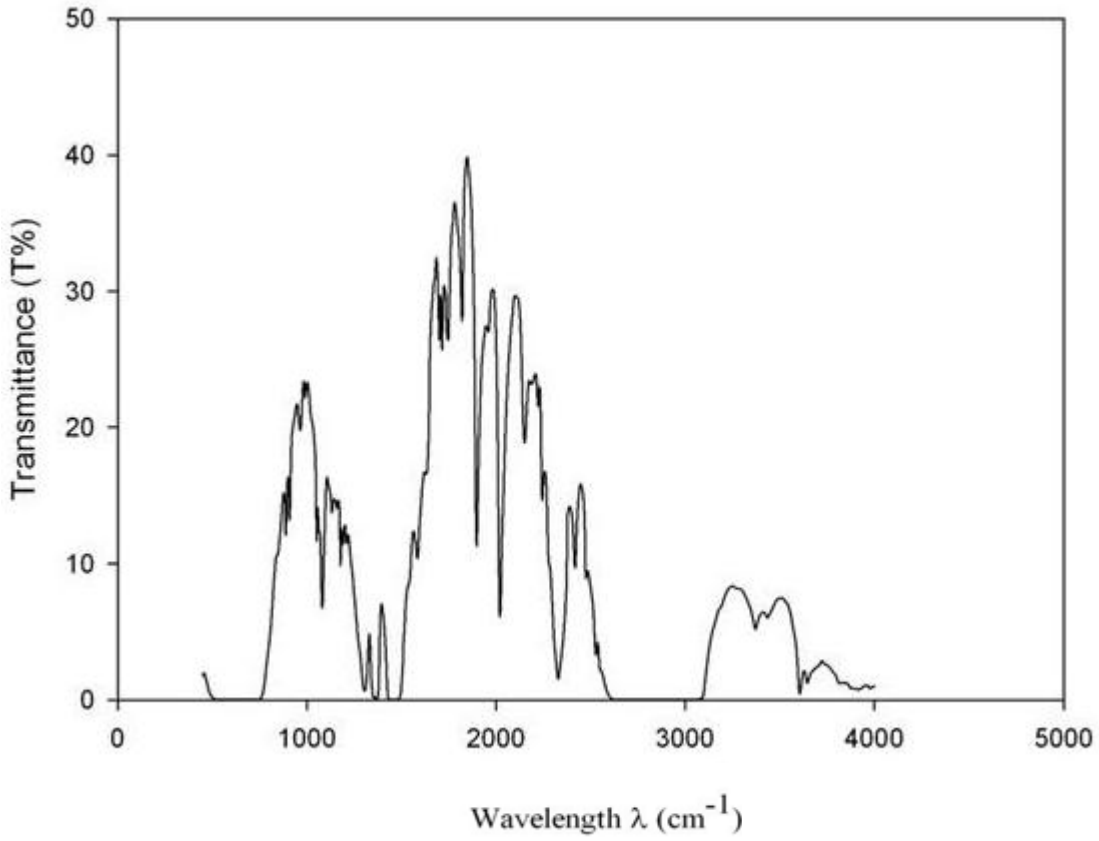

Figure 6.3: Transmittance of High density Polyethylene

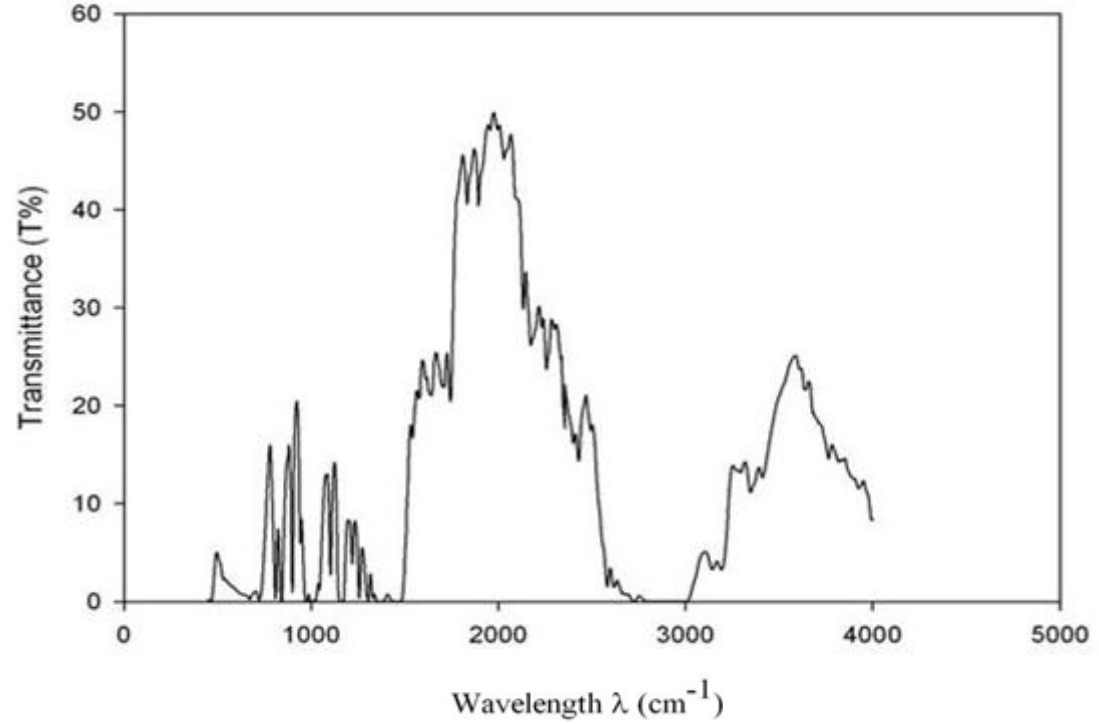

Figure 6.4: Transmittance of Polypropylene

According to previous figures, table 6.2 shows the approximate peak absorption values.

Table 6.2: Plastic samples and measured peak values

Sample	**Measured approximate peak absorption value**
LDPE	3.3 and 6.6μm
PET	3.3and5.5
HDPE	3.3 and 6.6μm
PP	3.3,4 and 6.6μm

6.4.1 Temperature measurement

Infrared systems have always been designed with accurate and reliable temperature control capabilities. Infrared heating systems need a precise reading of the actual product temperature during the heating process. Temperature measurement in the infrared systems is either contact or contactless: contact temperature measurement devices measure the temperature by direct contact with the object to be heated, whereas in the noncontact temperature measurement sensors, the temperature is measured without actual physical contact with the product.

An example of contact sensors are thermocouples. The main limitation of thermocouples, however, is that they may damage the product while contacting it. At the same time, thermocouples do not provide accurate measurement during heating process. Noncontact infrared temperature sensors are undoubtedly more accurate and precise as compared to the contact thermocouples. Infrared thermocouples receive emitted infrared radiation from the product. After radiation energy is intercepted by optics built in the sensor, the optics then focus the infrared radiation onto the detector which then converts it into electrical signal. The following are a few methods used for temperature measurement:

- **Thermocouples**: This type of temperature measuring device is considered to be the most types used in industrial environments. They produce voltage from the temperature gradient that develops at the junction of two dissimilar metals.
- **Resistance Temperature Detectors (RTD's)**: this type produces change in resistance of wire when temperature of the wire changes, they are more accurate than thermocouples but this type is not recommended for measuring high temperatures.
- **Thermistor:** this type changes resistance when temperature changes, but they are more sensitive than thermocouples or RTD's.

- **Infrared (non-contact) Sensors:** these are preferred when measurement taking place within the enclosures. They are used when the use of contact infrared sensors are not accurate in measuring specific application. Such applications are monitoring moving objects, environment with safety hazard present, where contamination of the target is likely and when the distance to the target is far.

Infrared sensors produce an output signal that corresponds to the amount of infrared that strikes the surface of the sensor. Infrared detectors can be classified as either thermal or photo type. Infrared sensors operate by detecting and converting incoming radiation into heat which results in the raising of the detector temperature. This change in temperature is then converted into an electrical signal and processed. The type of infrared sensor employed in this research is Optris CS infrared sensor available from Optris CS series. Their specifications include the following:

- Output voltage 0-5 or 0-10 free scalable
- Optical resolution of 15:1 at 90%energy
- Spectral response range from 8-14µm
- System accuracy ± 1.5%
- Repeatability of ±0.75% of reading
- Temperature coefficient ± 0.05 K/K
- Emissivity fixed at 0.100-1.100
- Response time of 25ms
- Temperature range -40˚C-1030˚C

6.5 installation considerations

Installing or configuring a sensor for a particular task is considered with sensitivity; therefore, it needs to be planned carefully in order for accuracy of the obtained measurement to be guaranteed (Ackland,1998).In order for the sensor to give accurate measurements, the area to be measured should fill the entire instrument field of view. In fact, it is recommended that the target size exceed the field of view by 50% because infrared sensors detect radiation from all sources (i.e. from energy transmitted, reflected and emitted by an object). Since the temperature sensor is a function of the emissivity, only the emissivity from the IR heater then has bearing on the temperature read in (Adonis,

2002). If the field of view is larger than the target size, the background will affect the temperature reading. The optical resolution of the sensor is defined by D:S ratios which compare the distance of the object to the sensor (D) to the size or diameter of the spot (S) being measured. Optical charts as the one shown in Figure 6.5and 6.6help determine the target spot size on a fixed focus instrument. Infrared sensors available have D:S ratios that range from low resolution (e.g. 2:1) to high resolution (300:1). The choice of D:S ratio depends on the size of the object to be measured and the distance the sensor is from the target.

The emissivity of the target material determines the spectral response of the sensor needed. Certain material can be transparent to a certain wavelength whereas other material maybe opaque to the same wavelength. The suitable spectral wavelength of plasticfilms such as polyethylene and polypropylene is 3.4 μm. Since high temperatures have a spectral response that lies within the short wavelength, the low temperature conditions have a spectral response between 8-14 μm wavelength ranges.

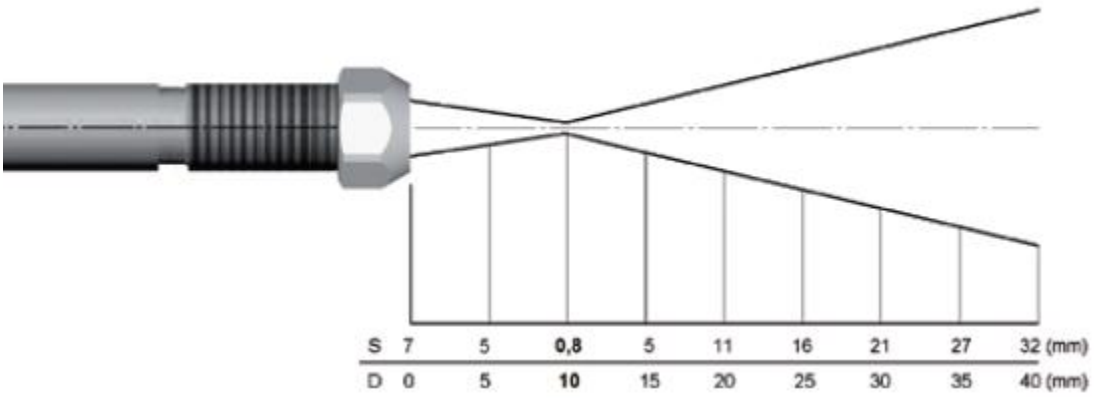

Figure 6.5: Optical resolution of sensor with CF-Lens(Optris, 2009)

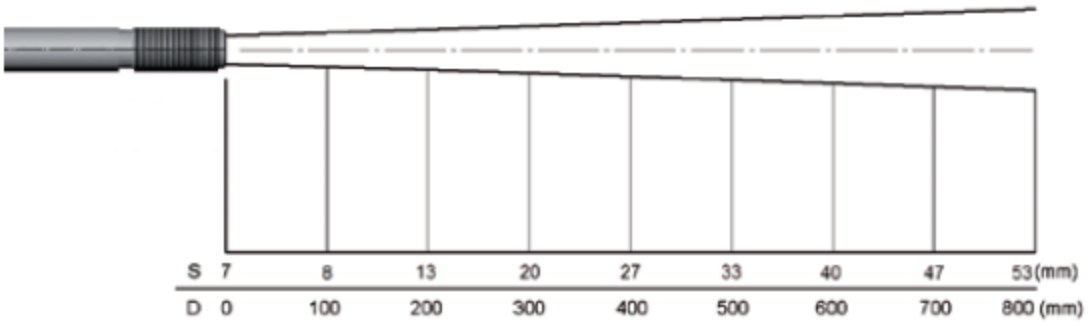

Figure 6.6: Optical resolution of a sensor (Optris, 2009)

6.6 Simulation and analysis of the results

6.6.1 Heating rate

In this section, the heat phase is analysed and the results discussed concern only the simulation of the filament wire. In order to verify the validity of the mathematical model of the heating phase of the filament, the model is simulated under the conditions such that the ambient temperature and the surrounding temperature are equal at 25˚C.

Simulation using MATLAB and Simulink to represent the response of the heating process was obtained and shown in Figure 6.7. Figures 6.8 to 6.11 show, as expected, the rising temperatures of the manufactured ceramic infrared heaters during testing. The variation between the model and the actual manufactured ceramic heater is due to reason that the manufactured ceramic heaters were not made in optimum conditions, and therefore they were not expected to act same way like the model.

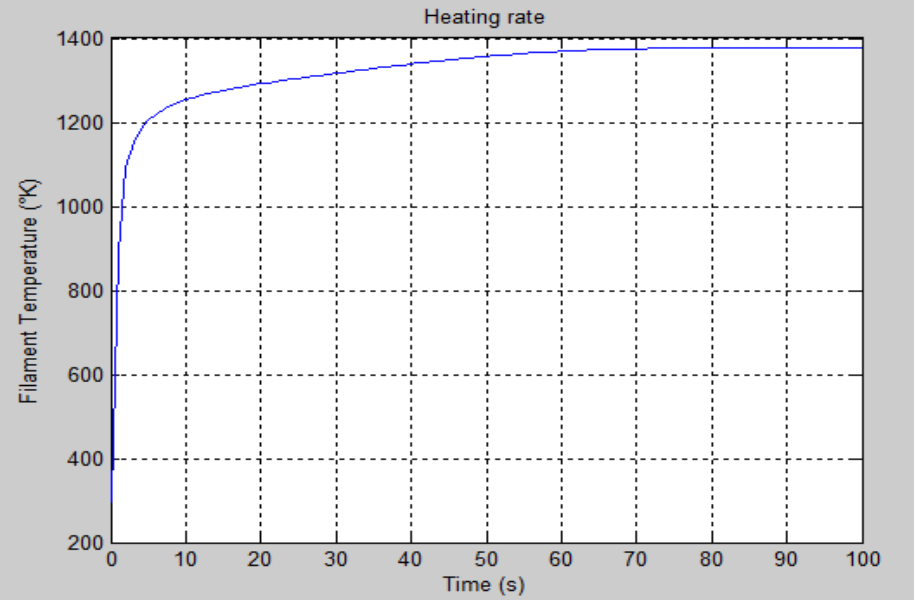

Figure 6.7: Heating Rate

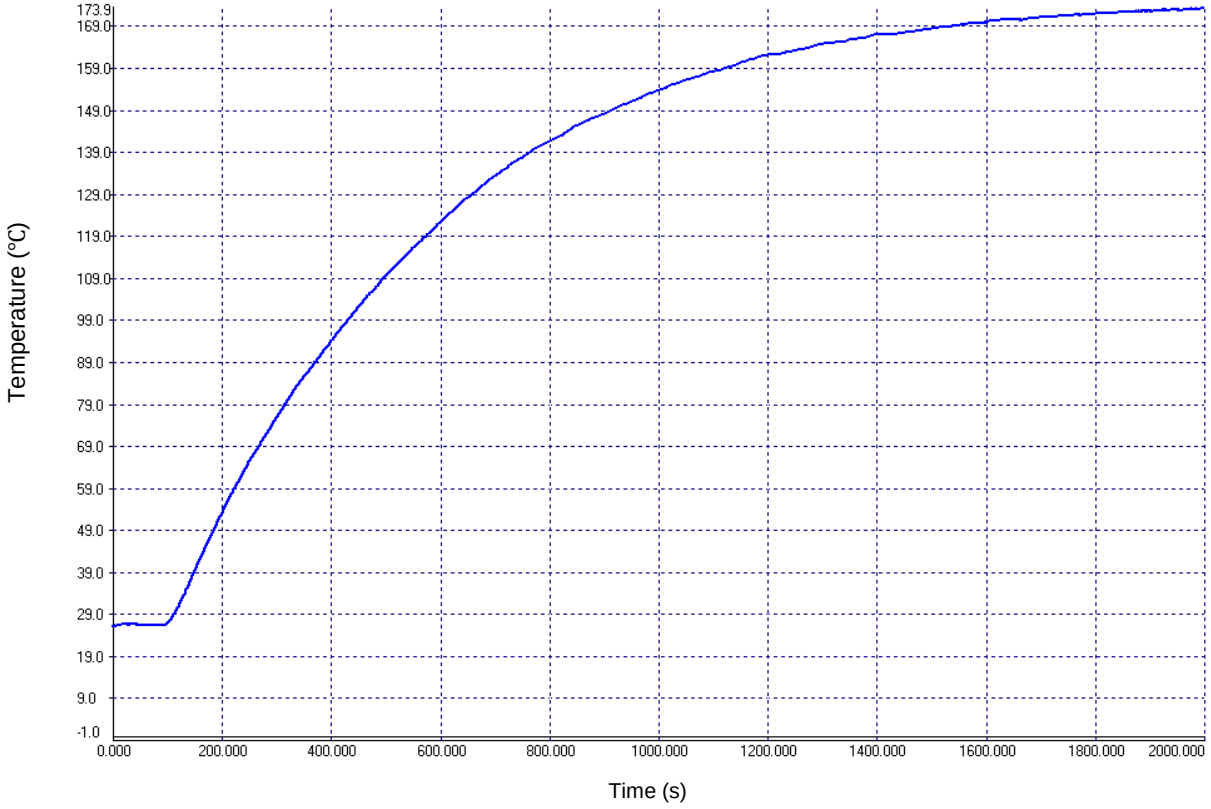

Figure 6.8: Heating rate of manufactured heater 1

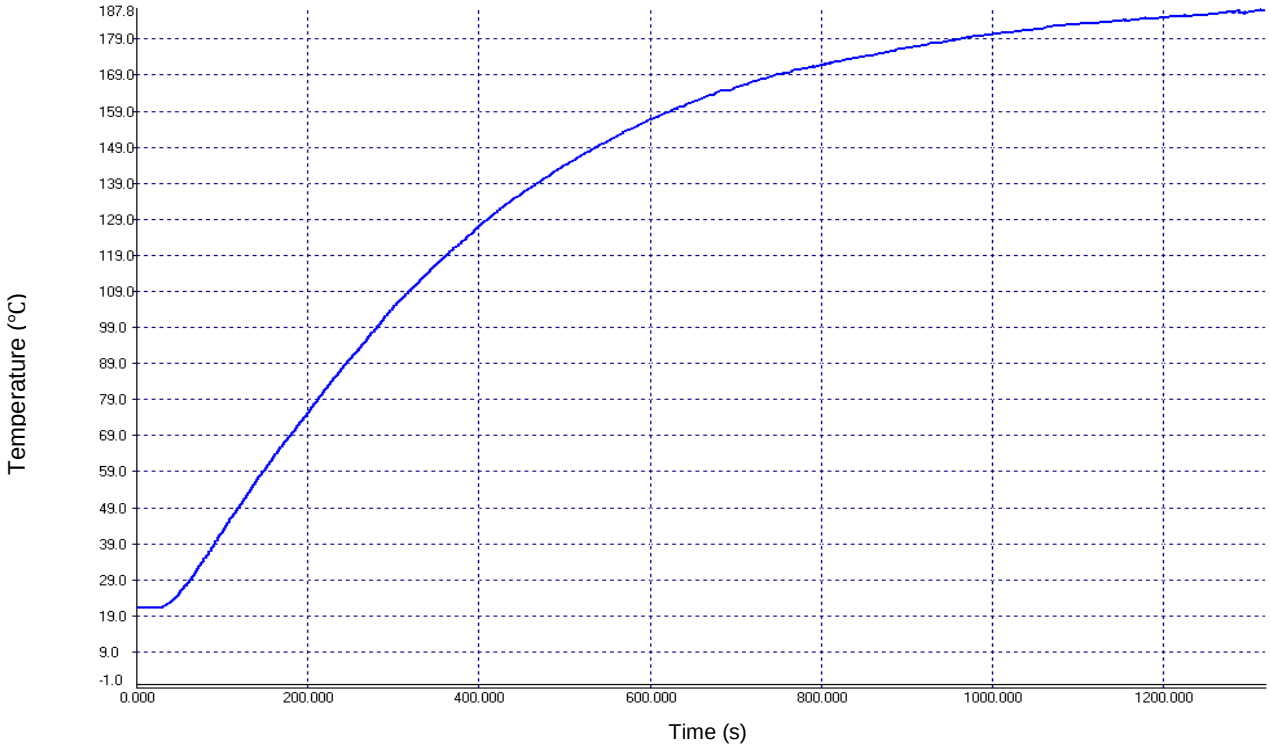

Figure 6.9: Heating rate of manufactured heater 2

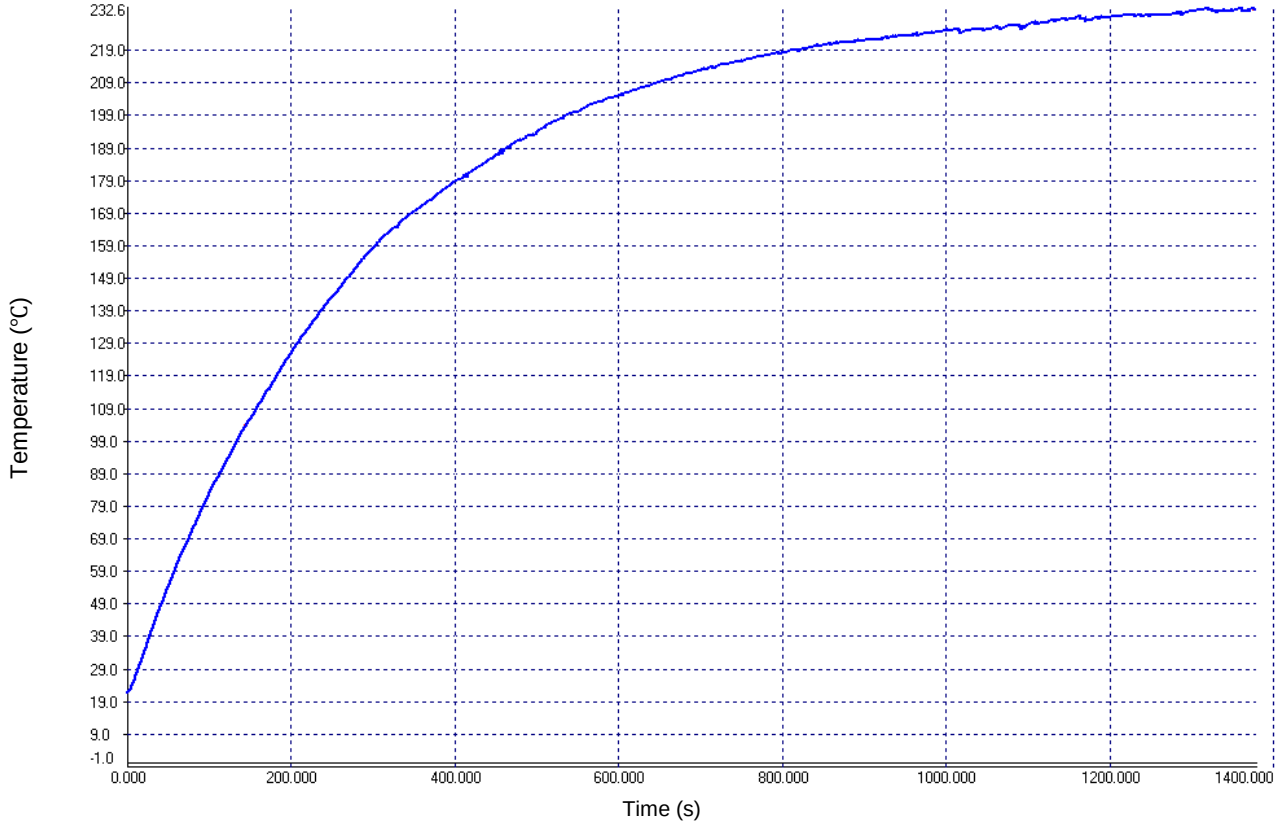

Figure 6.10: Heating rate of manufactured heater 3

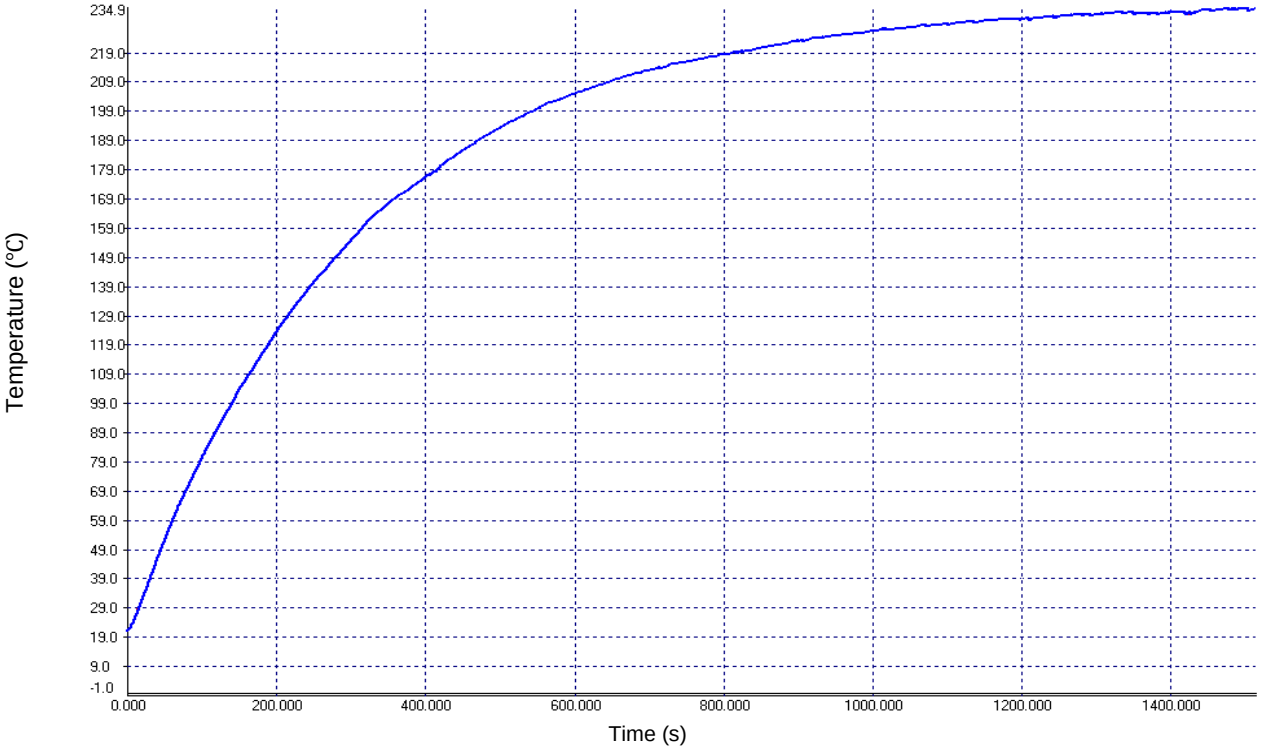

Figure 6.11: Heating rate of manufactured heater 4

6.6.2 Cooling rate

This section shows the cooling phase of an FIR heater. In the simulation, the heater is switched off, meaning that there is no heat generation. As soon as the FIR ceramic heater is switched off, cooling down is observed and presented in Figure 6.12. The dynamic is fast, similar to the heating phase one within the same period of time which is expected for an efficient heater with a low input voltage. Figures 6.13 to 6.16 represent the cooling down phase of the manufactured ceramic infrared heaters during testing.

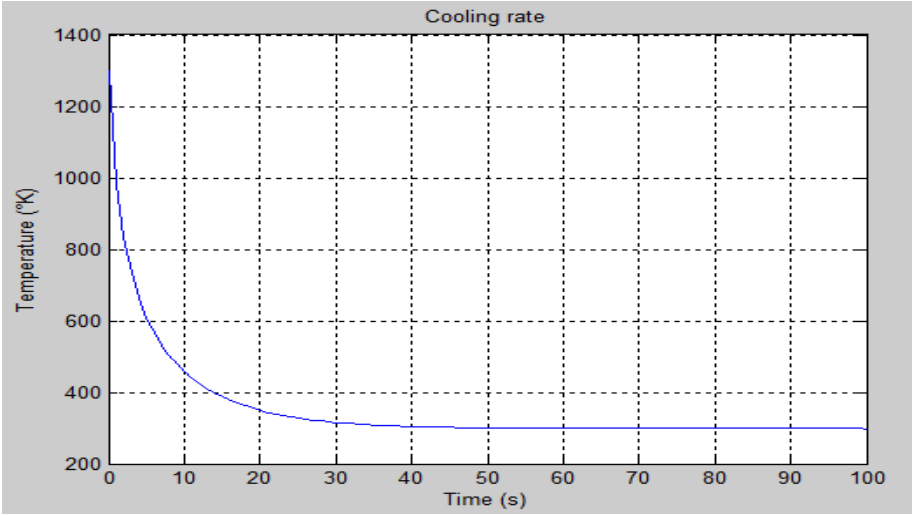

Figure 6.12: Cooling rate

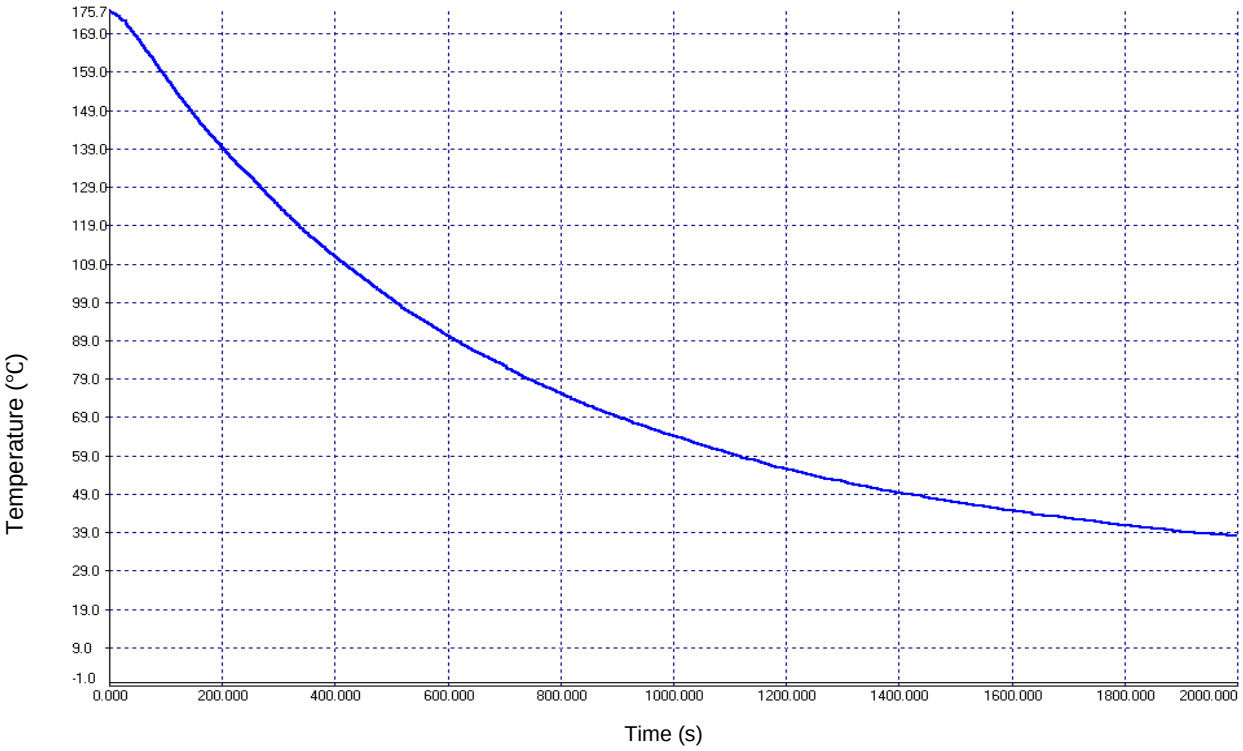

Figure 6.13: Cooling rate of manufactured heater 1

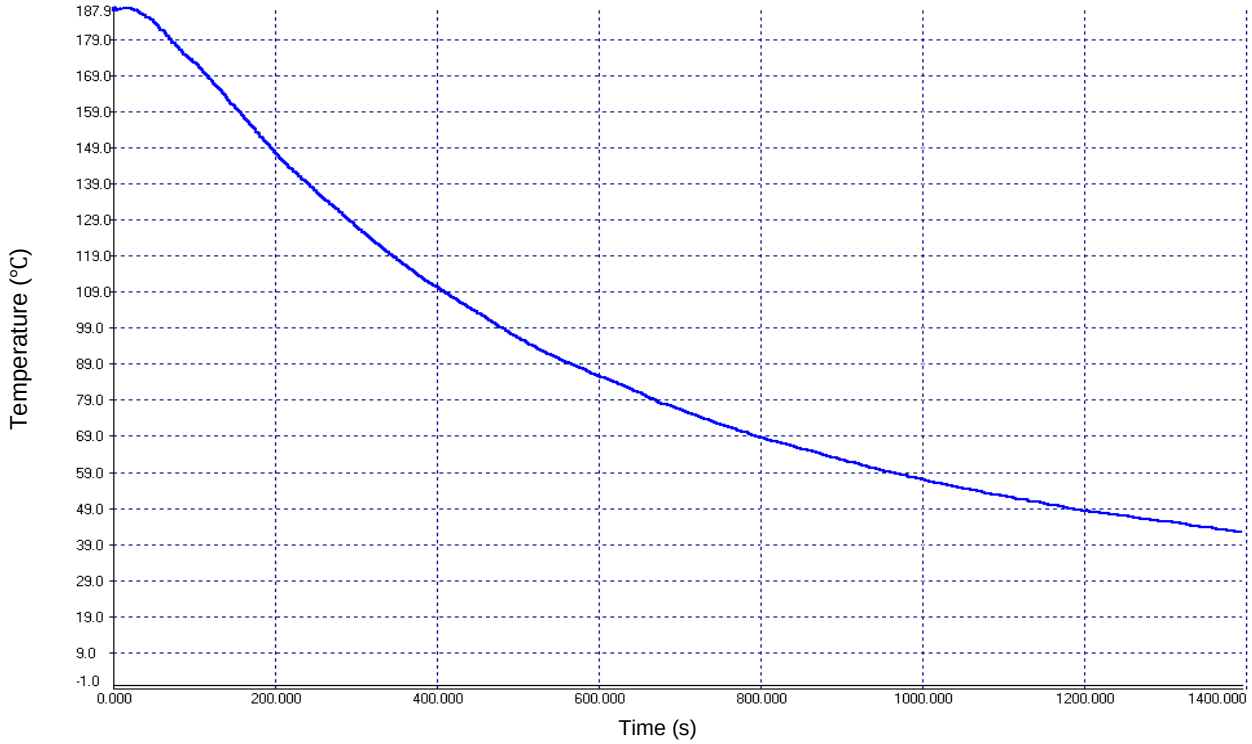

Figure 6.14: Cooling rate of manufactured heater 2

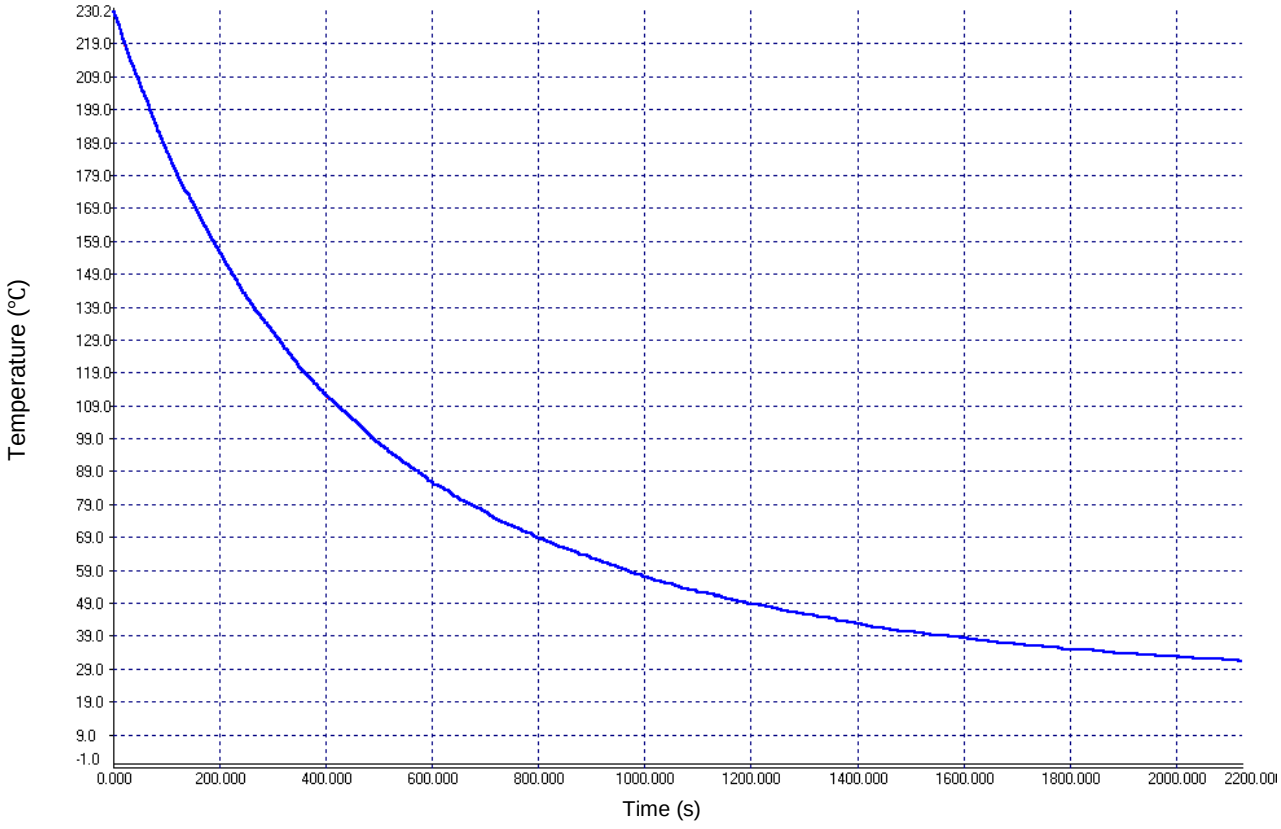

Figure 6.15: Cooling rate of manufactured heater 3

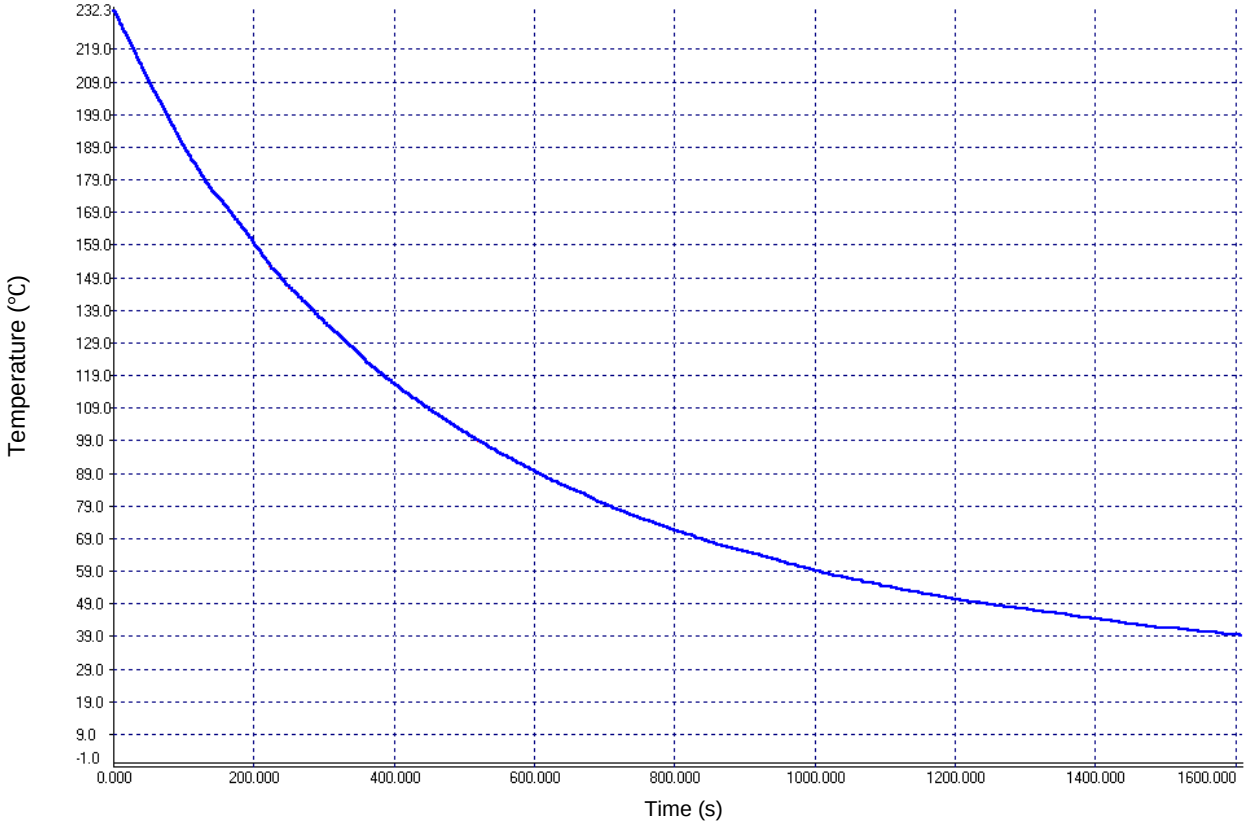

Figure 6.16: Cooling rate of manufactured heater 4

The following table shows the calculated lengths and temperatures corresponding to a particular diameter of the heating element. It also provides the wavelengths associated with different temperatures.

Table 6.3: Recommended lengths for heating element

Diameter	**Length (m)**	**Temperature (˚C)**	**Wavelength (μm)**
0.355	5	600	3.3
0.355	10	500	3.7
0.355	15	400	4.3
0.355	25	300	5
0.355	35	200	6.1
0.355	45	100	7.7

6.6.3 Experimental tests

Testing of the manufactured heaters has been conducted by connecting the heater leads to the wall socket, which normally gives 220 to 230 volts, and the temperature sensor has been mounted in front of the heater to sense the temperature of the heater surface. The maximum values of temperature recorded were as follows: 173.9˚C, 187.8˚C 232.6˚C and 234.9˚C.

The wavelength of the manufactured heaters is calculated using Wien's displacement law. The wavelength of the emitter is inversely proportional to the temperature. As the temperature increases, the wavelength decreases.

$$\lambda = \frac{\mathrm{b}}{\mathrm{T}} = \frac{2.8977685 \times 10^{-3}}{℃ + 273.15} \tag{6.1}$$

The power rating of the manufactured heaters is the amount of electrical energy that is consumed by the IR emitter. The formula calculating power is defined as the following:

$$P = \frac{V^2}{R} \tag{6.2}$$

Where V is the input voltage and R is the measured resistance of the heating element. The results from the testing of the manufactured heaters are summarised in Table6.4.variation in ceramic heaters temperature is due to Resistance wire configuration and the insulation fibre adjustment, drying process was also different for each heater.

Table 6.4: Manufactured heaters calculations

	Heater 1	Heater 2	Heater 3	Heater 4
Size (mm)	265×198	265×198	265×198	265×198
Typical operating temperature (˚C)	173.9	187.8	232.6	234.9
Wavelength (μm)	6.4	6.2	5.72	5.70
Input voltage (V)	228	228	228	228
Rated current (A)	1.05	1.05	1.05	1.05
Measured resistance (Ω)	216.5	216.5	216.5	216.5
Power rating (W)	240	240	240	240

6.7 Gasification of plastics

The manufactured ceramic infrared heaters were carefully placed inside the gasifier before establishing the electrical connections. The input voltage to the gasifier was 230 volts and the rated current was 4.2A. The gasification tests then conducted on each sample separately.

6.7.1 Sample preparation

The plastic samples were washed with hot water prior to the gasification tests to remove dirt and any possible contaminants that stick on the surface of the samples. Samples were also weighted using measuring scale to determine the mass of each sample before and after gasification. The following figures 6.17, 6.18, 6.19 and 6.20 shows the PP, HDPE, LDPE, PET samples before the gasification process whereas table 6.5 shows the weight of each sample before gasification. Heater to composite distance was set to be 10 centimeters as experimental condition.

Figure 6.17: HDPE sample before gasification

Figure 6.18: LDPE sample before gasification

Figure 6.19: PET sample before gasification

Figure 6.20: PP sample before gasification

Table 6.5: Mass of samples

Sample	Mass (grams)
LDPE	153.9
HDPE	190.05
PP	14.93
PET	22.05

6.7.2 Gasification results

The gasification experiments conducted were aiming to test and validate the manufactured ceramic infrared heaters for the gasification process and production of syngas. The temperature measurements inside and outside gasifier and the temperature of the samples during gasification were performed using a FlukeTi20 thermal imager and k type thermocouple. Comparison of temperature measurements has been conducted to determine the exact temperature inside the gasifier. Temperature measurements inside the gasifier using K type thermocouple was found more accurate than using a Fluke Ti20 because the maximum temperature range that Fluke Ti20 can measure is 360˚C and the actual temperature inside the gasifier was more than 360˚C. Temperature measurements using thermocouples have shown that the maximum temperature that the gasifier can reach is 457˚C.

Infrared gasifier was switched on and left for 20 minutes to reach temperature of 457˚C. During the gasification of LDPE the emission of syngas started after 10 seconds because the gasifier has been heated to reach temperature of 457˚C before feeding the samples to the gasifier. Syngas continues to yield for 12 minutes during the gasification of LDPE, results of gasification tests of HDPE, LDPE, PET and PP are shown in table 6.6 below. The total gas yields of LDPE, HDPE were 96.7wt% and 95 wt% each at temperature 457˚C. The formation of carbonaceous residue or coke was 3.3 wt%, 5.2 wt% for LDPE, HDPE respectively. After taking all the plastic samples, the test run is considered finished and the gasification then concluded.

Figure 6.21: LDPE sample after gasification

Figure 6.22: HDPE sample before gasification

Table 6.6: Gasification results

Sample	Mass of feed before gasification (gram)	Duration of gasification (Minute)	Mass of residue after gasification (gram)	Maximum temperature of gasifier(˚C)	Gas yield wt%
LDPE	153.9	10	5.06	457	96.7
HDPE	190.5	12	9.95	457	95.0
PET	22.05	6	5.91	457	74.0
PP	14.93	11	5.51	457	63.0

The percentage of produced gas was more than 90% of the total feed to the gasifier when comparing the mass of samples before and after gasification.

6.7.3 Analysis of results

The comparison of the wt% of coke residue and the wt% of the feed reveals the fact that the carbonaceous residue is very low, less that 5%, which makes the use of ceramic infrared heaters efficient. The plastics started react at 457˚C, the wavelength emitted by the manufactured infrared heaters was successfully absorbed by the plastic samples. The short period gasification time of the plastic sample during gasification confirms the high thermal efficiency of the infrared gasifier and therefore the validity of infrared technology used in gasification of plastics. Whereas in this experiments the difference of gasification residence time between samples referred to the difference in thickness. Gasification process shows that the amount of the produced gases increased when gasification temperature increased. Gasification results derived from this project were compared to other models (Toshiro, 2009) (Takatoshi, 2001). The comparison has shown that the production of syngas is comparable to models and the designed gasifier has low coke formation less than 5wt%. Gasification time and formation of residue needs further modification in the infrared gasifier compared to the two stage gasification procedures.

6.7.4 Gas analysis

Quadrupole Mass Spectrometer 200 gas analyser was used in this stage to further analyse the resultant gas derived from the gasification of plastic samples. Analog scan mode has been chosen for analysis, it is the spectrum analysis mode common to all gas analisers. X-axis represents the atomic mass range chosen in the mass spectrometer. The Y-axis represents the amplitude of every mass increment measured.

Atmospheric scan inside the gasifier was performed and set as reference for any increase in gas yield. Atmospheric scan is shown in figure 6.23. The experiments concentrated in the production of H_2, CO and CO_2. Samples of plastics then carefully injected to the gas analyser. Gas sample analyses have shown increase in hydrogen production for LDPE, PET and PP. increase in CO_2 was also observed for HDPE and PET. In all samples, the production of CO stayed unchanged during analysis. Figure 6.24, 6.25, 6.26, 6.27 shows the gas analysis of chosen samples. Table 6.7summerises the gas analysis results.

Table 6.7: Gas analysis results

Sample	Gasification temperature (˚C)	H_2 Production	COProduction	CO_2 Production
LDPE	457	Increased	No change	No change
HDPE	457	No change	No change	Increased
PET	457	Increased	No change	Increased
PP	457	Increased	No change	No change

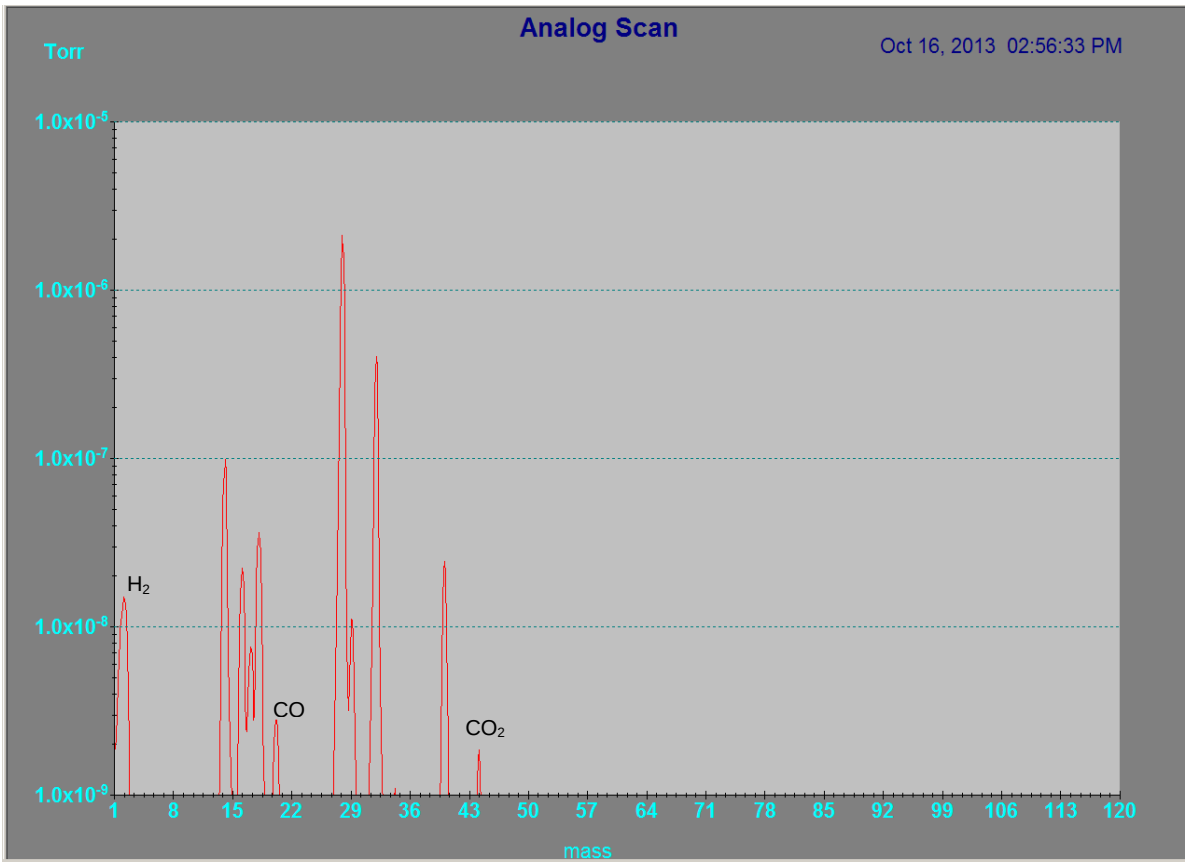

Figure 6.23: Atmospheric spectrum

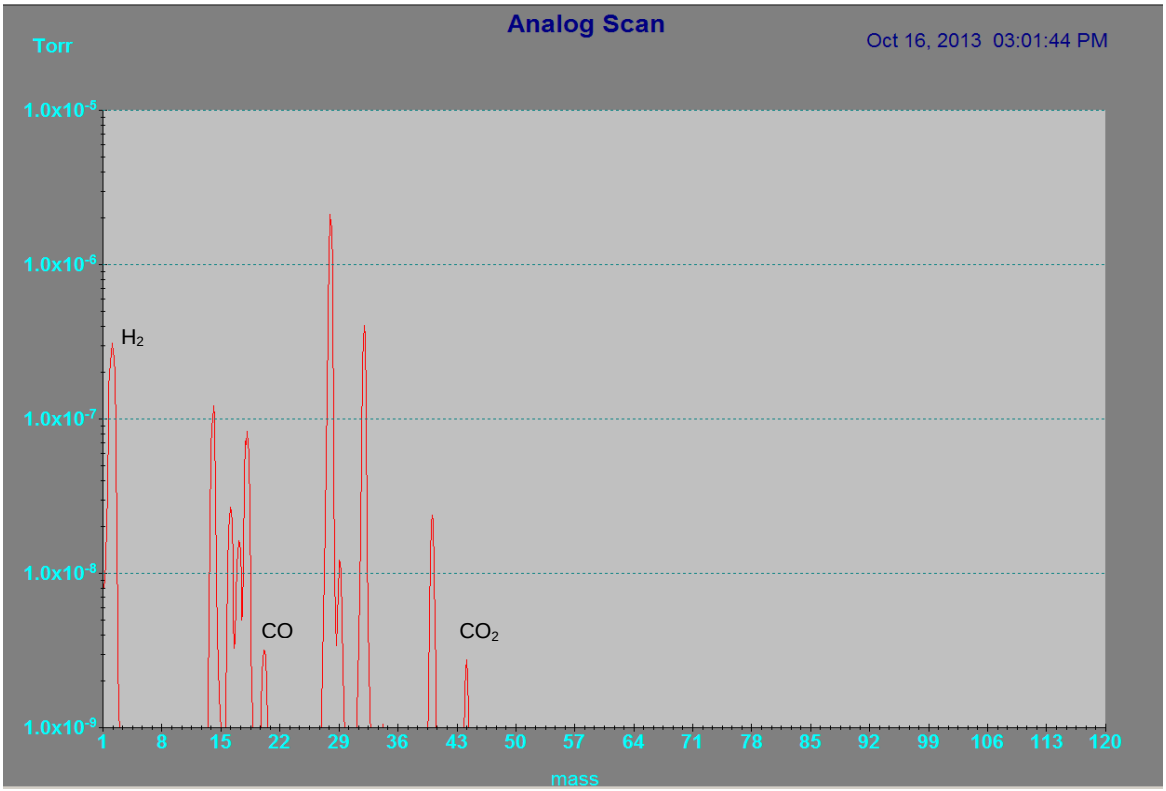

Figure 6.24: LDPE spectrum

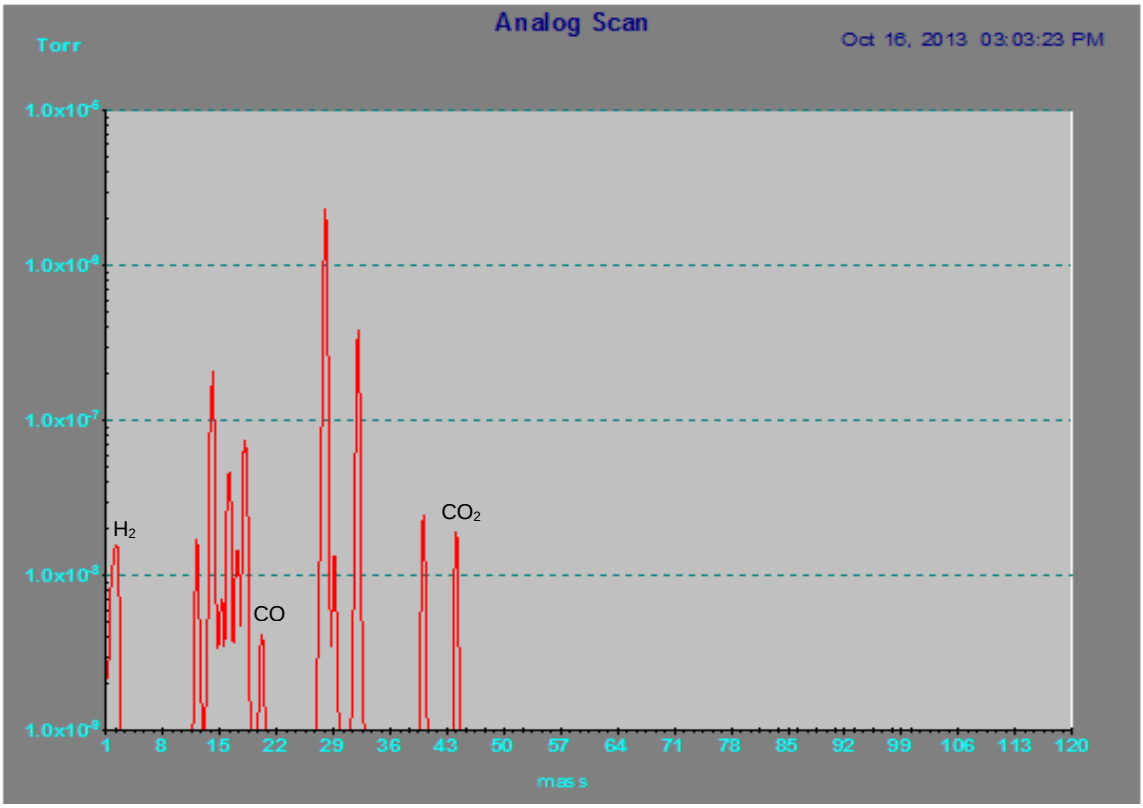

Figure 6.25: HDPE spectrum

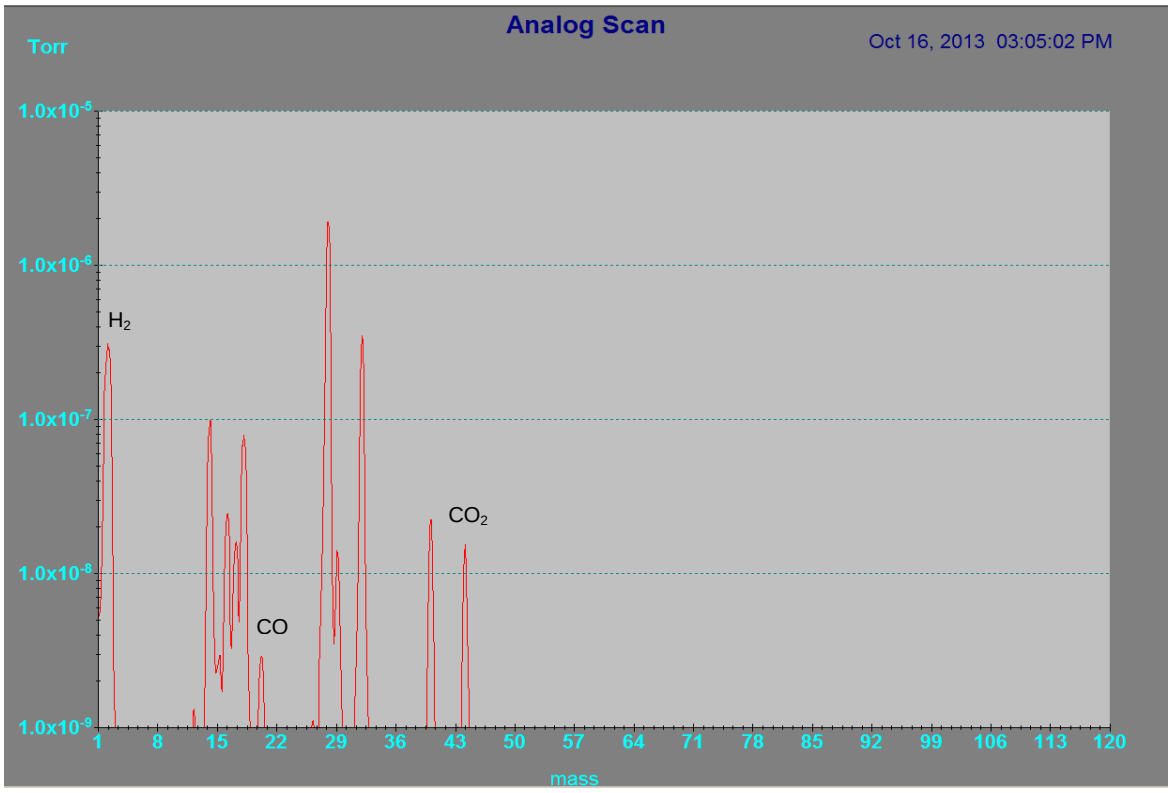

Figure 6.26: PET spectrum

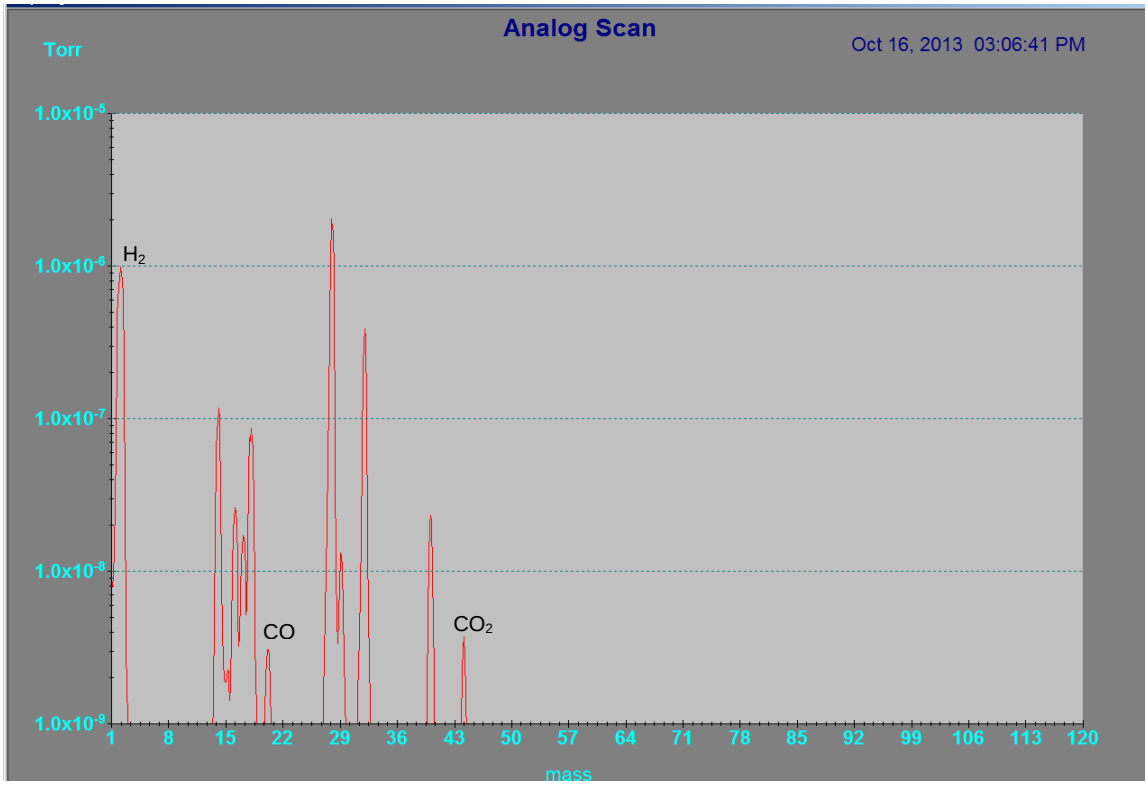

Figure 6.27: PP Spectrum

CHAPTER SEVEN
CONCLUSION AND RECOMMENDATIONS

This research is based on theoretical and practical work regarding the design of ceramic infrared heaters for far infrared heating applications. Both modelling and experimental techniques have been employed. The focus has been on developing and analysing ceramic infrared heaters that encompass the ability to produce wavelengths corresponding to the waste plastic absorption spectrum. This project considered only ceramic electric infrared heaters.

A design, model and manufacturing of ceramic electric infrared heaters, along with infrared gasifiers, have been proposed. The model of the gasifier is based on net radiation method, a widely used method in modelling and analysing heat transfer within enclosures. The results obtained from the tests revealed that the manufactured heaters have successfully emitted infrared energy and wavelengths matching the plastics absorption characteristics.

7.1 Problems solved in this research

The problems that this research sought to resolve were both the theoretical design and the hardware production of ceramic infrared heater suiting the plastics gasification applications. These problems were further divided into numerous sub-problems, including the following:

- To model and simulate ceramic infrared heaters that could be used in furnaces for gasification of waste plastics
- To design, manufacture and analyse a far infrared ceramic heater for waste plastic gasification;
- To design and manufacture an infrared gasifier;
- To use plastics from waste as feedstock in order to study the influence of infrared radiation on transforming thermoset plastics into syngas; and
- Production of syngas using the manufactured infrared gasifier.

7.1.1 To model and simulate ceramic infrared heaters that could be used in furnaces for gasification of waste plastics

In order to obtain an accurate mathematical expression of the IR heater used in this research, an intensive review of thermal system enclosures and infrared heating systems has been implemented. The model has been represented numerically, the results of the model were plotted graphically, and the curves were analysed.

7.1.2To design, manufacture and analyse a far infrared ceramic heater for waste plastic gasification

The ceramic heater design and manufacturing process has been described in detail, starting from the initial preparation of the mold board, all the way through the preparation of the plaster. The assembly of the heater parts started from making the front and back sides of the ceramic heater and placing the heating element and the fibre blanket. Figures have been introduced to show the manufacturing process.

7.1.3 Design and manufacture of an infrared gasifier

The infrared gasifier has been designed prior to the gasification stage, the aluminum body was found very helpful for retaining the heat inside the gasifier, Infrared gasifier has been designed and manufactured, waste plastics has been gasified using the manufactured infrared gasifier and gasification results were presented in table 6.6.

7.1.4 To use plastics from waste as feedstock in order to study the influence of infrared radiation on transforming thermoset plastics into syngas

Infrared radiation has been applied to the waste plastics usingthe manufactured ceramic infrared heater on gasification of plastics. Using an infrared heater for the gasification of plastics has successfully transformed 96.7wt%LDPE, 95wt%HDPE, 74wt% PET and 63wt% of the PP into gas, each at an approximate temperature of 457˚C.

7.1.5 Production of syngas using the manufactured infrared gasifier.

The designed infrared gasifier system has shown it is reliablefor the production of syngas. The gases yielded were analysed using a Quadrupole Mass Spectrometer. Gas analysis results were plotted and shown in chapter 6. Three of the four plastics samples tested were able to produce syngas with a significant proportion constituting of hydrogen while the production of carbon monoxide was same as atmospheric spectrum and stayed unchanged.

7.2 Application of results

The results obtained in this research provide for the following applications:

- The manufactured ceramic infrared heaters can be used in liquefaction and gasification of recyclable waste plastics in place of conventional plastic waste treatments such as landfills and incineration.
- The represented theoretical and mathematical models can be used to analyse the heat transfer of enclosures.
- The information presented on the making of ceramic infrared heaters can be used as the step-by-step basis of making of IR heaters.

- The measured wavelength values of the different plastic samples can be used as references on designing IR heaters.

7.3 Recommendations for further studies

A recommendation for further studies on this research acknowledges that IR processing of pyrolysis or gasification applications is still a modest underdeveloped research area. Much work still needs to be done in terms of optimisation of gasification of plastic using infrared thermal radiation. Parameters to be taken into consideration when designing infrared gasification systems are listed as follows:

- Number of heaters to be used in accordance with size of the gasifier;
- Distance between heaters and object to be processed;
- Electrical power consumed by the heaters; and
- Modification of the gasifier design in order to allow steam and oxygen injection.

REFERENCES

Abadie, L. M. & Chamorro, J. M. 2009. The Economics of Gasification: A Market-Based Approach. *Energies*, 2:662-694.

Adonis M, 2002, An investigation and design of an infrared readiation heat profile controller [unpuplished MTech.] Cape Town, Cape Peninsula University of Technology.

Ackland, K, 1998. Selecting the right infrared temperature sensor. *Temperature in Tech*.

Afzal, T.M., Abe T., & Hikida Y., 1999. Energy and quality aspects during combined far infrared convective drying of barley. *Journal of Food Engineering,* 42: 177-182.

Aguado, J. & Serrano D. 1999. Feedstock Recycling of Plastic Wastes. Royal Society of Chemistry, Clean Technology Monographs. Cambridge, UK.

Andrady, A. 2003. An environmental primer in plastics and the environment. Wiley Interscience, 3-76.

Andrady, A. L. 2003. Plastics and the environment. John Wiley and Sons Inc.

Androutsopoulos, G. P. & Hatzilyberis, K. S. 2001. Electricity generation and atmospheric pollution: the role of solid fuels gasification. *Global Nest: The Int. Journal*, 3(3): 171-178.

Anonymous, 2002. South Africa rejects hazardous waste incineration, Environmental Law Alliance Worldwide. http://www.elaw.org/system/_les/sa.rejects.incineration.pdf. Accessed 12/11/2012

Anonymous. 2009. Engineering: Aspects of radiation theory. http://www.noblelight/resources/pdf-downloads/technical-notes /Pdf [13 January 2011].

Anonymous, 2013. Gasification - An Investment in our Energy Future, Gasification Technology Council. http://www.gasification.org. Accessed 14/10/2011

Anonymous, 2013. The gasification of residual plastics derived from municipal recycling facilities, Environmental and Industry Council (EPIC) Canadian Plastics Industry. http//www.plastics.ca. Accessed 25/09/2012

Arena, U., Zaccariello, L., & Mastellone, M.L. 2009. Tar removal during the fluidied bed gasification of plastic waste. *Waste Management,* 29(2): 783-791.

Baeyens, J. 2010. Recycling plastics. http//: www.warwick.ac.uk/Knowledge/engineering/recycling [5 April 2011]. Accessed 16/10/2012

Barnes, D. K. A., Galgani, F., Thompson, R. C. & Barlaz, M. 2009. Accumulation and fragmentation of plastic debris in global environments. 364: 1985-1998.

Bejan, A. A.D.K., 2003. Heat transfer handbook. John Wiley and Sons Inc.

Bisho, H,. 1990. The answer is electrical infrared. *Journal of Microwave Power and Electromagnetic Energy,* 25(1): 47-52.

Bolshakove, A.S., Boreskov, V.G., Kasulin, G.N., Rogov, F.A ., Skryabin, U.P., & Zhukov, N.N. 1976. 22nd European meeting of metal research workers. Paper 15 (cited by Dagerskog, 1979).

Bredenhann, L. 1998. Minimum requirements for the handling, classification and disposal of hazardous waste. Department of Water Affairs and Forestry.

Brown, K. W., & Donnelly K. C. 1998. An Estimation of the Risk Associated with the Organic Constituents of Hazardous and Municipal Waste Landfill Leachate, *Hazardous Waste and Hazardous Materials,* 5:1-30.

Carvalho, M. G. & Farias, T. L. 1998. Modelling of heat transfer in radiating and combusting systems. 76(a), February.

Cihan, A. & Kahveck. 2007. Modelling of intermittent Drying of thin layer rough rice. *Journal of Food Engineering,* 79(1): 293-298.

Cosson, B., Schmidt, F., Emaouly, Y. I., & Bordival, M. 2011. Infrared heating stage simulation of semi-transparent media (PET) using ray tracing method. 4:1-10.

Cunningham, J. E., Monaghan, P. F., Borgan, M. T., & Cassidy, S. F. 1997. Modelling of pre-heating of preheating of flat panels prior to press forming, Composites Part A. *Applied Science and Manufacturing,* 28:17-24.

Da Graca C. & Fontes F. T. 1993. Multidimensional modelling of radiative heat transfer in scattering media. *ASME Journal,* 115:486-489.

Farah, N. F. 2011. The use of plastic bags. Golf News. Abu Dhabi: Al Nisr Publishing.

Fisher, M. 2003. Plastics recycling. In Plastics and the environment, Hoboken, NJ: Wiley Interscience. 563-627

Fostoria electric infrared heaters manual. www.fostoriaindustries.com. Accessed 05/05/2011.

Gilpin, R., Wagel, D., & Solch, J. 2003. Production, distribution, and fate of polycholori-nated dibenzo-p-dioxins, dibenzofurans, and related organohalogens in the environment. Dioxins and Health (eds A. Schecter and T. Gasiewicz), 2nd ed. Hoboken, NJ: John Wiley and Sons Inc.

Gregory, M. R. 2009. Environmental implications of plasticdebris in marine settings entan-glement, ingestion, smothering, hangers-on, hitch-hiking and alien invasions. *Phil. Trans. R. Soc. B.* 364:2013-2025.

Gruner, K. D. 2003. Principles of non-contact temperature measurements. *Raytek Technical Manual*, www.raytek.com. Accessed 20/11/2012

He, M., Xiao, B.,Hu, Z., Liu, S., Guo, X., & Luo, S. 2009. Syngas production from catalytic gasification of waste polyethylene, Influence of temperature on gas yield and composition. *International Journal of Hydrogen Energy*, 34(3):1342-1348.

Hebbar, U. H., Vishwanathan, K. H., & Ramesh, M. N. 2004. Development of combined infrared and hot air dryer for vegetables. *Journal of Food Engineering,* 65:557-563.

Heraeus, 1994. Technical brochure: productive heat in program form, infrared emitters.

Hodgson, A. T., Garbesi, K., Sextro, R. G., & Daisey, J. M. 2012. Soil-Gas Contamination and Entry of Volatile Organic Compounds into a House Near a Landfill. *Journal of the Air and Waste Management Association,* 42:3, 277-283.

Hopewell, J., Dvorak, R., &Kosio, E. 2009. Plastic recycling: challenges and opportunities. Philosophical Transactions of the Royal Society.

Hottel, H. C. & Cohen, H. S. 1958. Radiant heat exchange in a gas filled enclosure: allowance for nonuniformity of gas temperature. 4:3-14.

Howel, J. R. 1983. Radiative transfer in multi-dimensional enclosures with participating media. *ASME,* paper No.83-HT-32.

Howell, J. R. 1998. The Monte Carlo Method in Radiative Heat Transfer. *Journal of Heat Transfer*, 120:547.

Jackson, A. N. & Welch, D. A. 1998. Industrial applications of electric infrared heating. *Advanced Energy*. www.advancedenergy.org. Accessed 05/05/2012.

Jesus, A. S., Anzar, M.P., & Toledo, J. M. 2008. Catalytic air gasification of plastic waste PP in fluidized bed. *Ind. Eng. Chem. Res*, 47:1005-1010.

Jones, B. 2010. 10 steps to perfect plaster, Ceramic mold making techniques. www.ceramicsartsdaily.com. Accesed 10/09/2012.

Jones, J. C. 2010. Thermal Processing of Waste, Ventus Publishing.

Khalil, H., Shultis, J. K., & Lester, T. W. 1982. Comparison of three numerical methods for evaluation of radiant energy transfer in scattering and heat generating media. *Journal of Heat Transfer,* 5:235-252.

Kim, T. Y. & Baek, S. W. 1991. Analysis of combined conductive and radiative heat transfer in a two-dimensional rectangular enclosure using the discrete ordinates method. *International Journal of Heat Mass Transfer,* 34(9):2265-2273.

Kiran, N., Ekinci, E. & Shape, C. E. 2000. Recycling of plastic wastes via pyrolysis. 29:273-283.

Klein, A. 2002. Gasification: an alternative process for energy recovery and disposal of municipal solid wastes. *MSc thesis in Earth Resources Engineering*.www.columbia.edu/cu/earth. Accessed 01/02/2012.

Krishnamurthy, K., Khurana, H. K., Jun, S., Irudayarag, J., & Demirci, A. 2008. Infrared heating in food processing: an overview. *Comprehensive Reviews in Food Science and Technology,* 7.

Lampinen, M. J., Ojala, K. T., Koski, E. 1991. Modelling and measurement of infrared dryers for coated paper. *Drying Technology*, 9(4):973-1017.

Lawrence B., Berkeley. 2007. Improving process heating system performance. *Resource Dynamic Corporation,* Second Edition.

Lebaudy, P. & Grenet, J. 2001. Heating simulation of multilayer performs. *Journal of AppliedPolymer Science,* 80:2683-2689.

Lee, G. F. & Jones-Lee, A. 1994. Impact of Municipal and Industrial Non-Hazardous Waste Landfills on Public Health and the Environment: An Overview. (530): 753-9630.

Leong, M.S., Kooi, P. S. & Chandra. 1988. Radiation from a flanged parallel-plate waveguide: solution by moment method with inclusion of edge condition. 135(4).

Liu, J., Tiwari, S. N. 1994. Radiative interactions in chemically reacting compressible nozzle flows using Monte Carlo simulation. *6t AIAA/ASME Joint Thermophysics and Heat Transfer Conference,* 1-13.

Lloyd, B. J., Farkas, B. E., & Keener, K. M. 2003. Characterization of radiant emitters used in food processing. *Journal of Microwave Power and Electromagnetic Energy,* 38(4):213-224.

Lockwood, F. C. & Shah, N. G. 1981. A new radiation solution method for incorporation in general combustion prediction procedures. Eighteenth Symposium(International) on compustion, 18(1):1405-1414.

Long, C. 2009. Radiant infrared heating-theory and principles. Chromalox: Technical Information, Ventus Publishing Aps.

Mark A., John B., David B., Mario C., Joseph G., Alex M., Bill M., Preston L., Steve S., and Antony W., 2007. Improving process heating performance. U.S. Department of Energy Source Book.

Martin P., Von Thienen, N., Jochem, E. & Worrell, E. 1999. Recycling of plastics in Germany.

Masteral, F.J., Esperanza, E., Berrueco, C., Juste, M. & Ceamanos, J. 2003. Fluidized bed thermal degradation products of HDPE in an inert atmosphere and in air-nitrogen mixures. *Journal of Analytical and Applied Pyrolysis.* 70(1):1-17.

McKeen, L. W. 2008. The effect of temperature and other factors on plastics and elastomers. William Andrew.*Symposium on combustion* (Pittsburg, PA: The Combustion Institute):1405-1414.

Mella, J. Y. 2005. Recycling of Polymers, Department of Process and Environmental Engineering, Mass and Heat Transfer Process Laboratory.

Miller, A. 1994. Industry invest reusing plastics. *Environmental Science*. 28.

Miller, S. J., Shah, N. & Huffman, G. P. 2006. Conversion of waste plastic to lubricanting base oil. *Energy Fuels,* 19(4):1580-1586.

Modest, M. F. 2003. Radiative heat transfer, 2nd Ed. San Diego: Academic Press.

Monteix, S., Schmidt, F., Maoult, Y. L., Yedder, R. B., Diraddo, R. W. & Laroche, D. 2001. Experimental study and numerical simulation of perform sheet exposed to infrared radiation heating. *Journal of Materials Processing Technology,* 119:90-97.

Moran, M. J., Shapiro, H.N., Muson, B. R. & Dewitt, D. P. 2003. Introduction to thermal systems engineering – thermodynamics. Wiley and Sons Publishing.

Murthy, J .Y. & Choudhary, D. 1992. Computation of participating radiation in complex geometries. *28th National Heat Transfer Conference,* San Diego, CA (*ASME*, heat transfer), 153-160.

Nickrothal Handbook. 2001. Resistance heating alloys and systems for industrial furnaces. PRIMAtryck, Catalogue 1-A-5B-3 0.9, 5000.

Oehlmann, J. *et al.* 2009 A critical analysis of the biologicalimpacts of plasticizers on wildlife. *Phil. Trans. R. Soc.* B364, 2047-2062.

Ojolo, S. J. & Ismail, S. O. 2012. Mathematical modelling of plastic waste pyrolysis kinetics. *International Journal of Computational and Manufacturing Research,* 1:29-34.

Okuwaki, A. 2004. Feedstock recycling of plastics in Japan, polymer degradation and stability. 85 2005: 981-988.

Omega. 1998. Transactions in measurements and control, 2nd edition. Putnam Publishing Company, OMEGA press LLC.

Pan, Z. 2011. Infrared heating for food and agricultural processing. CRC Press, Taylor and Francis group.

Peter, K., Barlaz, M. A., Alix, P. R., Baun, A., Ledin, A. & Christen, T. H. 2010. Critical review in environmental science and technology.

Petrovskii, V.Y. 1998. Use of composites based on Si 33N4 in broadband electric heaters. II. Energy characteristics of an all-ceramic heater, powder metallurgy and metal ceramics. 37:3-4.

Petterson, M. & Stenstrom, S. 1998. Absorption of infrared radiation and the radiation transfer in papers, part 2: application to infrared dryers. *Journal of Pulp and Paper Science,* 24(11):365-363.

Petterson, M. & Stenstrom, S. 2000. Modelling of an electric IR heater at transient and steady state conditions, part 1: model and validation. *International Journal of Heat and Mass Transfer,* 43:1209-1222.

Plastics Europe. 2012. Association of plastic manufacturers. www.plasticseurope.org. Accessed 04/06/2012.

Radermacher, W. 2010. Using official statistics to calculate greenhouse gas emissions.

Roth, K. & Brodrick, J. 2007. Infrared radiant heaters. *ASHRAE Journal,* 72-73.

Ruoppolo, G., Ammendola, P., Chirone, R., & Miccio, F. 2012. H2-rich syngas production by fluidized bed gasification of biomass and plastic fuel. 32:724-732.

Sajid, H. S., Z. M. K., Raja, I. A., Mohamood, Q., Bhatti, Z. A., Khan, J., Farooq, A., Rashid, N. & Wu, D. 2010. Low temperature conversion of plastic waste into light hydrocarbons. *Journal of Hazardous Materials,* 179:15-20.

Sakuyama S., Uchida, H., Watanabe, I., Natori, K. & Sato, T. 1995. Reflow soldering using selective infrared radiation. Proceedings of IEEE/CPMT International Electronic Manufacturing Technology (IEMT) Symposium, 393-396.

Scobbo Jr., J. J. 1990. Radiative heating of thermoplastic graphite fiber composites. *22nd International SAMPE Technical Conference,* 22:39-49.

Scott, D. S., Czernik, S. R., Piskorz, J., & Radlein, D. S. A. G. 1990. Fast pyrolysis of plastic wastes. *Fuel and Energy,* 4:407-41.

Sgalari, G.,Camera-Roda, G., & Santarelli, F. 1998: Discrete ordinate method in the analysis of radiative transfer in photocatalytically reacting media, 25(5):651-660.

Shah, N.G. 1979. New method of computation of radiation heat transfer combustion champers. PhD thesis, Imperial College, University of London, London.

Sharma, G.P., Verma, R.C. & Pathare, P. 2005. Thin layered infrared radiation drying of onion slices. *Journal of Food Engineering,* 67:361-366.

Shoji, T., Shindoh, K., Kajibata, Y. & Sodeyama, A. 2001. Waste plastics recycling by an entrained flow gasifier, chemical and environmental department. Akash Technical Institute Kawasaki Heavy Industries, LTD, 29.

Shumacher, H. 1996. Infrared soldering from the view point of base material manufacturer. *Circuit World,* 22:4-8.

Siegel, R. & Howell, J. R. 1992. Thermal radiation heat transfer, 3rd edition. Washington: Hemisphere Publishing Corporation.

Smith, B. C. 1996, 2011. Fundamentals of fourier transform infrared spectroscopy. CRC Press, Taylor and Francis Group.

Song, H.J., Lee, J., Gaur, A., Park, J.J., &Park, J.W. 2010. Production of gaseous fuel from refuse plastic fuel via o-pyrolysis using low quality coal and catalytic steam gasification. 12:295-301.

Steward F. R. & Tennankore, K. N. 1979. *Journal of Institute of Energy*, 53: 107-112.

Sukhatme, S. P. 2005. *Textbook on heat transfer,* 4th edition, University Press.

Sweeney, G. J.,Monaghan, P. F., Brogan, M. I., & Cassidy, S. F. 1995. Reduction of infrared heating cycle time in processing of thermoplastic composites using computer modelling. 3rd *International Conference on Flow Processes in Composite Materials,* 94(6):255-262.

Tan, W. &Zhong, Q. 2010. Simulation of hydrogen production in biomass gasifier.*ASPEN PLUS.* IEEE.

Thermal ceramics (http:// www.thermalceramics.com) Accessed 2012/10/18.

Tsuji, T. &Hatayama, A. 2008. Gasification of waste plastics by steam reforming in fluidized bed. 11:144-147.

Tsuji, T., Tanaka, Y., Shebata, T., Uemaki, O. & Itoh, H. 2000. Two stage thermal gasification of plastics. 12.

United State Environmental Program Association (1980), planning workshop to develop recommendations for ground water protection strategy.

Vasile, C., Brebu, M. A., Karayildirim, T., Yanic, J., & Darie, H. 2007. Feedstock recycling from plastics and thermosets fractions of used computers. II. Pyrolysis oil upgrading. 86:477-485.

Viskanta, R. & Menguc, M. P. 1987.Radiation heat transfer in combustion system. *Program Energy Combust Science*, 13:97-160.

Wandless, P. A. 2010. How to make casting slip from your clay body – ceramic mold making techniques. www.ceramicartsdaily.org accessed 12/10/2012

Wu, C. & Williams, P. T. 2009. Hydrogen production from pyrolysis-gasification of waste plastics. *Energy and Resources Research Institute,* 90:147-156.

Wu, C. &Williams, P. T. 2010. Pyrolysis – gasification of post consumer municipal solid plastic waste for hydrogen production. *International Journal of Hydrogen Energy*, 35(3):949-957.

Yamawaki, T.2003. The gasification recycling technology of plastics WEEE containing brominated flame retardants. 27:315-319.

Yang, K. T. 1986. Numerical modelling of natural convection-radiation interactions in enclosures. *8th International Heat Transfer Conference* (WashingtonDC: Hemisphere), 1:131-140.

Yla Mella, J. 2002. Recycling of plastics from the waste electrical and electronic equipment (WEEE). *Department of Process and Environmental Engineering,*University of Oulu,Finland.

APPENDIX A: Filament wire specifications: Nikrothal 80 (Nikrothal Handbook, 2001)

Chemical composition

	C %	Si %	Mn %	Cr %	Ni %	Fe %	Trace elements
Nominal composition					Bal.		Added
Min	-	1.0	-	19.0	-	-	-
Max	0.10	1.7	1.0	21.0	-	2.0*	-

* Fe< 1.0 on request

Mechanical properties

Wire size	Yield strength	Tensile strength	Elongation	Hardness
Ø	$R_{p0.2}$	R_m	A	
mm	MPa	MPa	%	Hv
1.0	420	810	30	180
4.0	300	725	30	160

Mechanical properties (continue)

Mechanical properties at elevated temperature

Temperature °C	900
MPa	100

Ultimate tensile strength - deformation rate 6.2 x 10^{-2}/min

Mechanical properties (continue)

Creep strength - 1% elongation in 1000 h

Temperature °C	800	1000
MPa	15	4

Physical properties

Density g/cm^3	8.30
Electrical resistivity at 20°C Ω mm^2/m	1.09

Physical properties: Temperature

Temperature factor of resistivity

Temperature°C	100	200	300	400	500	600	700	800	900	1000	1100	1200
Ct	1.01	1.02	1.03	1.04	1.04	1.04	1.04	1.04	1.04	1.05	1.06	1.07

Physical properties: Coefficient of thermal expansion

Coefficient of thermal expansion

Temperature °C	Thermal Expansion x 10^{-6}/K
20 – 250	14.1
20 – 500	14.9
20 – 750	16.0
20 – 1000	17.2

Physical properties: Thermal conductivity

Thermal conductivity

Temperature °C	20	100	200	300	400	500	600	700	800	900	1000	1100
W m^{-1} K^{-1}	15	15	15	15	17	19	21	22	24	26	28	30

Physical Properties: Specific heat

Specific heat capacity

Temperature °C	20	100	200	300	400	500	600	700	800	900	1000	1100
kJ kg^{-1} K^{-1}	0.46	0.46	0.48	0.50	0.52	0.54	0.56	0.60	0.63	0.65	0.67	0.70

Physical properties: Melting point

Melting point °C	1400
Max continuous operating temperature in air °C	1200
Magnetic properties	The material is non-magnetic
Emissivity - fully oxidized material	0.88

APPENDIX B: Matlab Heating and cooling codes

```
ZuhairEltiganiMatarHaruon

Student number 210262958

Department of Electrical Engineering

Design and development of infrared heater for plastic Gasification purposes

clear;
clf;
clc;

Re= 61.67;                          % Resistance [?]
U = sqrt(12019.8);                  % Voltage [V]
L = 4;                              % Length of filament wire [m]
Tinf = 298.25;                      % ambient Temperature [°K]
Tsurr = 298.15;                     % Temperature surrounding [°K]
hc = 25;                            % Heat transfer coefficient by
Convection for air [W/m².K]
D = 3*1e-4;                         % Filament diameter [m]
epsi = 0.88;                        % Emissivity of filament
Cp = 460;                           % Specific heat of filament @20°C
[kJ/(Kg*K)]
rho = 8300;                         % Density of filament [kg/m³]
sig = 5.670*1e-8;                   % Stephan-Boltzmann constant [W/m².K?]

i = 1;
h = 1;
T(1) = 298.15;
t(1) = 0;
Rel = Re/L;
V = pi*(D^2/4)*L;
A = pi*D*L;
Eps = epsi*sig*A;
B = 1/(rho*Cp*V);

while t(i)<100
    k1=h*func4(T(i),B,U,Rel,Eps,Tsurr,hc,A,Tinf);
    k2=h*func4(T(i)+k1,B,U,Rel,Eps,Tsurr,hc,A,Tinf);
    k3=h*func4(T(i)+k2/2,B,U,Rel,Eps,Tsurr,hc,A,Tinf);
    k4=h*func4(T(i)+k3,B,U,Rel,Eps,Tsurr,hc,A,Tinf);
T(i+1)=T(i)+(1/6)*(k1+2*k2+2*k3+k4);
t(i+1)=i*h;
i=i+1;
end

plot(t,T);
gridon
xlabel('Time (s)');
ylabel('Filament Temperature (°K)');
title('Heating rate')
```

```
ZuhairEltiganiMatarHaruon

Student number 210262958

Department of Electrical Engineering

Design and development of infrared heater for plastic Gasification purposes


function f=func4(T,B,U,Rel,Eps,Tsurr,hc,A,Tinf)
f=B*((U^2/Rel)-Eps*(T^4-(Tsurr)^4)- hc*A*(T-Tinf));

clear;
clf;
clc;
holdoff;

L = 4;                                  % Length of filament wire [m]
Tinf = 298.25;                          % ambient Temperature [°K]
Tsurr = 298.15;                         % Temperature surrounding [°K]
hc = 25;                                % Heat transfer coefficient by
Convection for air [W/m².K]
D = 3*1e-4;                             % Filament diameter [m]
epsi = 0.88;                            % Emissivity of filament
Cp = 460;                               % Specific heat of filament @20°C
[kJ/(Kg*K)]
rho = 8300;                             % Density of filament [kg/m³]
sig = 5.670*1e-8;                       % Stephan-Boltzmann constant [W/m².K?]

i = 1;
h = 1;
T(1) = 1300;
t(1) = 0;
V = pi*(D^2/4)*L;
A = pi*D*L;
Eps = epsi*sig*A;
B = 1/(rho*Cp*V);

while t(i)<100
    k1=h*func3(T(i),B,Eps,Tsurr,hc,A,Tinf);
    k2=h*func3(T(i)+k1,B,Eps,Tsurr,hc,A,Tinf);
    k3=h*func3(T(i)+k2/2,B,Eps,Tsurr,hc,A,Tinf);
    k4=h*func3(T(i)+k3,B,Eps,Tsurr,hc,A,Tinf);
T(i+1)=T(i)+(1/6)*(k1+2*k2+2*k3+k4);
t(i+1)=i*h;
i=i+1;
end
plot(t,T);
gridon;
xlabel('Time (s)');
ylabel('Temperature (°K)');
title('Cooling rate')
```